Introduction..3

MVs and tumor progression 6

MVs and extracellular matrix remodeling....11

MVs and thrombosis..16

MVs and angiogenesis.....18

MV mediated tumor-immune system interaction.....23

Clinical studies involving MVs 27

MVs: structure and biogenesis 31

Techniques for separating membrane vesicles and exosomes 37

MV protein composition 39

Shed MVs and mammary carcinoma.....43

Aim....46

Materials and Methods.....49

Cell Culture.....50

Vesicle collection 50

Cell Lysate Preparation.....51

Bradford assay 51

Gel permeation cromatography 51

Filtration/centrifugation 52

Transmission Electron Microscopy analysis 52

Monodimensional electrophoresis 52

2D-PAGE 53

Spot detection: Ammoniacal Silver Staining or Comassie Brilliant Blue.....54

Ammoniacal Silver Staining..54

Gel acquisition and analysis .55

Blue Comassie Staining.....56

Preparation of samples for mass spectrometry 56

Destaining and in gel digestion 56

Extraction of tryptic peptides 57

Purification of tryptic peptides with zip-tip ..57

Acquisition of mass spectra through MALDI-TOF...57

Protein Labeling with fluorescent dye Cy5 58

Labeling of cells with radioactive S35 methionine.....59

Western Blotting.....60

Immunofluorescence.....61

Immunofluorescence of cells grown on 3D collagen.....62

Antibodies 62

Results and discussion.....63

Purification and characterization of 8701 BC derived MVs.....64

Proteomic analysis of 8701 BC derived MVs. 68

Attempts of vesicles purification 71

Induction of vesicle shedding by Scatter Factor addition.....74

Purification and characterization of MDA MB 231 derived MVs.....76

Immunofluorescence of MDA MB 231 cells 79

Proteomic analysis of MDA MB 231 shed vesicles.....81

Conclusions...105

References.....109

Introduction

"When a plant goes to seed, its seeds are carried in all directions; but they can only live and grow if they fall on congenial soil" (Paget, 1889).

This theory was elaborated for describing breast cancer invasiveness. Actually, tumor growth and metastasis are associated to an active cross talk between tumor and surrounding microenvironment. On this setting, the *"seed"* is represented by the initiating cancer cell while the *"soil"* corresponds to the stromal environment, composed by the extracellular matrix, fibroblasts, immune cells, endothelial cells and adipocytes. The interaction among all these components and the tumoral mass can promote tumor regression at the beginning while favors tumor feeding and immune escape to establish a suitable environment for tumor progression, later on.

Cell-cell and cell-matrix interactions can be induced by secreted growth factors, cytokines, chemokines, small molecular mediators (such as nucleotides, nitric oxide ions, bioactive lipids) and adhesion molecules. Recent observations suggest a mechanism by which cancer cells and surrounding stromal cells can exchange signals through a mutual release of micro-vesicles (MVs). In the last decade, the attention of the research has been focused on MVs as vehicle for horizontal transfer of informations among cells.

In vitro, numerous eukaryotic cell types, deriving from hematopoietic system - B and T lymphocytes, platelets, dendritic cells, mast cells, reticulocytes - as well as neurons, intestinal epithelial cells and especially tumor cells have shown to shed heterogeneous vesicle populations in the extracellular milieu. *In vivo*, their presence has been documented in several biological fluids, such as blood, urine or ascites from malignant effusions.

This phenomenon, observed in normal condition, increases in various pathologies and disorders, like a tumor condition. In 1969, Tarin was the first to report that membrane vesicles were released *in vivo* by murine breast carcinoma cells and bound to collagen fibers in areas where fibril degradation was observed (Vittorelli, 2003). *In vivo* MV shedding has been also documented in 1978, from spleen nodule and lymph node cultures of a patient affected by Hodgkin disease.

Later on, in 1980 Poste and Nicolson observed the malignant invasive properties conferred by shed extracellular vesicles to tumor cells cultured *in vitro*. These findings represented the basis for further studies on characteristics and functions of different origin vesicles.

Nowadays MVs are grouped in two main kinds: membrane vesicles and exosomes, that differ first for the dimensions. Membrane vesicle diameters range between 200 nm and 1 micron while exosomes are a more uniform population of smaller vesicles (20-80 nm diameter) with a characteristic cup-shaped morphology. The two vesicle populations are frequently collected together. However in some studies they are attempted to be separated and differences between them are appreciated.

MV transported molecules have been implicated in several mechanisms of cancer progression, such as neoangiogenesis, extracellular matrix remodeling and immune response modulation. Tumor released MV have the potential to alter the normal cell activity and to increase tumorigenicity, thereby promoting a suitable environment, stimulating cell migration and invasiveness (Castellana et al., 2009).

MVs and tumor progression

Tumor progression involves the transition from normal to malignant cells, through a series of cumulative alterations. During this process, cells acquire invasive and migratory properties, reaching and growing in tissues far from their origin. Loss of cellular adhesion, increased invasiveness, intravasation and survival in the vascular system, extravasation, survival and proliferation in a new site are all prerequisites for the establishment of distant metastases.

Host and tumor microenvironment play a central role in tumor progression and metastasis. Malignant cells do not exist in isolation but they are intimately connected to the cells of their microenvironment. Non tumor cells, such as endothelial cells, leukocytes, macrophages, fibroblasts, bone marrow-derived cells and other tissue components, including adipocytes and neural elements, are involved in every step of tumorigenesis (fig. 1). Actually, interactions between neoplastic cells and their microenvironment components orchestrate progression from *in situ* disease to invasion and metastasis. Some authors have proposed cancers as ecosystems operating in a complex manner between tumor cells and their microenvironment (Mareel et al., 2009). In this scheme, communication within the ecosystem between tumor cells, receptors, soluble mediators and resident and recruited host cells is critical, at both the primary site and metastatic *foci*.

Migration and metastasis in tumor cells are complex and involve levels of cooperation between subsets of disseminating cells. Single migrating cancer cells at the invasive front of a primary tumor create 'migration tracks' in the extracellular matrix, signposted with cell membrane adhesion molecules, such as the integrins (Kirfel et al. 2004). Such paths form a conduit for subsequent ranks of migrating tumor cells. Further cooperation between groups of disparate migrating cells can be seen at distant metastatic sites, thereby increasing metastatic efficiency (Mareel et al., 2009).

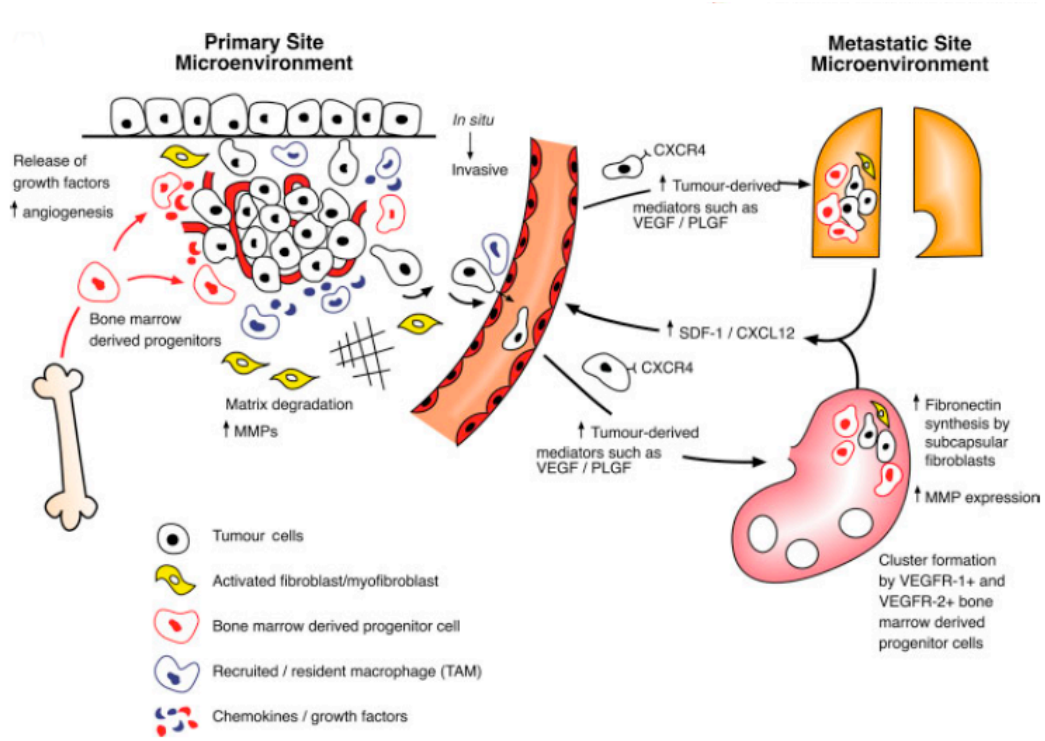

Fig. 1 Schematic representation of the microenvironment at the primary and metastatic sites. An ecosystem of host cell types, including bone marrow-derived progenitor cells, activated fibroblasts, tumour-associated macrophages (TAMs) and endothelial cells, interact with tumour cells at every step from in situ proliferation through invasion to intravasation and metastasis *(*Coghlin and Murray, *J Pathol 2010; 222: 1–15).*

In animal models of transplanted tumors, the site of implantation determines malignant behavior. Orthotopic transplantation produces aggressive and metastatic tumors, whereas ectopic transplants (i.e. in the subcutis) lead to more indolent growths (Mareel et al., 2009). This remarks that the reciprocal interplay between tumor cells and host microenvironmental elements is crucial.

The extracellular matrix (ECM) surrounding tumor cells not only acts as a barrier to invasion and migration but also functions as a repository for growth factors essential to malignant progression. Hydrolysis of matrix components by proteases such as metalloproteases (MMPs), cysteine cathepsins and serine proteases is largely, but not exclusively, carried out by tumor-recruited host cells, such as macrophages, endothelial cells and fibroblasts (Mareel et al., 2009). The concerted actions of a number of extracellular proteinases promote invasion and intravasation by several mechanisms, including disruption of tumor cell adhesion molecules and degradation of basement membranes and other matrix components.

Invasion of the extracellular matrix and migratory ability are closely linked, requiring coordinated expression of morphological changes in the tumor cell phenotype (including epithelial–mesenchymal transition) and activation of matrix proteases at the invasive front. Interaction of successive waves of tumor cells in an organized ‘class action’ may enable successful colonization of distant sites in a complex manner, with initial pioneering groups of migratory cells producing a favorable microenvironment, through release of MMPs and establishment of angiogenesis, for successive groups of less biologically invasive tumor cells (Mareel et al., 2009). Therefore it is not surprising that increased expression and activity of serine and metalloproteinases have been shown to be correlated with the metastatic behavior of tumor cells. In particular, MMP-2 and MMP-9 are thought to be involved in the invasive phenotype of tumor cells (Coussens and Werb, 1996).

In order to metastasize effectively, a solid tumor must first invade matrix and basement membranes and gain access to the lymphatic or vascular system. Highlighting the significance of MMPs in the tumor microenvironment, a recent study showed that alterations in MMPs and tissues inhibitors of matrix metalloproteinases (TIMPs) were a crucial event in early colorectal polyp cancers. Increases in MMPs 1, 2 and 3 and in TIMPs 1 and 2 were observed in carcinomatous epithelium compared with adenomatous or normal epithelium. In addition, MMP 7 (matrilysin) was expressed exclusively in carcinomatous epithelium (Jeffery et al. 2009).

The metastatic tropism of a given primary tumor may be also governed by specific tumor-derived chemokines which facilitate cellular alterations in target tissues, such as fibroblast activation and fibronectin synthesis. Tumor-derived soluble mediators act to mobilize progenitor cells from the bone marrow, causing them to migrate into, and prepare, specific pre-metastatic niches before the arrival of tumor cells. In turn, the nascent metastases, fueled by their niche interactions, may secrete factors which influence the primary tumor cell mass. This process constitutes a self-amplifying feedback loop, in which the primary tumor drives

metastasis, not only as a source of migrating malignant cells, but also as a chemokine producing factory, the output of which increases with tumor cell mass.

Into the metastatic multi-step process, one of the mechanisms responsible of host-tumor interaction is represented by vesicle shedding (fig. 2).

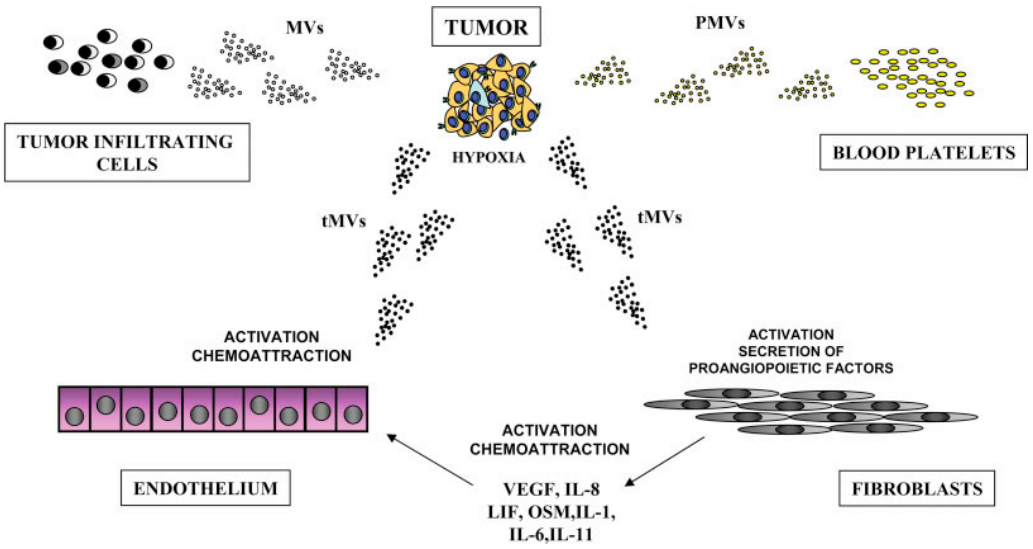

Figure 2 – Tumor microenvironment is enriched for biologically active MVs. MVs that are present in the tumor microenvironment are derived from several sources. Accordingly, MVs are shed by tumor cells themselves (tMVs), platelets activated by lung cancer expressed tissue factor (PMVs), and cancer infiltrating cell monocytes. The tMVs activate and chemoattract endothelial cells, induce secretion of several pro-angiopoietic factors by stroma fibroblasts, and activate bone osteolysis. Simultaneously, stroma fibroblasts stimulated by tMVs in turn affect tumor cells by enhancing their metastatic potential *(*Wysoczynski and Ratajczak, *Int. J. Cancer, 2009; 125: 1595–1603).*

Some researchers talk about a mixed population of different vesicle kinds, referred as microvesicles (MVs). Some others look at specific vesicle classes, namely membrane vesicles or rather exosomes. Herein both them will be mentioned, according to the authors' will.

In vivo MV shedding has been firstly documented in 1969, from murine breast carcinoma cells. Afterwards, the ability of those particles to cause horizontal transfer has been found. In 1980, Poste and Nicolson demonstrated that fusing membrane vesicles released by highly aggressive murine melanoma cells with less aggressive melanoma cells, the latter ones became able to metastatize to the lung.

These studies encouraged further investigations on vesicle involvement in tumor progression.

Dolo and coworkers reported that membrane vesicles, either shed *in vitro* by breast cancer cells or present in the pleural effusion of a breast carcinoma patient, carry tumor-associated antigens. So tumor markers detected in the circulation of carcinoma patients are, at least in part, carried by these structures (Dolo et al., 1995a).

Nowadays, molecule transferring mediated by vesicles to adjacent or remote cells is considered to influence several aspects of tumor progression, such as extracellular matrix remodeling, thrombosis, angiogenesis and immune response modulation.

Recently, EGFRvIII, oncogenic receptor found in a subgroup of aggressive gliomas, has demonstrated to be transferred in a population of non aggressive tumor cells, by micro-vesicles. As consequence, recipient cells show the activation of signaling pathways leading to morphological transformation and acquisition of a more aggressive phenotype, able to grow in anchorage non dependent way (Al-Nedawi et al. 2008). This report confirms and explains the observation reported in 1980 by Poste and Nicholson, described above.

MVs and extracellular matrix remodeling

Tumor microenvironment is highly enriched in MVs shed by tumor cells, platelets, monocytes and lymphocytes infiltrating the tumor tissue as well as stroma cells. Since fibroblasts represent the main constituents of the tumor stroma, attention of researchers has been focused on assessing the biological effects of tumor MVs on this cell type. Fibroblasts are associated with tumor cells and, when activated, are believed to play a central role in cancer migration and invasion (Kalluri et al., 2006). For example, human and murine lung cancer cells exposed to conditioned media, harvested from tumor MV affected stroma cells, show enhanced motility and higher metastatic potential in *in vivo* models. These findings suggest that some of the factors secreted by stroma cells may enhance the metastatic potential of lung cancer cells. On their own, lung cancer cells release vesicles activating stromal fibroblasts and endothelial cells (Wysoczynski and Ratajczak, 2009). In other studies, the activity of MVs obtained from two prostate carcinoma cell lines with different metastatic potentials has been tested. These MVs, as other tumor shed vesicles, are known to exhibit matrix metalloproteinases (MMP) and extracellular MMP inducer (EMMPRIN/CD147) at their surface, suggesting a role in extracellular matrix degradation. When they were added to fibroblast cultures, they were able, at first, to induce the activation of fibroblasts, assessed through extracellular signal-regulated kinase 1/2 (ERK1/2) phosphorylation and MMP-9 up-regulation, increased motility and resistance to apoptosis. On the other hand they promote MV shedding from activated fibroblasts able in turn to increase migration and invasion of highly metastatic prostatic cancer cells (fig. 3).

These findings strongly remark a mechanism of mutual communication attributable not only to soluble factors but also to determinants harbored by MVs, possibly contributing to the constitution of a favorable niche for cancer development (Castellana et al., 2009b).

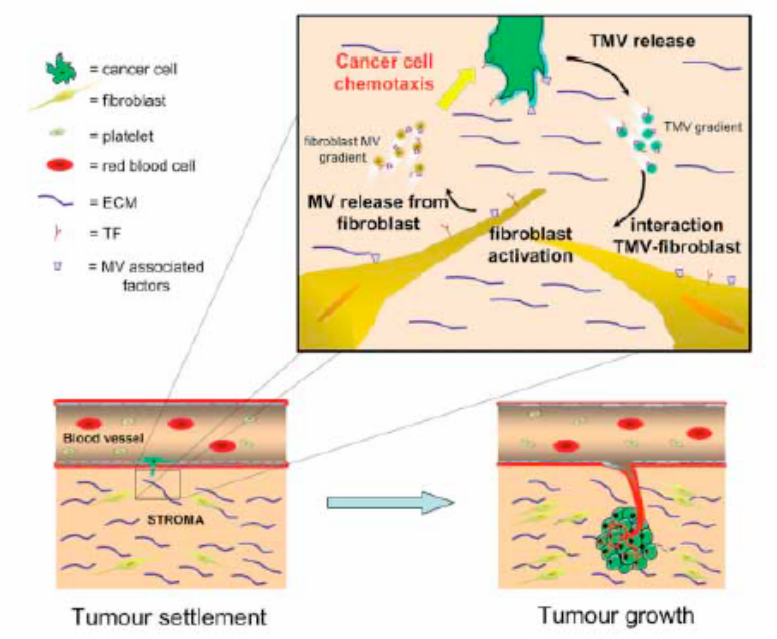

Fig. 3 Model for the role of procoagulant MVs in the intercellular communication between cancer cells and their local micro-environment: Extravasation is one of the early events in metastatic growth. After endothelial cells retraction, cancer cells interact with the perivascular stroma (bottom left). They can communicate with host cells, by soluble as well as MV associated factors. In this sense, MVs take part in a noxious circle between cancer and normal cells, amplifying the chemotaxis process (magnifi-cation scheme, upper right). Once induced to migrate, cancer cells settle within the new location, various events determining their fate. The establishment of a favourable environmental niche can lead to tumour growth (bottom right) (Castellana et al., *Hämostaseologie 2009; 29(1):51-7).*

A crucial cross-interaction has been found also between cancer cells and platelets. In particular, platelet derived MVs modulate metastatic potential of lung cancer cells by direct stimulation and by transferring platelet-derived integrins to the membranes of those cancer cells, thus efficiently facilitating interaction with the endothelium. As such, this enhances metastasis of cancer cells circulating in the peripheral blood (Wysoczynski and Ratajczak, 2009).

The large array of bioactive molecules incorporated into tumor-produced MVs prompts speculation that these structures might potentially play a paracrine role in shaping host environment. It is conceivable that in a small primary tumor, vesicular activity is locally restricted. Later, tumor-derived MVs may become systemic by distribution through the blood stream. In addition of becoming distributed, MVs may have to be taken by recipient cells in order to exert their biological effect. Phosphatidylserine (PS) or milk fat globule epidermal growth

factor eight (MGF-E8)/lactadherin carried by MVs are considered as “eat me” signal at the surface allowing uptake by appropriate cells via specific uptake mechanisms (Keller et al., 2009).

At molecular level, the action of MVs in the tumor microenvironment is due to several factors. Studies on exosomes present in ascites and blood of ovarian cancer patients showed that the protein cargos of exosomes differed from patient to patient and displayed proteinases responsible of ECM remodeling such as EMMPRIN/CD147 that plays a critical role in tumor progression and was identified before in membrane vesicles (Sidhu et al., 2004). The active form of the metalloproteinase ADAM10 and matrix degrading enzyme pro-heparanase have also been found in those exosomes. Gelatinolytic activity associated with exosomes is reported also from other research groups. In particular, Graves and coworkers found that vesicles from early *versus* late stage epithelial ovarian carcinomas were equally effective at stimulating invasion of ovarian cancer cells. This invasion stimulation was largely MMP and uPA dependent because blockage of these enzymes inhibited vesicle-stimulated invasion for all tested vesicles. Most vesicles contained active MMP-2 or MMP-9, which may facilitate cellular invasion through cleavage of ECM components and activation of other enzymes. In addition all tested vesicles contained active uPA which could lead to additional uPA activation, through a positive feed back loop, and could also promote MMP activation. Proteinase activation likely contributes to vesicle-stimulated invasion, because the combination of vesicles and cultured cells resulted in enhanced uPA activation. Although just as effective in stimulating invasion, vesicles from early stage cancers were less numerous than those from late-stage cancers. An increase in vesicle shedding with associated tumor volume may facilitate metastasis by providing larger quantities of invasion-stimulating membrane vesicles. Such vesicles were found to stimulate invasion of cultured ovarian cancer cells in a dose-dependent fashion, and therefore more vesicles would likely lead to greater invasive potential (Graves et al., 2004).

Also breast cancer cells shed *in vitro,* from selective membrane areas, vesicles enriched in MMP-2, MMP-9, MT1-MMP in association with β1 Integrin (Dolo et al., 1998). These findings suggest a model in which membrane vesicles can adhere to ECM components, through integrinic receptors, and release locally their proteolytic content favoring the action of MMPs on ECM, thus representing a way to interact with the microenvironment. The high proteolytic amount shared amongst vesicles of different origin could be beneficial for the growing tumor to modify its local environment in order to gain access to matrix-imbedded growth factors.

Studies on ovarian cancer membrane vesicles demonstrated that MVs and their proteolytic content can be useful as potential biomarkers for diagnosis and follow-up of the pathology. Actually, vesicles were found both in benign and tumor fluids. Vesicle amounts were however extremely low in endocystic fluids of ovarian serous cysts, relatively low in endocystic fluids of ovarian cyst of serous and mucinous cystoadenomas and in ascitic fluids of fibromas. They were definitely more elevated in ascitic fluids of malignant tumors. Among these ones, the very invasive ovarian carcinomas appeared to produce especially large amounts of vesicles. Regarding the gelatinolytic content, lytic activities were low or undetectable in vesicles recovered from serous cysts. However, all samples of vesicles obtained from other benign or malignant pathologies carried gelatinolytic activities corresponding to MMP-9 and to MMP-2. A significant correlation between the amount of vesicle-associated MMP-9 activity and the kind of pathology was not observed. On the contrary, the activity of vesicle-associated MMP-2 appeared to correlate with the malignancy of the pathologies (Ginestra et al. 1999), in agreement with previous studies reporting MMP-2 as the predominant gelatinolytic activity involved in ovarian cancer invasion and metastasis (Fishman et al. 1997). Similarly, in mammary cancer cells, the number and proteolytic activity of MVs correlate with their invasiveness *in vitro* (Ginestra et al., 1998). In particular, HT-1080 and MDA MB 231, that are the most invasive cells among the ones used in these studies, shed the maximal amounts of vesicles

both in serum-free and in complete media. 8701 BC and MCF 7 cells, less invasive, were found to shed lower amounts of vesicles. Serum usually stimulates vesicle shedding. However the most invasive cell lines shed vesicles containing proteolytic activities, although reduced, also in serum-free media. Under these conditions 8701 BC cells did not shed measurable amounts of vesicles and MCF 7 cells shed a small amount of vesicles which was almost devoid of proteolytic activity. MCF 10A, an immortalized epithelial breast cell line, did not release vesicles even if cultured in serum supplemented medium. Not only the amount, but also the kind of proteolytic enzymes carried by shed vesicles appeared to correlate with invasive potential of the cell. HT-1080 vesicles carry both MMP-2 and MMP-9 while MDA MB 231 vesicles were devoid of MMP-2 activity when shed in serum-free medium. Moreover, vesicles shed from both most aggressive cell lines contained uPA. Plasmin, once activated by vesicle-bound uPA, in turn activates progelatinases carried by vesicles; therefore the presence of uPA is such vesicles appear to have a central role in triggering the proteolytic cascade (Ginestra et al. 1998).

Cathepsin B is an acidic pH activated cysteine-protease. In a tumoral environment, where pH is typically acidic, cathepsin B can induce degradation of several ECM components - fibronectin, laminin, tenascin C and type IV collagen - directly or indirectly, by the activation of other proteolytic enzymes (MMPs, uPA) and degradation of MMP inhibitors. Cathepsin B has also found to be transported by tumor vesicles in the tumor environment, where it could play a key role in ECM degradation and angiogenesis (Giusti et al. 2008).

Taken all together, these data show that tumor shed MVs carry several proteases degrading extracellular matrix components, thus opening the way to cancer cells. In this perspective, MVs become crucial in ECM modification, essential aspect of tumor growth and metastasis.

MVs and thrombosis

Another feature of tumor progression is represented by hypercoagulability, that has been documented in virtually all kind of cancers and is the second leading cause of death in cancer patients. Activation of the coagulation system generates thrombin and promotes the formation and subsequent deposition in blood vessels of fibrin, thereby generating a process of disseminated intravascular coagulation, which is partially controlled by the fibrinolytic system. Tumor vesicles shed *in vivo* have been frequently associated with a network of fibrin fibers (Castellana et al., 2009b). The observed association between vesicles and fibrin fibers raises the possibility that vesicles contain some procoagulant activities that account for the fibrin deposition associated with many types of malignancy. The association between vesicles and fibrin fibers had been so far reported for ascitic fluids of ovarian carcinoma (Dolo et al., 1999). More recently, procoagulant activity of vesicles has been proved. Proteins that regulate the fibrinolytic system, plasminogen activators such as u-PA are shown to be enriched in tumor derived vesicles, thus becoming involved in tissue remodeling and proliferation. Moreover, the presence of MVs carrying Tissue Factor (TF) in venous blood of cancer patient has been correlated with the pathogenicity of cancer. In giant-cell carcinoma patients, high amounts of TF positive tMVs strictly associate with a hypercoagulable state. Coagulation activation is also attributable to anionic phospholipids, especially phosphatydilseryne (PS). Surface-exposed PS strongly propagates the coagulation process by facilitating the assembly and activation of tenase and prothrombinase complexes. In particular, accessible PS at the MV surface is an important cofactor for TF activity, providing the indispensable negatively charged surface and promoting thrombin generation (Castellana et al., 2009b). The pool of TF enriched tMVs probably interacts with platelets, endothelial as well as stromal cells producing local blood coagulation and thrombosis. In venous blood, MVs from different origins are subjected to ligand-receptor interactions or mechanisms of membrane fusion, allowing mixture of

antigens and modulation of their functionality. It is still unclear whether MVs present in plasma of cancer patients derive exclusively from cancer cells, but it is largely accepted that even if these MV are secreted by monocytes, endothelial cells, platelets or stromal cells, the shedding is influenced by the presence of the tumor itself. In the context of tumor microenvironment, tMVs are able to promote TF activity and PS externalization, one of the hallmarks of cellular activation, on normal fibroblasts (Castellana et al., 2009b). Due to high permeability of tumor microenvironment, coagulation factors normally sequestered in the vascular compartment, could diffuse within the stroma and initiate a coagulation process mimicking the thrombotic lesions observed in the atherosclerotic plaques. In this regard, tMVs may contribute to promote and amplify the pathogenicity of cancer, linking thrombotic complications and tumor malignancy.

MVs and angiogenesis

Angiogenesis, the formation of new blood vessels from preexisting ones, occurs through activation and proliferation of endothelial cells. In physiological processes, angiogenesis is finely tuned by a balance of stimulatory and inhibitory factors. However, persistent and unregulated growth of new capillaries is crucial for sustained tumor growth, because it allows oxygenation and nutrient perfusion to the tumor as well as removal of waste. Furthermore tumor-associated angiogenesis provides conduits into the tumor for circulating host cells and allow egress into the circulation of disseminating cancer cells. The expression of pro-angiogenic factors such as VEGF by solid tumors correlates with a poor prognosis and metastatic propensity (Mareel et al., 2009). Successful colonization of distant sites by tumor cells is dependent on their survival within the circulatory system.

It is believed that tumor and stromal cells secrete angiogenic factors such as vascular endothelial growth factor (VEGF) and basic fibroblast growth factor (bFGF), thus favoring tumor associated angiogenesis.

Growing evidence suggests that MVs also possess angiogenic activities; in particular, tumor derived MVs seem to stimulate secretion of pro-angiogenic factors in stromal cells and induce endothelial cell proliferation (Coghlin and Murray, 2010). Matrix reorganization from endothelial cells - process facilitated by matrix degrading proteases - is crucial for vascularization in both normal and pathological condition. Taraboletti and coworkers demonstrated that endothelium derived MVs contain MMP, like MMP2, MMP9 and MT1-MMP, facilitating autocrine stimulation of endothelial cells in Matrigel invasion (Taraboletti et al. 2002). The same group showed also that ovarian cancer MVs vehicle VEGF and MMP, stimulating endothelial cell motility and invasiveness, *in vitro* (Taraboletti et al. 2006).

Tumor MVs can make active endothelial cells by delivering glycoproteins involved in protein-protein interactions and catalysis. CD147/Basigin/EMMPRIN is a membrane-spanning molecule highly expressed in tumor cells and one of the

promising actors implicated in this kind of transcellular protein activation. Over a role in ECM degradation, mentioned in the section “MVs and extracellular matrix remodeling”, EMMPRIN may be involved in promoting neo-angiogenesis, as documented by Millimaggi and colleagues. In fact, tMVs can induce an angiogenic phenotype in HUVEC endothelial cells *in vitro* and this event is strictly correlated with the relative EMMPRIN enrichment of tMV (Millimaggi et al., 2007). As well as tMV, platelet MVs (pMVs) can also support angiogenesis in lung cancer, *in vitro*. They stimulate the expression of pro-angiogenic factors like MMP-9, MT1-MMP, VEGF, IL-8, or hepatocyte growth factor (HGF) and support adhesion of lung carcinoma cells to fibrinogen. In addition, they transfer CD41, a platelet specific glycoprotein corresponding to α chain integrin subunit, to the cancer cell plasma membrane, stimulate their proliferation, show chemoattractant capacity and induce phosphorylation of MAP kinases. Importantly, pMVs stimulate lung carcinoma cells in their metastatic spread to the lung (Janowska-Wieczorek et al. 2005).

Although it is not clear which is the primary signal inducing platelet activation and subsequent pMV shedding, reported data indicate a strong link between the coagulation system and metastatic spreading and growth. Moreover, high plasmatic levels of pMVs in association with VEGF, IL-6 and RANTES were detected among patients with gastric cancer, suggesting that the presence of high plasmatic levels of PMV could be a predictive marker for metastastic lesions (Kim et al., 2003). Developmental endothelial locus-1 (DEL-1) has been found on MVs shed from mesothelioma cells that can act as a strong proangiogenic factor and promote vascular development in the tumor neighborhood (Hegmans et al., 2004).

Addition of hepatic carcinoma vesicles to endothelial cells stimulated chemotaxis and uPA production, through a bFGF-2 mediated mechanism (Taverna et al., 2003).

In three dimensional systems of co-cultures with neurons and astrocytes, endothelial cells became able to organize a barrier with properties similar to the

hematoencephalic barrier. In those experiments, the different cell lines were not in physical contact, thereby endothelium behavior can be modulated by only neuronal secreted factors. Actually, neurons produce either VEGF or FGF, modulating endothelial cell growth and differentiation and inducing the formation of such a barrier. Experimental evidences indicate that those factors are released by neurons, at least in part, by MVs (Schiera et al., 2007).

It has also been demonstrated that tMVs vehicle factors to endothelial cells. In particular, MVs produced by cancer cells expressing a mutant active form of EGFR vehicle this receptor to endothelial cells, inducing in the target cell the expression of VEGF and his receptor, VEGFR (Al-Nedawi et al. 2009).

MV transported lipids can also interfere with cell migration and angiogenesis. For example, sphingomyelin, that is a component of cell membrane, has found to be enriched in membrane vesicles and it confers migratory properties to endothelial cells (Kim et al. 2002). Rigogliuso et al. reported that hepatic carcinoma vesicles can carry CDase and Sph-K1, that are enzymes responsible of sphingosine-1 phosphate synthesis. Moreover, they demonstrated that those vesicles can be incorporated into endothelial cells (fig. 4). Experimental evidences suggested that CDase and Sph-K1 are transferred inside the recipient cells, probably by vesicle endocytosis, and exert profound angiogenic effects, promoting endothelium survival and proliferation (Rigogliuso et al., 2010).

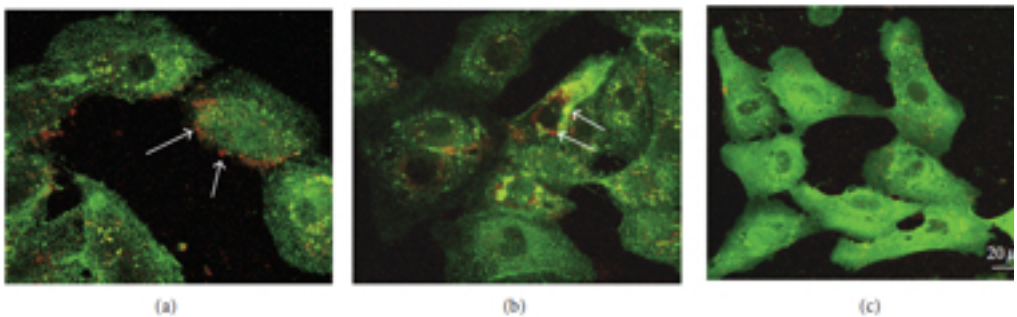

Fig. 4: Interactions of shed vesicles with endothelial cells. Vesicles shed by SK-Hep1 cells, labelled with lipid styryl dye FM4-64 (red fluorescence), were added to GM7373 endothelial cells in which β1 Integrin was stained using FITC-conjugated secondary antibodies (green fluorescence). Cells were incubated with vesicles, respectively, for (a) 10 min, (b) 20 min, and (c) 30 min. The arrows indicate vesicle localization (Rigogliuso et al., *J. Oncol. 2010)*.

Recent studies have shown that human cancer cells release vesicles containing ADAM10, a disintegrin and metalloproteinase, and L1, a type 1 membrane glycoproteine that is overexpressed in many types of carcinoma. ADAM10 cleaves L1, which in turn stimulates *in vitro* and *in vivo* angiogenesis via the activation of endothelial αvβ3 integrin and promotes migration, invasion and growth of tumor cells. ADAM10 itself has also angiogenic activity, suggesting that MVs containing ADAM10 should be involved in tumor related angiogenesis (Choi et al., 2007).

The transmembrane glycoprotein CD8 promotes tumor growth via the induction of systemic angiogenesis and its expression is associated with poor prognoses in patients with gastrointestinal cancer. CD-8 containing vesicles derived from rat pancreatic adenocarcinoma cells strongly induce angiogenesis, both *in vivo* and *in vitro*. In colon-rectal and pancreatic cancer, the expression of CD8 is up-regulated in tumor cells, suggesting that the presence of CD-8 on MVs could serve also as diagnostic marker for these cancers (Choi et al., 2007).

Angiogenic effects are also induced by horizontal transfer of mRNAs and miRNAs through vesicles shed by tumor glioblastoma cells and taken up by endothelial cells (Skog et al. 2008).

Tumor MVs directly chemoattract endothelial cells and activate phosphorylation of MAPKp42/44 and AKT. Moreover, endothelial cells stimulated by tMVs secrete more IL-8 and increase expression of the adhesion molecules iCAM and vCAM. This fact, in connection to increased secretion of tMVs during hypoxia, provides evidence that pro-angiopoietic tMVs should be considered as one of the main actors in tumor neo-vascularization. Thus, a more complex network of mutual pro-angiopoietic interactions is emerging in which tMVs play an important and under appreciated role (Wysoczynski and Ratajczak, 2009).

Tumor MVs may increase angiogenesis indirectly by activating stroma cells. Accordingly, experimental evidences provide that tMVs induce expression of several pro-angiopoietic factors in stromal cells such as IL-8, VEGF, LIF, OSM,

IL-11 and MMP-9 (Wysoczynski and Ratajczak, 2009). These data, taken all together, remark that vesicular components such as sphingomyelin, EMMPRIN, CD-8, VEGF, bFGF are likely involved in MV mediated neovascularization. On this basis, the presence of pro-angiopoietic tMVs in the tumor microenvironment should be considered while developing more effective anti-angiopoietic therapeutics.

MV mediated tumor-immune system interaction

In the initial phases of tumor progression, the immune system acts to block the growth. Nevertheless, during progression tumor cells can develop mechanisms of immune escape. Cancer cells are believed to mould microenvironment components and affect the immune system mainly by pathways involving cell-to-cell contacts and the release of suppressive soluble factors. Moreover, tumors are able to successfully mask their immunogenic profile losing surface antigens and become invisible to immune cells.

In the scenery of cancer elusion from immune system, shed MVs play a key role as immune-suppressors (fig. 5). Actually, B-lymphocytes, T-lymphocytes, and antigen-presenting cells such as dendritic cells are important participants of the anti-tumoral immune response, and are all known to produce exosomes.

Experimental evidences show that systemic application of patients derived exosomes can promote the growth of human xenografted carcinoma in mice. By the way, these exosomes do not significantly affect cell proliferation *in vitro*, suggesting that such a function might be due to an immune modulation, rather then a direct growth promoting effect (Keller et al., 2009).

Andre and colleagues reported the purification of exosomes from cancerous ascitic fluid and demonstrated the induction of a specific anti-tumoral response by autologous exosome-loaded dendritic cells (DCs) (Andre et al., 2002). This study confirms that exosomes are secreted in human malignant ascites effusion and demonstrated that exosomes have the capacity to transfer specific tumoral antigens to DCs, inducing a specific antitumoral response. Tumor shed vesicles have been reported also to be recognized by immune cells, thus working as bait for tumor escape from immune system.

Several researchers, independently working on this field, reported a T lymphocyte cytotoxicity exerted by tumor derived MVs. First vesicles shed from breast tumor cells were shown to inhibit lymphocyte proliferation, *in vitro*. In particular, after addition of breast cancer membrane vesicles (released by 8701-BC and MCF-7cell lines) to peripheral blood lymphocytes, a strong and dose

dependent inhibition of the lymphocyte capability to incorporate 3H-thymidine was observed. The inhibitory effect was found to be specifically associated with the immune suppressing cytokine TGF-β1 that is transported by those vesicles. According to this model, TGF-β1 could be specifically delivered to lymphocytes which react with HLA positive vesicles, thus having as main effect the blocking of lymphocyte growth (Dolo et al., 1995b).

Moreover, MVs were shown to vehicle some tumor-associated antigens (TSAs) in association with HLA class I molecules (Dolo et al. 1995a). T lymphocytes, by specifically recognizing TSAs, adhere to tumor membrane vesicles. Such an interaction may result in the inhibition of proliferation of anti-TSA lymphocytes (Dolo et al., 1998).

Recent evidences confirm a role of MVs in T cell cytotoxicity. MVs derived from several human tumors, including melanoma and colorectal carcinoma, are found to carry Fas-ligand (FasL) and Tumor Necrosis Factor related apoptosis inducing ligand (TRAIL), thus triggering apoptosis of cytotoxic T lymphocytes expressing the death receptors. This action is believed to increase the possibility of tumor cells to escape from the immune system (Andreola et al., 2002; Kim et al., 2005). The induction of apoptosis and T cell receptor (TCR) alterations in effector T cells could be reproduced with MV isolated from plasma of cancer patients, thus helping to explain the high frequency of apoptotic lymphocytes that are often found in the peripheral circulation of these patients (Taylor et al., 2005). Definitively MVs may represent a mechanism by which cancer cells elude infiltrating lymphocytes (Wysoczynski and Ratajczak, 2009). This hypothesis appears to be in contrast with the initial evidence of immunogenicity (Vittorelli, 2003). Hence, only *in vivo* studies focused on evaluating how cancer cell released vesicles affect immune functions could clarify the role these micro-vesicles play in tumor immunity (Iero et al., 2008).

Natural killer cells are not spared from these negative influences, as they lose their cytolytic potential through the down-modulation of perforin expression, upon contact with tMVs (Liu et al. 2006).

Due to their antigenic profile, MVs can affect immune cell behavior. On the one hand, tMVs can modulate monocyte cytotoxicity through the transfer of CCR6 and CD44v7/8 antigens to monocytes, exerting antiapoptotic effect and activating AKT kinase, starter of survival pathways (Baj-Krzyworzeka et al., 2006). Moreover, tMV-treated monocytes showed an increased anti-tumor activity in regard of the enhanced cytotoxicity against tumor cells *in vitro* (Baj-Krzyworzeka et al., 2007). On the other hand, in the context of tumor escape, tMV retain a large part of the protein repertoire of the producing cells, including molecules involved in immune suppression and deviation, producing additional effects on antitumor immune responses. Indeed, crucial components of the immune response, such as antigen presenting cells, are profoundly affected by the encounter with tMVs. These MVs not only impair the capacity of circulating CD14+ monocytes to differentiate into functional dendritic cells, but they also skew the differentiation of these cells towards altered CD14+ monocytes expressing low or absent levels of HLA class II histocompatibility molecules (Iero et al., 2008). These cells, present in relatively high numbers among peripheral blood mononuclear cells of melanoma patients, exert suppressive activity on lymphocyte proliferation and impair the expression of effector molecules (such as perforin and α-IFN) in a TGF-β1-mediated fashion. Eventually, immunosuppressive effects of tMV could potentially be exerted at least on two distinct steps of the process. First, during cross-priming by dendritic cells, with the impaired differentiation of monocytes into dendritic cells, and second, at T cell level, where myeloid suppressor cells release TGF-ß, blocking proliferation and effector functions, and with the induction of apoptosis in activated cells (Valenti et al., 2006).

Generally, horizontal transfer mediated by vesicles can convert immune cells in altered phenotypes, thus helping the cancer evasion from immune surveillance. Moreover, cancer cells can fuse with MVs derived from non cancer cells, masking their tumoral phenotype behind lipids and proteins typical of non transformed cells.

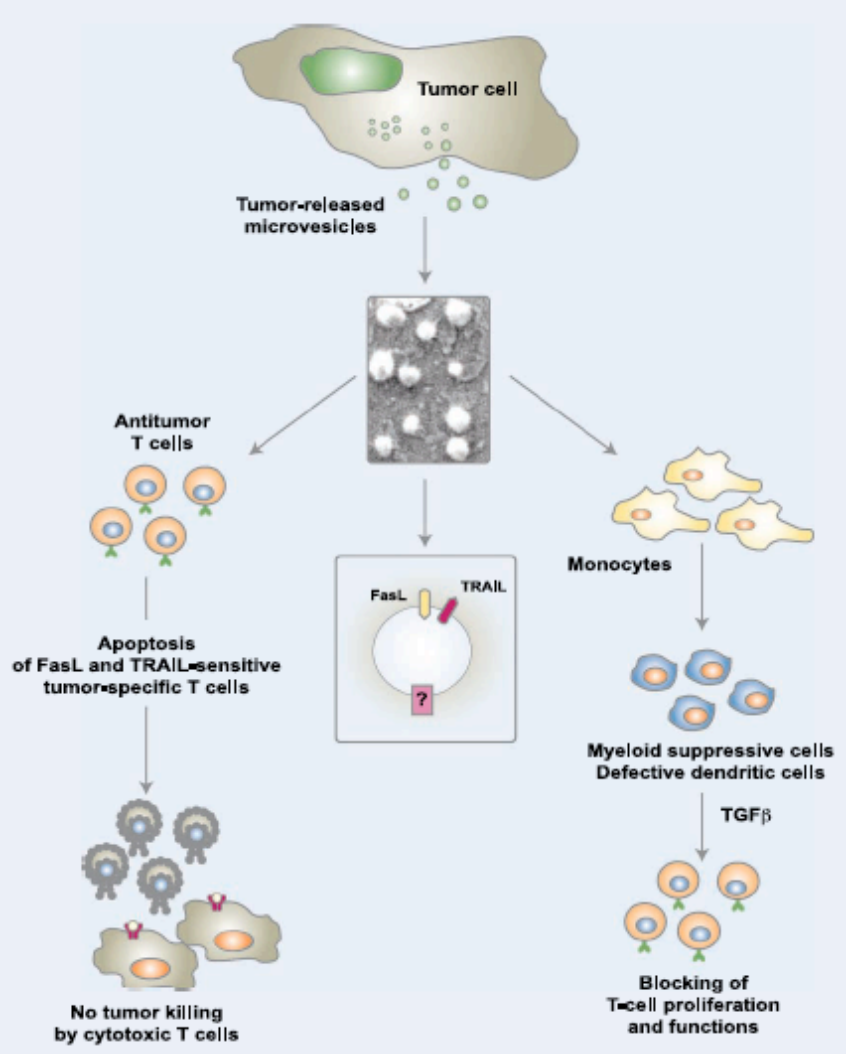

Fig. 5. Immuno-suppressive pathways mediated by tumor-released microvesicles. Tumor cells release microvesicular organelles (also known as exosomes) that express a large array of bioactive molecules. Through FasL and TRAIL, these vesicles can induce apoptosis in activated antitumor T cells, abrogating the potential of these effectors to kill tumor cells. By mechanisms still under investigation, the same vesicles can skew monocyte differentiation into myeloid suppressive cells, exerting inhibitory activity on T cell proliferation and functions through TGFh secretion. Switching off T cell responses at upstream levels (i.e., by affecting cross-priming by antigen-presenting cells) as well as downstream levels (i.e., by eliminating antitumor effector cells) would be expected to efficiently abrogate antitumor immune potential (Valenti et al., *Cancer Res. 2007; 67, 2912-2915*).

Clinical studies involving MVs

In cancer patients, serum levels of MVs are both significantly elevated and positively correlated with malignancy, suggesting that they could serve as important diagnostic indicators for cancer (Ginestra et al., 1999). So MVs from tumor patients' blood and ascites could become a source of material for clinical testing.

Indeed MVs are promising in clinical applications for disparate purposes. First they are shown to vehicle molecules closely associated to affected cells, such that they can be studied to identify new tumor markers. In addition, tumor surface antigens MV-harbored could be used to stimulate immunological responses against tumor growth. Vesicle shedding may represent also a drug efflux mechanism through which anticancer drugs (i.e. doxorubicin) are discarded by tumor cells, thereby developing drug resistance (Shedden et al., 2003). These observations suggest that inhibition of vesicle secretion and uptake as well as modulation of MV function may represent important new targets for therapeutical intervention.

The initial identification of MVs released by tumor cells was envisaged as the discovery of a new cell-free source of tumor antigens for *in vivo* immune priming or tumor vaccine design. Indeed, MVs are close replicas of the originating cells for selected protein content and they express a large array of tumor antigens when secreted by neoplastic cells. To name a few examples, melanoma-derived exosomes contain the highly immunogenic antigens MelanA/Mart-1 and gp100, those released by colon carcinoma cells express carcino-embryogenic antigen (CEA) and Human Epidermal Growth Factor Receptor-2 (HER2), which can be detected also in vesicles secreted by breast carcinoma (Andre et al., 2002).

Antigenic content is not only a feature of *in vitro* released MVs, but it can also be found in MVs isolated from plasma of cancer patients. Proteomic analysis proved definitively that exosomes of different cell origin are commonly enriched in several members of the heat shock protein family (Hsp) which are known to

favor antigen presenting cell (APC) activation through delivery of danger signals (Mears et al., 2004). These findings inspired vaccination studies in animal models, which pointed at tumor-derived exosomes as an antigenic source for T-cell priming, while *ex vivo* experiments in cancer patients were performed to demonstrate the ability of exosomes purified from ascitic fluids, to generate anti-tumor T cells when cross-presented by autologous dendritic cells (Andre et al., 2002).

MVs could be used, more generally, as physiological vehicle for molecule distribution to the cells. For example, healthy blood cell shed MVs are proposed to transfer CD5 and CD59 to erythrocytes in hemoglobinuria affected patients, lacking these proteins. Moreover, MVs could help the setting of cells in the new post-transplant environment. Eventually, tumor MVs can be used to support immune response against tumor or, on the contrary, to induce tolerance of new implanted organs.

Solid tumors are spontaneously infiltrated by T lymphocytes. Among them, memory effector cells are responsible of clinical outcome while regulator T cells compromise long term survival. This led to identification of tumor associated antigens able to develop immune responses and useful as vaccines in cancer immunotherapy. Recently, great interest has been developed in using exosomes as potential vaccines, especially dendritic cell derived exosomes that are useful as antigen presenting entities. Clinical studies based on exosomes have been applied to patients affected by lung carcinoma and melanoma. Phase I clinical trials showed that injection with dendritic cell shed exosomes is safe and associated with regression in some cases and long term stabilization. These studies revealed also that injected exosomes increase the levels of circulating “Natural-Killer” cells and NK group 2 dependent functions in the majority of patients (Viaud et al., 2009).

By the way, a risk factor in isolating exosomes is represented by possible retroviral contaminations. For example, exosomes and HIV-1 particles have similar biophysical properties such as size and density and both of them are able

to activate immune cells. Recent strategies of purification, adopting immune-affinity capture in combination with density gradient ultracentrifugation, led to obtain virus-free hemopoietic cell shed exosomes (Cantin et al., 2008).

Circulating EpCAM positive exosomes have been isolated from serum in patients affected by early stage ovarian cancer. Firstly, plasmatic levels of exosomes are increased in patients with more advanced stage disease. miRNA profiling indicates a potential use of exosomes as diagnostic markers in characterizing biopsy profile and identifying asyntomatic populations (Taylor et al., 2008).

Exosomal preparations from human malignant pleural effusions may contain also immunoglobulins and complement proteins that do not belong really to the exosomal fractions but they are co-isolated by the usual purification methods (Bard et al., 2004). Therefore the use of such exosomes may have deleterious consequences, especially in the case of heterologous cross-utilization. Induction of polyantigenic immune responses targeted to noncancer proteins could be not only responsible for a decrease of the anti-tumoral effect of the vaccine but could also induce an autoimmune response potentially dangerous to the patient. Although the use of exosomes as antigen source for cancer immunotherapy is promising, the risk of presence of contaminating proteins must be taken into account before their *in vivo* use can be generalized.

Increased levels of exosomes in plasma or in malignant effusions belonging to cancer patients underline their importance as possible source of diagnostic markers. Another possible obstacle in such body fluid based exosome analysis is the presence of contaminating exosomes secreted by normal cells (e.g., normal colon cells as compared to colon cancer cells) and other cell types (e.g., non colon cell types).

To better understand the molecular properties of disease cell derived exosomes, such exosomes need to be isolated free of normal cell-derived exosomes from the complex mixture in blood. Purification strategies that discriminate between complex exosome mixtures in blood could be aided by the knowledge of exosome

tissue-specific signatures, especially disease cell signature (Mathivanan et al., 2010).

MVs: structure and biogenesis

Vesicle shedding is a physiological phenomenon associated with cell growth. Cells with higher growth rate release a major amount of vesicles, in comparison with slowly growing cells. Generally, the release increases upon cell activation, hypoxia, irradiation and oxidative stress. Shedding is an energy-requiring mechanism that is known to be associated with several events such as increase of cytosolic calcium and degradation of membrane cytoskeleton. Moreover, there is an increase in phospholipid movement inside the membrane bilayer, that brings to a perturbation of the lipid asymmetry with the consequent shift of phosphatidylserine to the external membrane leaf-left and the segregation of proteins to the lipid rafts (fig. 6).

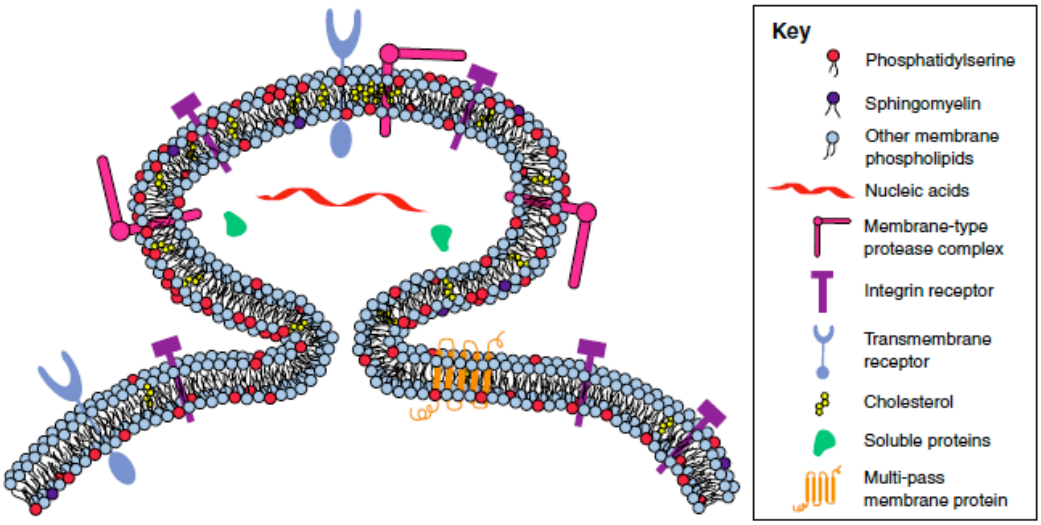

Fig. 6 Microvesicle shedding. Microvesicles are formed by the outward budding of the plasma membrane, as shown. Not all plasma-membrane proteins are incorporated into shed vesicles, although the topology of membrane proteins remains intact. Membrane proteins such as oncogene and other growth-factor receptors, intergrin receptors and MHC class I molecules, soluble proteins such as proteases and cytokines, as well as nucleic acids, have been found in microvesicles. Microvesicles appear to be enriched in some lipids such as cholesterol, whereas phosphatidylserine is relocated to the outer membrane leaflet specifically at sites of microvesicle shedding *(*Muralidharan-Chari et al., *J. Cell Science 2010; 123, 1603-1611).*

MVs represent an unconventional exocytosis mechanism for numerous proteins, secreted in the extracellular space but lacking the classical signal peptide sequence that usually is recognized by endoplasmic reticulum-Golgi secretion system (fig. 7). For example, although galectins lack conventional signal sequences, they reach the cell surface and bind to glycoconjugates on the plasma membrane and in the extracellular matrix. Actually galectins are suggested to be vehicled by vesicles (Nickel et al., 2003). The literature is not unique in considering the route of release for some proteins. In particular, bFGF-2, that is a secreted factor lacking the signal peptide, has been found in extracellular vesicles shed by tumor cells (Taverna et al., 2003). Nevertheless other authors demonstrated that FGF-2 reaches the extracellular space by direct translocation across the plasma membrane (Nickel et al., 2003).

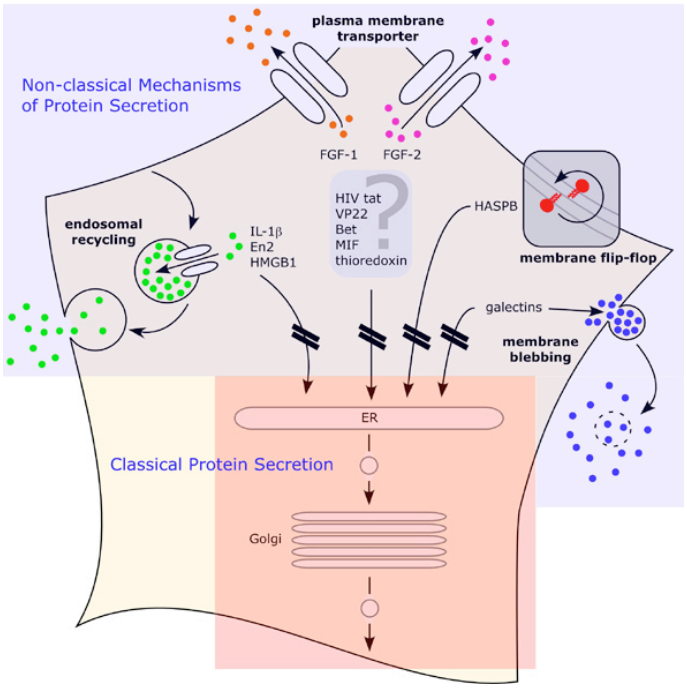

Fig. 7 Cargo proteins and potential export routes of unconventional protein secretion. At least four distinct types of nonclassical export can be distinguished. For some proteins (i. e. IL-1b, En2 and HMGB1) export involves import into intracellular vesicles, which are probably endosomal subcompartments. FGF-1 and FGF-2 probably reach the extracellular space by direct translocation across the plasma membrane, but they apparently use distinct transport systems. In other cases (i. e. Haspb) a flip-flop mechanism is required to locate theprotein in the outer leaflet of the plasma membrane. The final postulated pathway of unconventional protein secretion involves the formation of exosomes, vesicles that form on the outer surface of the cell in a process known as membrane blebbing. Exosomes are labile structures that release their contents into the extracellular space. It has been suggested that this pathway may be used by the galectins *(*Nickel, *Eur. J. Biochem. 2003; 270(10):2109-2119).*

MVs are mainly classified in two kinds: membrane vesicles and exosomes, that differ firstly for the dimensions (fig. 8A). Membrane vesicles are heterogeneous in size, with diameter ranging between 200 nm and more than 1 micron, while exosomes are a more uniform population of smaller vesicles (20-80 nm diameter) with a characteristic cup-shaped morphology. This distinction concerns also the mechanism of biogenesis and release (fig. 10A). Exosomes are intracellularly generated, from inward budding of the limiting membrane of late endosomal compartments, and they form intra-luminal vesicles (ILVs) inside structures known as multivesicular bodies (MVBs). Afterwards, MVBs can fuse with the plasmatic membrane, releasing their content - namely exosomes - into the extracellular space (van Niel et al., 2006).

Caby and collaborators reported the presence of exosomes in the blood of healthy donors and they were able to collect those particles by differential centrifugation or, in alternative, immuno-capture mediated by anti-CD63 antibody bound latex beads (Caby et al. 2005).

Membrane vesicles are so called because they are shed directly from the plasma membrane by a fission event, similar to the cytokinesis. This mechanism is similar to the events associated with virus budding (Cocucci et al., 2009). As in the case of virus budding during the propagation of viral infection, vesicle shedding is more evident along the microvilli and along free margins of the cell surface. Such events are reasonably associated with having specific biological roles in the cell surrounded by extracellular matrix (Dolo et al., 1998).

Structural similarities are found also between membrane vesicles and apoptotic bodies. Nevertheless, membrane vesicles do not contain neither nuclear nor cytosolic organelles, that are enriched in apoptotic blebs (Taylor et al. 2008) (fig. 8B). Indeed purified MVs lack endoplasmic reticulum proteins such as calnexin and the mitochondrial protein cytochrome C (Mears et al., 2004). These properties lead to discriminate easily among MVs and apoptotic vesicles, by using specific nuclear or organelle markers.

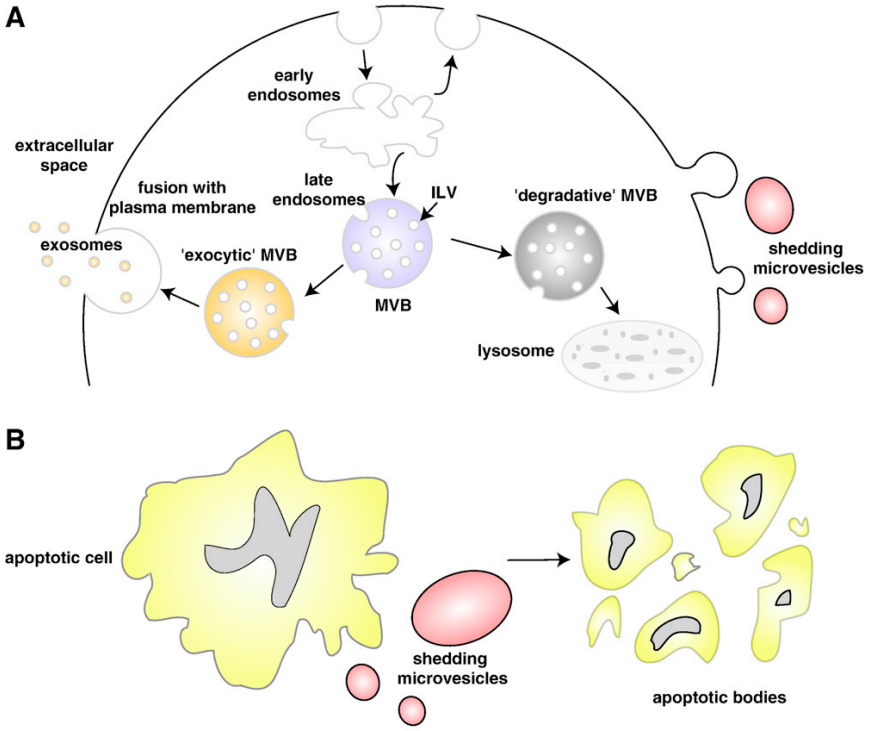

Fig. 8 – Scheme of the release of extracellular membranous microvesicles into the extracellular space. A, Release of exosomes and SMVs is shown. In early endosomes, proteins are either recycled to the PM or sequested in ILVs of the larger MVBs. ILVs of MVBs are generated by budding from the limiting membrane into the lumen of endosomes. Owing to the biophysical properties, MVBs either can be degradative (evolving into lysosomes) regulated by ESCRT or ubiquitination or can be exocytic (i.e., fuse with PM with sub sequel release of their contents— exosomes). SMVs are released by the process of blebbing or shedding from the PM.

B, Apoptotic or dying cells with cell shrinkage, a hallmark of apoptosis, leads in generation of ABs. These vesicles are remnants of the degrading apoptotic cell with nuclear and cytoplasmic content *(*Mathivanan et al., *J. Proteom. 2010; 73: 1907–1920).*

It is known that different cells can produce both membrane vesicles and exosomes. In a landmark paper, Heijnen et al. described the characteristics of these two types of vesicles released by platelets (Heijnen et al., 1999). When activated with a thrombin receptor agonist, platelets release two distinct populations of vesicles. The first, corresponding to exosomes, were sized between 40 and 100nm, bound annexin V poorly and were enriched in the tetraspannin protein CD 63 - known to be marker for late endocytic and multi-vesicular compartments. The relatively low number of exosomes that bound annexin-V suggests that the outer leaflet of platelet exosomes is probably not enriched in phosphatidylserine. The second vesicle type, being shed from the cell surface, were sized between 100 and 1000 nm, expressed many plasma membrane

glycoproteins and bound annexin V, readily indicated an enrichment in phosphatidylserine (PS).

Interestingly, the properties of the two types of vesicles also differed; for instance, exosomes did not allow the prothrombinase complex to form, whereas factor X and prothrombin were found to bind the membrane vesicle associated PS. These distinctions were taken up by many authors. The presence of only trace amounts of PS on exosomes of reticulocytes had already been observed by Johnstone (Heijnen et al., 1999). Though more recent studies have shown the presence of PS on specific tumor and other exosomes (Al-Nedawi et al., 2009; Keller et al., 2009).

In the literature, various mechanisms of MVs modulating cell target activity are described. Firstly, MVs can vehicle membrane proteins interacting with the cell target in juxtacrine manner. Similarly, vesicle membrane proteins can be activated by proteolytic cleavage and the sub sequel fragment can acts as ligand for a cell surface receptor. Moreover, MVs can fuse directly with the cell target, bringing to a RNA, protein non selective transferring. This fusion could alter some properties of the cell target (fig. 9).

For what concerns the function, it has not been completely clarified if the two mentioned classes of vesicles play the same or different roles, i*n vivo*. At the beginning, membrane vesicles were considered to be involved in several tumor progression aspects, such as extracellular matrix degradation, angiogenesis and immune response escape. Exosomes, instead, were believed to be active promoters of immune response against tumor progression (Vittorelli, 2003). In the last decade, experimental evidences showed that exosomes can also promote tumor progression.

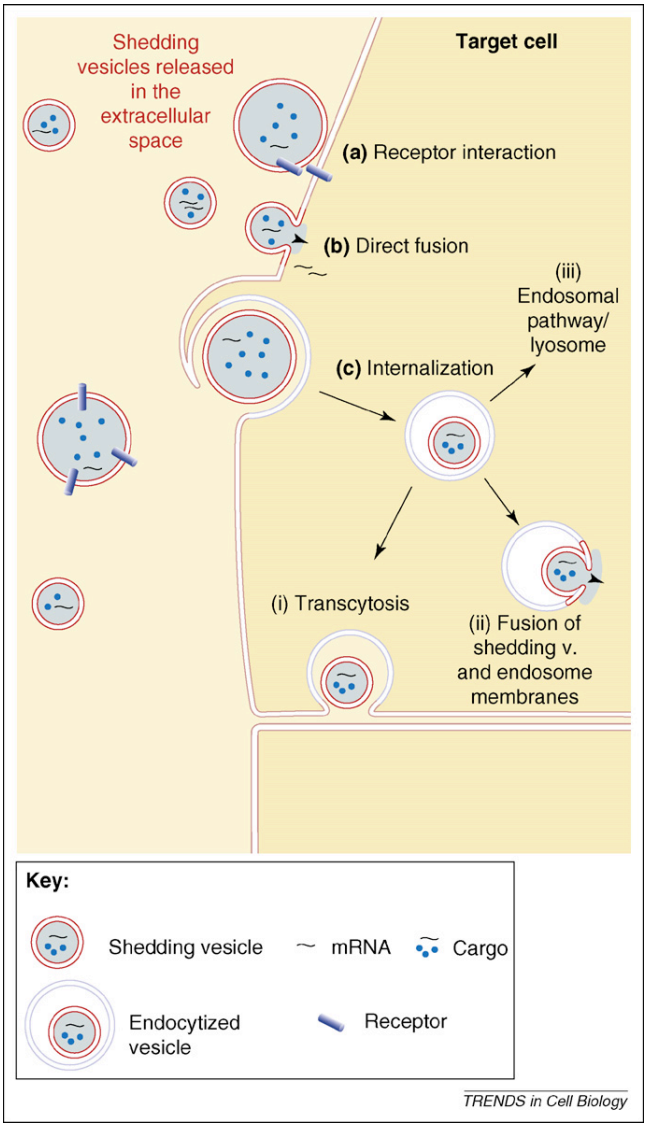

Figure 9. Interactions of shedding vesicles with their target cells. The shedding vesicles, released by a donor cell to the extracellular space can: (a) bind via specific receptors (blue cylinders) to the surface of the target cell; (b) fuse with the target cell plasma membrane discharging their cargo, including mRNA, into the cytosol; or (c) be taken up by the target cell by endocytosis (shown as a form of macropinocytosis). The internalization can be followed by: (i) transcytosis (i.e. the fusion of the endosome membrane with the plasma membrane followed by release of the intact shedding vesicle back to the extracellular space); (ii) the discharge of the cargo to the cell cytosol upon fusion of the shedding vesicle membrane with that of its endosome; or (iii) the endocytosed shedding vesicle can also be targeted to the lysosome by entering the endosomal pathway. The cargo contained within the shedding vesicles along their pathway includes material sorted out from the cytosol of the donor cell. The arrows indicate the direction of cargo discharge taking place upon vesicle membrane fusion (Cocucci et al., *Trends in Cell Biol. 2009; 19 (2):43-51).*

Eventually, membrane vesicles and exosomes may not be functionally different and their roles could be rather determined by their specific protein content which could vary depending on the cell from which they are produced. Some authors describe characteristics and roles of microvesicles (MVs), without distinction between different categories. Others refer to membrane vesicles or exosomes specifically.

Techniques for separating membrane vesicles and exosomes

Culture media conditioned by exponentially growing cells are enriched in micro-particles that can be considered as cell debris or cell fragments, by flow cytofluorimetry. Electronic microscopy reveals that these “fragments” are similar to vesicles, namely phospholipid bilayer sacs holding cytoplasmic material. Therefore, cell culture supernatants represent a source of micro-vesicles, useful for isolating and characterizing them.

In the last years, several studies focus on characterization of vesicles collected from conditioned culture media *in vitro* or biological fluids *in vivo*. Exosomes have been isolated from numerous biological fluids such as urine, malignant pleural effusions, bronchial washing fluid, ocular liquid, seminal liquid, amniotic liquid, milk, pregnancy associated liquid and synovial liquid (Mathivanan et al., 2010).

The importance of MVs as tumor markers is related to their availability from blood in easy and non invasive manner (fig. 10).

In particular, the greatest number of works are based on isolating a mixed vesicle population, by ultracentrifugation. Therefore, most of the works report results obtained with a mixture of membrane vesicles and exosomes.

Nevertheless, several procedures have been applied to separate different vesicle populations. For example, exosomes - the smallest vesicles - can be obtained by porous membrane filtration (0,1-0,2 micron porosity). In other cases, sucrose density gradients are used to separate particles having different density. Immunoaffinity based capture techniques have been recently employed to isolate highly purified exosomes. In particular, HER2 based antibodies are used to isolate exosomes from mammary adenocarcinoma and from ovarian cancer ascites. This approach is advantageous to remove histones - apoptotic bleb markers - that are otherwise enriched in exosomal preparations obtained by filtration or

ultracentrifugation. The main limit of this technique is the necessity of previous knowledge of the interesting particle composition.

Considering the diversity in size and density of membrane vesicles (200-1000nm) and exosomes (20-80nm), they can be separated by differential centrifugation. It has been documented that membrane vesicles sediment at lower speed centrifugation (about 10-15,000 gravity) than exosomes, pull down at 100,000 gravity circa (Heijnen et al., 1999).

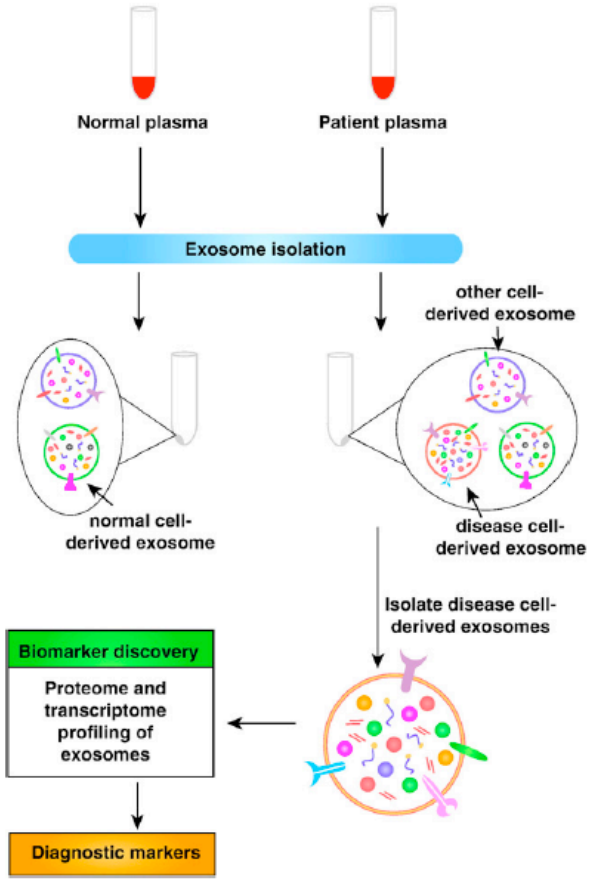

Fig. 10 – Circulating exosomes can be a rich source for identifying potential biomarkers. Patient plasma contains exosomes that are released by disease cells (e.g., colorectal cancer cells), normal counterpart (e.g., normal colon cells) and other normal cells (e.g., liver). Exosomal tissue signatures can be used to isolate disease cell-derived exosomes for proteomic and transcriptomic profiling (Mathivanan et al., *J. Proteom. 2010; 73: 1907–1920)*.

MV protein composition

Vesicle composition depends upon cell type origin. Anyway, MVs are enriched in specific components, in comparison with the cell membrane from which they take origin, because they are generated from selective areas of plasma membrane, enriched of sphyngolipids, cholesterol, integrin receptors and other specific proteins.

Proteomic analysis is the elected technique for characterizing MVs, since a wide knowledge of MV protein content can help in elucidating their potential roles, *in vivo*.

Recently numerous proteomic studies have been applied to MVs, generally, and to exosomes, more specifically. The great number of data concerning transcriptomic and proteomic studies on exosomes are collected in a database - ExoCarta - (Mathivanan and Simpson, 2009). A total of 2624 proteins, 901 mRNA and 274 miRNA from 4 different organisms are herein cataloged. Additionally, the compendium lists proteins that are more often identified in exosomal studies based on the number of occurrences of these molecules in 75 published proteomic studies. Some of these molecules can be used as reliable exosomal markers, which is currently one of the important steps in characterizing the presence of exosomes in a preparation. Interestingly, tissue-specific proteins that are identified in exosomes are also listed in ExoCarta.

By the way, several molecules are shared among MVs of different cell origin (fig. 11). Proteins playing distinct roles are actually conserved in exosomes irrespective of their origin. The list of common proteins includes Rab GTPases, a family of more than 60 ubiquitous proteins necessary for coordinating various steps of intracellular trafficking, like vesicle formation, transport and fusion to cell targets. Numerous studies have established that different Rab proteins are localized to distinct intracellular compartments where they play central roles in the proper targeting and fusion to vesicles with the correct destination organelles. Although most Rab proteins are constitutively expressed in all mammalian cells,

several of them have been shown to be up-regulated in human tumors and especially enriched in tumor shed vesicles. Therefore, it is believed that dysregulation of Rab gene expression may cause elevated MV shedding in actively growing tumors.

Moreover, MVs are enriched in annexins and endosomal sorting complexes required for transport (ESCRT) that are involved in vesicle trafficking and fusion processes, proteins involved in antigen binding and presentation like molecular chaperons (i.e. Hsp70, Hsp60, Hsc71) and class I, class II MHC histocompatibility molecules, proteins responsible of targeting and cell adhesion such as tetraspannins (i.e. CD63, CD81, CD9 and CD82), several members of integrin and immunoglobulins, cytoskeletal proteins such as actins and tubulins, cytoskeletal-related proteins cofilin and profilin-1, metabolic enzymes (alpha-enolase, pyruvate kinase, thioredoxine peroxidase), ribosomal proteins and ubiquitins (Mathivanan et al., 2010). In particular, tetraspannins and ESCRT proteins are exclusively exosomal markers because they belong to intraluminal vesicles generated by the endosomal pathway; therefore these proteins can be used to discriminate between exosomes and membrane vesicles.

Exosomes recovered by malignant pleural effusions showed also to be enriched in extracellular matrix organization and cell-matrix interaction related proteins as bamacan (basement membrane chondroitin sulfate proteoglycan) protein or thrombospondin-2 which interacts with cell surface receptors such as integrin or heparan sulfate proteoglycan (Bard et al., 2002). The binding of extracellular matrix proteins on exosomes may be explained by the presence of matrix-binding proteins like integrins on their surface.

Proteomic analyses demonstrate a constant presence of serum bovine proteins in MV preparations from cell cultures *in vitro*. Cells are usually grown in the presence of fetal bovine serum (FBS) that stimulates proliferation and, thus, a higher amount of vesicles is obtained in the extracellular medium. Both vesicle shedding and clustering of selected molecules are greatly induced by the addition of serum. As result, proteome profile of vesicles is largely contaminated by serum

proteins such that vesicular proteins are under represented. To overcome this problem, several researchers adopted the strategy of high-speed centrifugation of the serum prior of adding it to the cell culture. Nevertheless, the presence of bovine proteins in those preparations probably reflects the stick adherence of the more abundant bovine serum proteins to lipid membranes. This contamination was also observed in exosomes prepared from human peripheral blood dendritic cells (Mears et al., 2004).

Proteomic analysis of MV underlined that although several molecules are shared between MV of different cellular origins, MV functionality seems to be determined by their specific protein content that reflects the cells from which they are released. In fact, the presence of tumor specific antigens and tumor associated proteins has been documented in MVs. For example Mart-1, Mel-CAM and Her2/neu are found in melanoma exosomes (Mears et al., 2004). Moreover, the A33-antigen is specific to colorectal cancer-derived exosomes and future studies based on immunoaffinity capture of colon-specific exosomes can be performed with this knowledge (Mathivanan et al., 2010). As another example, APC derived exosomes carry antigens in association with histocompatibility molecules. These demonstrations may render MVs as an attractive source for proteomic mining in the field of marker or antigen discovery.

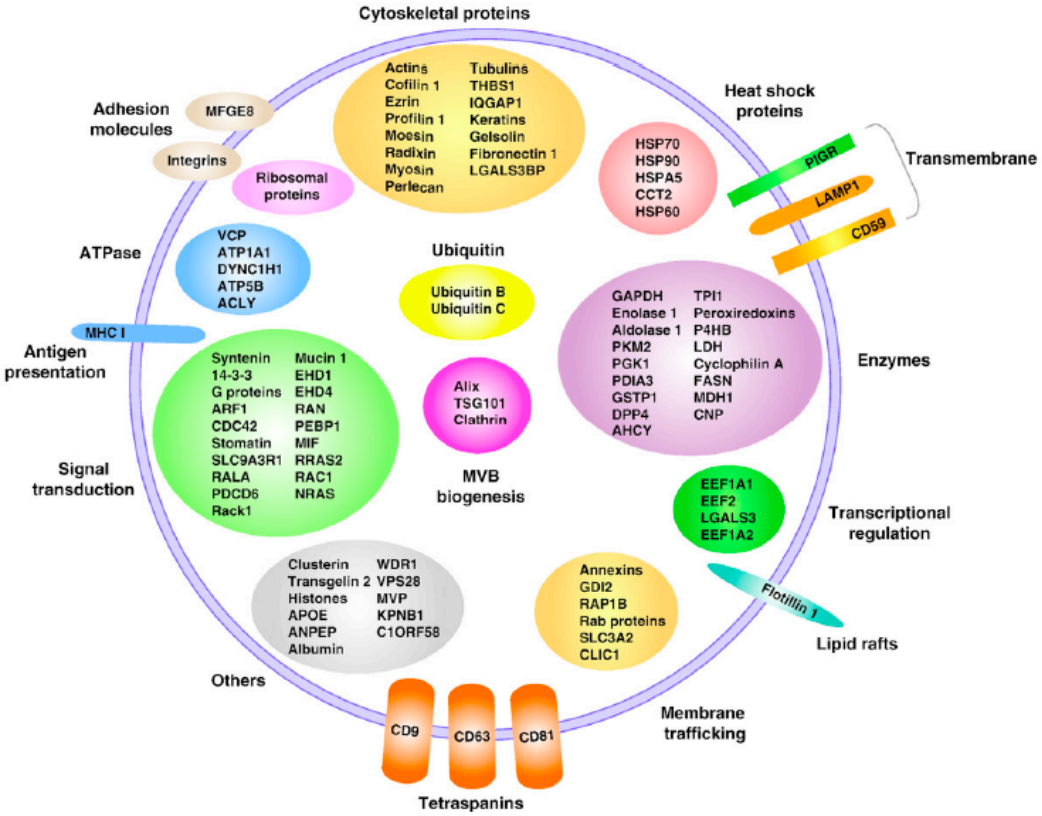

Fig. 11 – A graphical representation of the protein composition of exosomes categorized for the function performed. ExoCarta was used to download 19 exosomal proteomic studies that had identified at least 30 proteins. Protein molecules that are identified in more than 26% of the proteomic studies are depicted in the figure as gene symbols or protein names *(*Mathivanan et al., *J. Proteom. 2010; 73: 1907–1920).*

Shed MVs and mammary carcinoma

Breast cancer is still the most common form of cancer diagnosed in women, other than skin cancer, and the fifth leading cause of cancer related death (fig. 12) (International Agency for Research on Cancer, 2003, retrieved 2009).

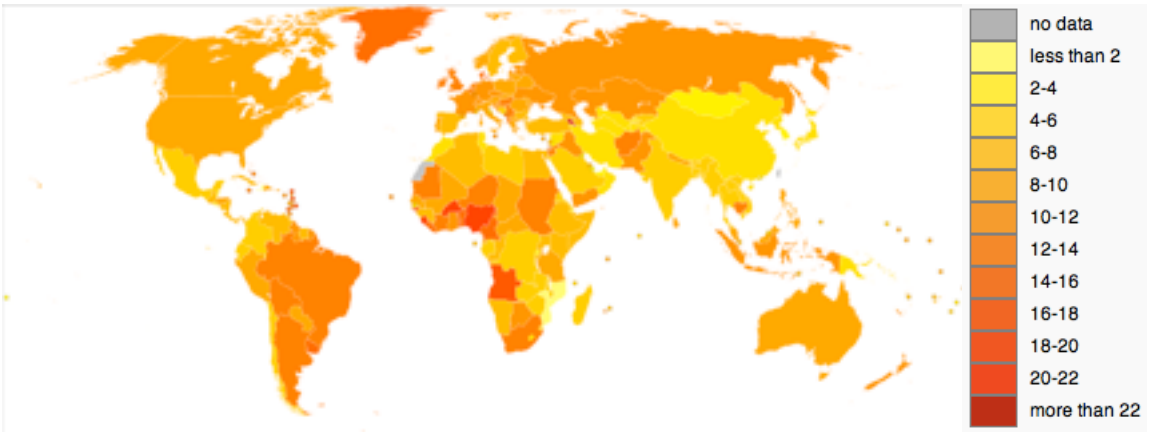

Fig. 12 Age-standardised death rates from breast cancer by country (per 100,000 inhabitants) *World Health Organization*. 2009

Breast cancer is cancer originating from breast tissue, most commonly from the inner lining of milk ducts or the lobules that supply the ducts with milk. From the origin site, cells can overcome the basal lamina and reach the blood stream. Then, cells can extravasate and infiltrate in other tissues (for breast cancer, the preferential secondary sites are bones, brain, liver, lung and lymph nodes) where they generate metastasis (fig. 13).

A deep understanding of tumor progression mechanisms and involved factors could help to eradicate primary tumors, before they extend and metastatize.

Unfortunately, no single biomarker is currently available with sufficient sensitivity and selectivity for prediction of breast cancer. Although remarkable advances have been done in early diagnosis, prognosis and management of patients with breast cancer, no independent and strong prognostic marker, that is suitable for accurate prediction of the disease course in all individuals and predicts treatment outcome in all the categories of mammary carcinoma, has been found (Arciero et al., 2003).

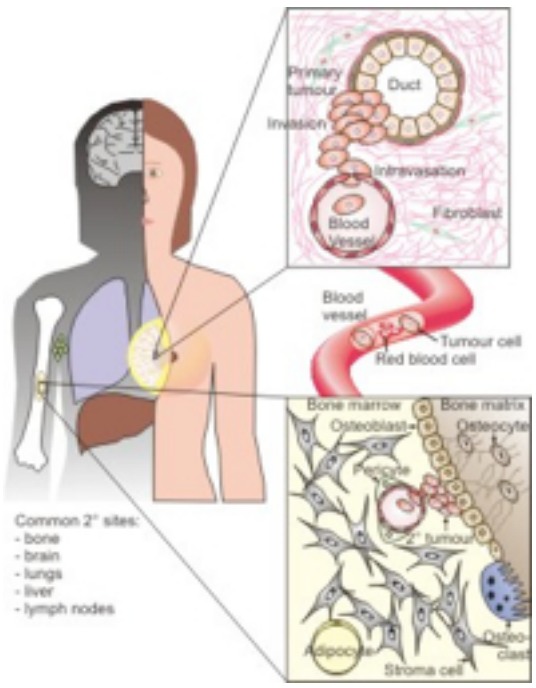

Fig. 13 Scheme of breast cancer primary sites and progression via.

Current literature strongly suggests that good management of breast cancer will require the assessment of the status of multiple biological markers. At the present, clinically validated predictive biomarkers of breast cancer include estrogen receptor (esr1), progesterone receptor (pgr), BRCA1, BRCA2 and the extent of amplification of ERBB2 gene and/ or overexpression of erbb2 protein product (Dowsett et al., 2000).

The primary prognostic factors for breast cancer still remain those determined by clinical or standard pathological approaches. These include axillary lymph node status, tumor size, histological or tumor grade, histological subtype and the presence or absence of metastasis. About 62 genes have now been associated with the onset, progression and severity of breast cancer. However, the specific roles of the majority of these genes are yet to be clearly elucidated and only a small number are now putatively associated with breast cancer. New developments in functional genomics and proteomics have enabled high throughput parallel analysis of thousands of genes in individual patients and amongst populations, and opened up the possibility of providing more details on the molecular mechanisms associated with breast cancer. The most common markers are associated with hormonal reception (Esr e Pgr), cell cycle regulation (ErbB2, p53, cyclin D and so on), ECM modifications (MMPs, uPA, Serpin1, Serpin2, cathepsin, VEGF), tumor associated antigens (cytokeratin 19, MUC1, BRCA1, BRCA2).

Some currently employed breast cancer biomarkers were found to be present in vesicles shed *in vivo* by breast carcinoma cells or, in alternative, obtained from

cancer cell cultures *in vitro*. For example, membrane vesicles from two breast carcinoma cell lines, MCF-7 and 8701-BC are shown to carry most antigens expressed on the cell surface (β1, α3 and α5 integrin chains, tumor-associated antigens, HLA class I molecules, and so forth). In particular, nonrandomized distribution of HLA class I molecules, β1 integrin subunit, proMMP-9, and TIMP-1 occurs on the plasma membrane of breast carcinoma 8701-BC cells when vesicle shedding takes place (Dolo et al. 1998).

These experimental evidences show that tumor markers detected in the circulation of carcinoma patients, at least in part, are carried by shed membrane vesicles. Thus, breast cancer related biomarker research can be focused on vesicle characterization and new markers with diagnostic value could be identified in MVs.

For those studies, available tools are mainly Western Blotting, E.L.I.S.A., flow cytofluorimetry and especially transcriptomic and proteomic analysis.

Aim

Extracellular vesicle shedding is a physiological phenomenon observed both *in vivo* and *in vitro*. It increases in pathological conditions such as cancer and it seems to correlate with several cancer progression mechanisms such as promotion of tumor invasiveness, metastasis formation, angiogenesis and immune escape.

Literature data report two kinds of microvesicles, i.e. membrane vesicles and exosomes, that differ for both dimensions and biogenesis mechanism. In fact, membrane vesicles with diameter ranging from 100 to more than 1000 nm, are produced by shedding from the plasma membrane while exosomes (20-80 nm in diameter) are produced by exocytosis of multivesicular bodies. Nevertheless, differences in physiological roles between membrane vesicles and exosomes are not yet completely clarified.

8701 BC human breast carcinoma cells represent a good model for the characterization of shed vesicles, since the presence of those vesicles has been already described (Dolo et al., 1994). In particular, it has been found that, in serum supplemented medium, 8701 BC cells shed membrane vesicles which carry tumor-associated antigens and class I HLA molecules (human lymphocyte antigens), suggesting a mechanism of escape from immune surveillance (Dolo et al., 1995a). Moreover, they vehicle integrin-β1 and MMP-9, responsible of the adhesion to the extracellular matrix (ECM) and degradation of ECM components, that could promote cell migration (Dolo et al., 1998). Indeed all the data concerning 8701 BC shed vesicles are focused on membrane vesicles while the production of exosomes has not yet revealed.

MDA MB 231, another cell line derived from breast adenocarcinoma, has been reported to shed microvesicles, even without serum stimulation (Ginestra et al., 1998). Although this cell line has been extensively studied, extracellular vesicles are not yet analyzed.

The aim of this work is to separate different vesicle populations shed by breast carcinoma and analyze separately the protein content of these extracellular vesicles. 8701 BC and MDA MB231 cell lines have been chosen as models of vesicle release. The instruments used for this analysis are various: western blot,

transmission electron microscopy, immunofluorescence and especially proteomic analysis. Nowadays proteomic analysis represents a tool for investigating the global protein content and it has become the technique elected for studying extracellular shed vesicles. A deeper knowledge of vesicle transported proteins could help to elucidate their potential roles *in vivo*. More specifically a different protein content between different vesicle fractions could highlight upon their different origin and their different functions. Eventually, identification of the vesicular proteins can be useful in discovering new tumor biomarkers, opening new insights into tumor diagnosis and therapy.

Materials and Methods

Cell Culture

Neoplastic cells, 8701 BC, derived from ductal malignant breast cancer (Minafra et al., 1989) and MDA MB 231, derived from American Type Culture Collection (ATCC), were seeded in RPMI 1640 culture medium (CELBIO), with 2mM L-glutamine and antibiotics (100 units/ml penicillin and 100units/ml streptomycin), supplemented with 10% fetal bovine serum (CELBIO) and grown in a humidified incubator with 5% CO_2 in air at 37°C.

Vesicle collection

Media conditioned by subconfluent healthy 8701 BC cells for 3 and 24 h were centrifuged at 2000 x g for 10 min and 4000 x g for 15 min to remove cellular debris. The supernatant was therefore differentially centrifuged. In particular, the medium was initially centrifuged at 15,000 x g (JA 20 Rotor, Beckman) for 30 min at 4°C and the pelletted vesicles were collected. The supernatant was then ultracentrifuged at 100,000 x g (Ti 60 Rotor, Beckman) for 90 minutes at 4°C and the new pellet was collected.

Both the vesicle fractions were resuspended in phosphate-buffered saline (PBS) and stored until use at -80°C. Protein concentrations were determined using Bradford method.

MDA MB 231 cells were grown in the presence of serum until 80-90% confluence. Then they were washed twice in PBS and fresh medium depleted of serum was added. In the first set of experiments, after 24 h starvation, conditioned medium was collected and treated as described above to obtain vesicles. In the second experimental part, an additional washing step was introduced. In particular, after 4 h starvation, conditioned medium was discarded, fresh medium was added in absence of serum and the latter one was collected after 24 h.

Cell Lysate Preparation

Cell cultures, after conditioned medium collection, were washed in cold PBS. Then, they were carefully scraped and incubated on ice for 30 minutes with RIPA buffer (50mM Tris, pH 7.5, 0.1% NP40, 0,1% deoxycolate, 150 mM NaCl and 4mM EDTA) and a mixture of protease inhibitors (0.01% aprotinin, 10 mM sodium pyrophosphate, 2 mM sodium orthovanadate and 1 mM PMSF). The total cellular lysate was centrifuged at 14,000 RPM for 8 min to clear cell debris and then stored at -80°C. Protein concentration in the cellular extracts was determined using the Bradford method.

Bradford assay

Protein concentration was determined measuring the absorbance at 595 nm through the spectro-photometer. Initially BSA (Sigma) was used at different concentrations (10 μg/mL to 140 μg/mL) to build a standard curve used as reference to calculate the protein concentration of the sample.
Bradford reactive (1ml) was added to the samples and BSA aliquots and the reaction occurred in 5 minutes, before the analysis.
Bradford reactive consists of 0,01 % Comassie Brillant Blue G-250, 5% Ethanol, 10% Phosphoric Acid. The solution is filtrated and stored at 4°C.

Gel permeation cromatography

To separate microvesicles from serum proteins an approach of gel permeation chromatography (GPC) was used. The GPC column is prepared by packing sepharose 4B gel beads (Sigma-Aldrich) with 45-165 μm bead diameter and 60,000-2,000,000 Da fractionation range (cut off), into the glass column. The length of the packed material was about 35-40 cm. This technique may allow the

separation between microvesicles, being larger than pore size, that are quickly eluted and serum proteins, smaller analytes, that enter the pores more easily, increasing their retention time. For this separation a gravitational column - Glass Econo-Column (BioRad lenght 50 cm, diam 1 cm) attached to an ÄktaPrime system (GE Healthcare) for monitoring only (280 nm) has been used.

Filtration/centrifugation

To separate microvesicles from BSA, Amicon Ultra-15 Centrifugal Filter Units with cut off = 100kDa (Millipore) were used, according to the manufacturing instructions. In particular, the sample was added to the reservoir of the centrifugal device. The centrifugation was performed at 4,000 xg for 30 minutes. After that, both the filtrate and the held fraction were collected and analyzed by gel electrophoresis.

Transmission Electron Microscopy analysis

Size and morphology of the nanoparticles were examined using transmission electron microscopy (TEM, FEI Morgagni). For the analysis vesicles were negatively stained. In particular, a 5 µl drop of sample has been placed onto spacemen support grid (Cu 200M), and let to adsorb for 60 seconds. Then they were washed twice in double-distilled water, once in uranyl acetat 2% solution. Eventually, they were adsorbed for 10 sec in uranyl acetat 2% solution.

Monodimensional electrophoresis

1D- SDS polyacrilammide gel electrophoresis allows the separation of proteins on the basis of their molecular weight.

To obtain this separation, protein samples (15 µg) were resuspended in ratio 1:2 in loading buffer 3X (SDS 6% (w/v), β-mercaptoethanol 15% (v/v); Glicerol 30%

(v/v); Bromophenol Blue 0,25% (v/v)). They were denatured at 95°C for 5 minutes and loaded into polyacrilamide gels, produced as described below.
The running was performed at 100V.

Recipe for separating gel			stacking gel	**Reagent**
10%	12,5%	15%	3,5%	
3,3 ml	4,2 ml	5 ml	1,2 ml	Acrilamide/bisacrilamide (30:0,4%)
2,5 ml	2,5 ml	2,5 ml	-	Tris HCl 1.5M, pH 8.8
-	-	-	2,5 ml	Tris HCl 0.5 M, pH 6.8
100 µl	100 µl	100 µl	100 µl	SDS 10%
225 µl	225 µl	225 µl	225 µl	Ammonium Persolphate 10%
14 µl	14 µl	14 µl	14 µl	TEMED
to 10ml	to 10ml	to 10ml	to 10ml	H_20

2D-PAGE

Both the vesicle fractions and the cell lysate were dialyzed against ultrapure distilled water at 4°C with three changes (3h, Over Night, 3 h) and lyophilized. Dried samples were solubilized in a buffer containing 4% CHAPS, 40mM Tris, 65mM DTE (1, 4 dithioerythrol) and a trace of Bromophenol Blue in 8M UREA.
To achieve a proteomic study, a 2D-PAGE analysis was performed. This technique sorts proteins according to two independent properties in two discrete steps: the first-dimension step, isoelectric focusing (IEF), separates proteins according to their isoelectric points (pI); the second-dimension step, SDS-PAGE, separates proteins according to their molecular weight (MW). Each spot on the resulting two-dimensional array corresponds to a single protein species in the sample.

The isoelectric focusing was performed at 20°C on commercial IPG strips, 18cm long with non linear pH range 3,5-10 (GE) using the IPGphor system (Amersham Biosciences, Uppsala, Sweden). Strips were rehydrated in 350 microliters of 8M urea, 2% CHAPS, 10mM DTE and 0,5% carrier ampholytes (Resolyte 3.5-10), containing aliquots of 45 micrograms (analytical gels) and 1 milligram (preparative gels) of protein samples. After 1h strip hydratation at 10V, the isoelectric focusing was carried out by linearly increasing voltage from 200 to 3500 V during the first 3 hours, after which focusing was continued at 8000V for 8 h. After the run the IPG strips were equilibrated with a solution containing 6 M urea, 30% glycerol, 2% SDS, 0.05 M Tris-HCl pH 6.8 and 2% DTE (dithioerythrol) for 12 min, in order to resolubilize proteins with SDS and reduce disulphide bonds. The –SH groups were then blocked by substituting the DTE with 2.5% iodoacetamide in the equilibration buffer for further 5 min.
The focused proteins were then separated on 9-16% linear gradient polyacrylamide gels (SDS-PAGE) with a constant current of 40 mA/gel at 10°C.

Spot detection: Ammoniacal Silver Staining or Comassie Brilliant Blue

Ammoniacal Silver Staining

After electrophoresis, gels are washed in ultrapure water for 5 min.
Then, they are fixed in 40% Ethanol-10% Acetic acid for 60 min. and in 5% Ethanol-5% Acetic acid for further 60 min. The fixing step is followed by a 10 min washing step in ultrapure water at room temperature. After that, gels are incubated in 2% glutaraldehyde - 0.5M Sodium Acetate at 4°C for 30 min, washed three times (each one 10 min) in ultrapure cold water and further incubated with 0.05% 2-7 Naftalendisulfonic Acid (NDS) at 4°C. Again they are washed four times (each one 15 min) in ultrapure cold water.

Then they were incubated in staining solution containing 0.8% (w/v) $AgNO_3$, 0.33% (v/v) NH_3 and 0.02N NaOH, for 30 minutes in dark at room temperature.
After the staining, the gels were washed four times (each one 4 min) in ultrapure water at room temperature. The developing step was performed with a solution containing 0.005% Citric Acid and 1.11% formaldehyde, in which gels were incubated for about 12 minutes, until they reached the desired level of spot detection.
The reaction is stopped by a solution of 5% Acetic Acid for 2 minutes and the gels can be stored in ultrapure distilled water.

Gel acquisition and analysis

Silver stained gels are digitized using a computing densitometer and analyzed with Image Master 2D Platinum software, MELANIE 5° edition (Amersham Biosciences, Sweden), that allows a qualitative/quantitative analysis of the electropherograms.
The first step of *in silico* gel analysis consists of removing artifacts associated with the scanning process (shadows and bubbles are considered also protein spots by the software). Then gel calibration is carried out using proteins, whose molecular weight (MW) and isolectric point (pI) are known, as internal standards. In this way, spatial coordinates for each spot are converted into the correspondent pI and MW values.
For gel matching of several electrophoretic images the software uses algorithms that allow to match shape and position of spots present on different gels. The automatic matching can bring to errors for different migrating gels. Therefore it is recommended to match manually some reference spots (10-15), useful as anchors for a more precise matching.
Quantitative analysis is performed calculating the percentage volume (% Vol) for each spot, that corresponds to the ratio between single spot volume and the whole volume of the detected spots. This method decreases the differences due to silver staining among the gels.

Blue Comassie Staining

To identify the proteins through mass spectrometry, the gel containing 0,5-1mg proteins was incubated two hours in Blu Comassie staining solution (0,2% Blu Comassie, 40% Methanol, 10% Acetic Acid). Afterwards the gel was maintained for 1 hour in strong destaining solution (40% Methanol; 10% Acetic Acid) and then overnight in weak destaining solution (7% Methanol; 5% Acetic Acid). Finally all the visible spots were cut from the gel and stored in 20% Ethanol at 4°C.

Preparation of samples for mass spectrometry

Destaining and in gel digestion

Solutions. Sol 1. NH_4HCO_3 (ammonium bicarbonate) 20mM pH 8.3; **Sol 2.** CH_3CN/H_2O (acetonitrile/water)(50/50); **Sol 3.** NH_4HCO_3 (ammonium bicarbonate) 50mM pH 8.3; **Sol 4.** HCOOH (Formic Acid) 5%; **Sol 5.** CH_3CN (acetonitrile); **Sol 6.** Trypsin (sequencing grade modified, Promega) dissolved in Ammonium Bicarbonate [0,1μg/μl].

Procedure. After blue comassie staining, visible gel spots are cut and stored at 4°C in 20% Ethanol until use. The gel pieces selected for mass spectrometry analysis are further cut in smaller pieces and washed in 200 μl **sol 1**, by incubation at 30°C for 15 min. Then the supernatant is discarded and gel pieces are destained in 200 μl **sol 2** at 30°C for 15 min. This step is followed by a washing in nanopure water at 30°C for further 15 min. After that, gel pieces are dried in speed vacuum for 60 min and then they can be stored at -20°C or treated directly for in gel digestion.

For trypsin digestion the ratio enzyme/protein has to be 1/10. For low concentrated proteins you can use 0.5μg trypsin while higher concentrated proteins can be digested with 0.1-0.2 μg trypsin. At first, 2μl trypsin can be

added to dry gel pieces. To avoid autolysis of trypsin, after the addition of the enzyme, gel pieces are centrifuged at 9000 rpm for 3 min. Overlay gel pieces with the necessary amount of sol 3, centrifuge again at 9000 rpm for 3 min and incubate at 37°C at 1350 RPM over night.

Extraction of tryptic peptides

After digestion, samples can be spin down by centrifugation at 9000 rpm for 3 min and trypsin solution containing digested peptides can be collected in eppendorf tubes. Gel fragments are washed in **sol 5** (adding the same volume used before to overlay the fragments) at 28°C for 10 min under shaking. After centrifugation at 9000 rpm for 3 min, the solution is collected and another washing step in **sol 4** is performed at 28°C for 10 min. This is followed by centrifugation, supernatant collection and washing in **sol 2**. After that, again centrifugation and supernatant collection are done. Eventually all the supernatants for the same sample are joined and dried in speed vacuum. In these conditions extracted peptides can be stored at -20°C.

Purification of tryptic peptides with zip-tip

Solutions. Sol 1. CH_3CN; **Sol 2.** CH_3CN/H_20 (50:50 (v/v)), TFA 0.1%; **Sol 3.** TFA 0.1%. **Procedure.** This procedure is aimed to remove the salts and to concentrate the sample. At first the dry extracted peptides are rinsed in 10µl **sol 3.** The zip-tips are washed once with 10µl **sol 1,** three times with **sol 2** and other three times with **sol 3**. Then, the peptides are taken with absorbed on the ZIP-TIP, pipetting Up/Down ten times. Then the solution can be discarded and ZIP-TIP is washed with 10 µl **sol 3**. The elution is performed in sol 2 by pipetting ten times. At this point, purified peptides can be dried in Speed-Vacuum.

Acquisition of mass spectra through MALDI-TOF

The sample preparation includes the following step:

a. prepare the matrix dissolving 2,5-dihydroxybenzoic acid (DHB) [5mg/ml] in a solution containing CH_3CN/H_20 (70:30 (v/v)), TFA 0.1%;

b. rinse the peptides previously purified with zip-tips in DHB matrix (1-2 µl);
c. wash the MALDI plate with distilled water and dry with Kimwhites paper; cover with anti-oxidant agent and finally wash with acetone. Air dry;
d. load 1 µl DHB matrix onto a position of the plate to test if it correctly cleaned: if the droplet forms easily crystals, it is possible to start with sample loading;
e. load 1 µl of each sample into the different positions of the plate;
f. wait for matrix-peptide co-crystallization;
g. introduce the plate into the mass spectrometer, set the instrument parameters through Voyager software and acquire at least three spectra for each spot.

MALDI-TOF mass spectra are recorded on the Voyager DE-PRO (Applied Biosystems) mass spectrometer, in the 500-5000 Da mass range, using a minimum of 100 shots of laser per spectrum. Such spectra are run into Data Explorer software, which allows appropriate calibration and elaboration of the peaks. In particular, delayed extraction source and reflector equipment allow sufficient resolution to consider MH+ of monoisotopic peptide masses. Internal calibration is carried out using trypsin autolysis fragments at m/z 842.5100, 1045.5642, and 2211.1046 Da.
At this point, mass spectra are ready for an extensive research throughout online databases. Peptide mass fingerprinting is compared to the theoretical masses from the Swiss-Prot or NCBI sequence databases using Mascot http://www.matrixscience.com/. Typical search parameters are as follows: 50 ppm mass tolerance, carbamido-methylation of cysteine residues, one missed enzymatic cleavage for trypsin, oxidation of methionine. Moreover, a minimum of four peptide mass hits is required for a match.

Protein Labeling with fluorescent dye Cy5

Cy5 is a water-soluble fluorescent dye belonging to the cyanine family and it contains a NHS (*N*-hydrossisuccinimide) reactive group binding covalently to the ε amminic group of the lysin, present in the proteins. The reaction is optimized so that only 1-2% of the total lysin residues are bound in the sample. This approach,

known as "*minimal labeling*" permits that labeled proteins don't change their pI and MW and therefore they will separate in 2D-PAGE as well as the unlabeled proteins.

The powder stock of fluorescent molecules has to be resuspended in N,N-Dimetilformamide (DMF) to obtain a final concentration of 1 nmol/µl. Afterwards a volume of the stock solution can be diluted in 1.5 volumes of DMF, to obtain a working solution of 400 pmol/µl.

For the labeling, the proteins (50 µg) are incubated with 400pmol CyDye on ice in the dark for 30 min. The reaction is blocked adding 10 mM lysine and incubating on ice in the dark for further 10 min. Labeled proteins can be stored at -80°C in the dark, until the use.

Labeling of cells with radioactive S^{35} methionine

Radioactive methionine is the most used aminoacid in biochemical studies because it can be incorporated in all the neosynthetized proteins; moreover, S^{35} isotope has a long mean life-time (around three months) that emits β radiations detectable by autoradiography.

Subconfluent 8701 BC cells were starved in methionine free RPMI medium for 1 hour. Afterwards, cells were fed with methionine free medium containing 0,4 µl/ml of S^{35} methionine (10 µCi/µl) for 24 hours and then, radioactive medium was discarded and cells were cultured in unlabelled medium. Conditioned medium (3-24 hours) was finally collected and, after removal of cell debris, it was directly ultracentrifuged at 100000xg for 90 min at 4°C to pellet vesicles. After medium collection, cells were also lysed to obtain total labelled cell proteins.

Conditioned medium and cells were labeled with Cy5 and treated as described above for sample preparation before 2D-PAGE.

Besides the protein quantification by Bradford assay, radioactivity quantification was carried out by scintillation. For this analysis 1 µl of proteins were precipitated in 20% Trichloroacetic acid added with 50 µg Bovine Serum Albumin, on ice for

30 min. The proteins were pelletted by centrifugation at 13.000 rpm for 15 min, washed with 200 µl acetone and again centrifuged at 13.000 rpm for 5 min. Finally, the proteins were resuspended in 20 µl PBS and put on a filter paper disk and air dried.

The disk was positioned into a propilene tube in the presence of 2 ml of scintillation liquid (Ready Safe liquid scintillation cocktail *Beckman*). Then the amount of S^{35} isotope was measured.

The proteins were separated by 2D-PAGE and the gels were acquired by Typhoon 9400 scanner (GE), selecting the excitation and emission wave lengths of Cy5 Dye.

Then gels were prepared for the autoradiographic detection of protein spots. In particular, gel were fixed in 10% Acetic Acid-60% Methanol for 30 min under shaking. Then they were incubated with signal amplification liquid (Amplify NAMP100 *Amersham*) for 30 min.

Then, the gels were put on 3MM paper and dried at 80°C for 1 h. Finally they were put on an autoradiographic X-ray film (Hyperfilm ECL, Amersham, *GE Healthcare*) in the dark for 10 days; the films were treated with development and fixing solutions in the dark (Kodak, *Sigma*).

Alternatively, the scanning laser PhosphorImager (*Biorad*) can be used for the autoradiography of labeled spots; this method offers the possibility to reduce exposure times and obtain an image with higher resolution. In this case, the gel is put in contact with a photosensitive slide called slide K.

The slide is then scanned by a scanning that reveals absorbed energy during the exposition to the gel and converts this energy into an image.

Western Blotting

For western blotting analysis, 15 µg of vesicle proteins and cellular lysate were electrophoresed on a SDS-PAGE and electro-transferred onto nitrocellulose membrane (Hybond, Amersham) using following transfer buffer: 25 mM Tris, 190

mM glycine and 20% methanol. Protein transfer was performed at 50 V for 2 h at 15°C. Following transfer, the nitrocellulose membrane was stained using Ponceau Red (0.2% Ponceau Red, 3% TCA) and destained with distilled water. Blocking of the membrane was achieved using 5% nonfat milk in TBS-T (20 mM Tris Base, 30 mM Tris HCl, 150 mM NaCl, 0.05% Tween 20). The membrane was after incubated with the primary antibody in 5% nonfat milk in TBS-T, overnight at 4°C. Following incubation, the filter was washed 3 times for 10 min to remove the unbound antibody. Then the membrane was incubated with horseradish peroxidase-conjugated anti-IgG antibody for 1 h at room temperature. After secondary antibody incubation, the membrane was washed 3 times for 5 min and 2 times for 10 min with TBS-T. Immunoreactive bands were visualized by the enhanced chemiluminescence Western blotting kit (Amersham) using Hyperfilms (Kodak).

Immunofluorescence

Cells were grown on glass slides. Once subconfluent, they were softly washed in PBS. They were fixed in 96% cold Ethanol for 10 min on ice; After a washing with cold PBS, cell membranes were permeabilized with 0.1% triton x100 in PBS for 5 min.Then the slides were washed three times in PBS and after treated with a blocking solution containing 20% fetal bovine serum, 5% Bovine serum albumin, 0.02% sodium azide in PBS, for 1h at room temperature.

After three washings in PBS, the slides were covered with 20 µl of primary antibody solution and incubated in humidified chamber for 1 h at room temperature. This step is followed by three washings in PBS and incubation with the fluorophor-conjugated secondary antibody for 30 min at room temperature. This is followed again by three washings in PBS and one in distilled water.

Finally, the slides were put on a bigger slide on which a droplet of DABCO solution (2% DABCO, 20mM Tris-HCl pH 8, glycerol (1:9, v/v) in water) was

previously put. Cells were observed in an Olympus BX-50 microscope equipped with Vario Cam B/W camera.

Immunofluorescence of cells grown on 3D collagen

Cell suspension was added with 50 mM $NaHCO_3$ and mixed with type I collagen (rat tail BD Biosciences, sold as a 3.9mg/ml solution in 0.02M acetic acid) (1:1, cell suspension:collagen) at a concentration of 300000cells/ml.

Quickly 100 µl of this suspension were seeded onto 96-well plate and incubated 2 minutes at 37°C for polymerizing collagen. Then medium plus serum was added to the cells that were incubated to favor the growth inside the collagen matrix.

The cells, once grown, were fixed in 3,72% formaldehyde for 10 minutes. After fixing, gels were washed three times in PBS and incubated with primary antibody over night at 4°C.

After four washings in PBS, gels were incubated with the secondary antibody at 37°C in the dark for one hour. They could be again washed four times in PBS and put on a support for microscopy. Cells were observed in an Olympus fluoview FV300 confocal microscope, equipped with two laser multipliers.

Antibodies

Primary antibodies: anti-beta1 Integrin C27 rat mAb (1:5000, WEN-TIEN CHEN Lab.); anti Hsc70 mouse mAb (1:2500, Santa Cruz); anti Cytochrom C Clone 7H8.2C12 mouse mAb (1:500, BD Pharmingen); anti Lamp1mouse mAb (1:200 for Western Blot, 1:50 for immunofluorescence, Santa Cruz).

Secondary antibodies for Western Blotting: horseradish peroxidase-conjugated anti rat IgG (1:20000, Sigma Aldrich); horseradish peroxidase-conjugated anti mouse IgG (1:5000, Sigma Aldrich).

Secondary antibodies for immunofluorescence: FITC-conjugated anti rat IgG (1:200); TRITC-conjugated anti mouse IgG (1:400).

Results and discussion

Purification and characterization of 8701 BC derived MVs.

In the initial phase of this study, 8701 BC cells, derived from infiltrating ductal breast cancer (Minafra et al., 1889), have been used. These cells are known to release membrane vesicles in the presence of fetal bovine serum (fig. 14), while exosome production has not yet been revealed.

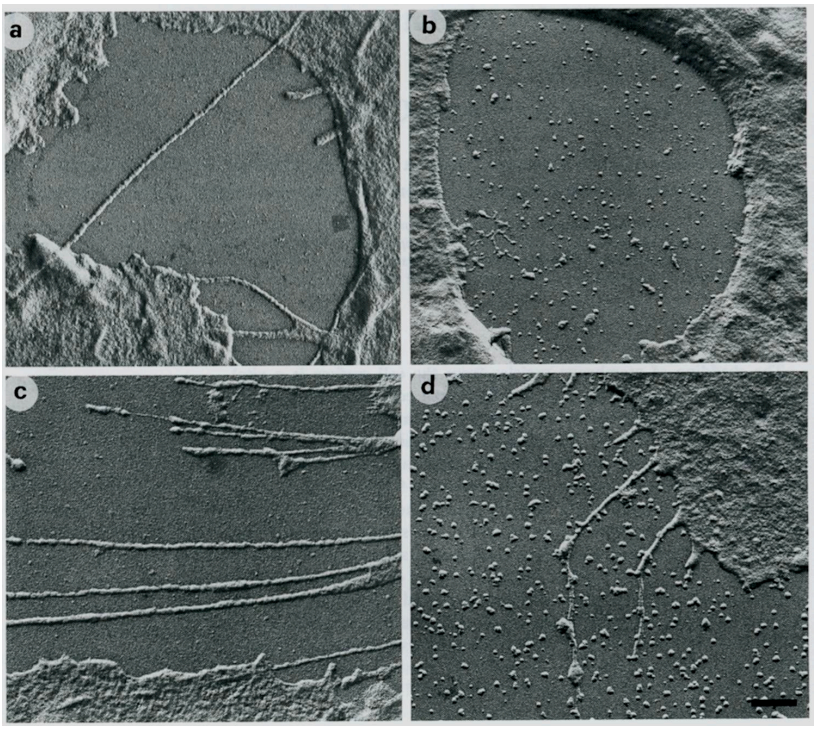

Fig. 14: **TEM analysis of 8701-BC breast carcinoma cells** cultured in serum-free (a and c) and in 10% FCS (b and d) show release of vesicles occurring in complete media (Dolo et al., 1994).

The first goal of this research was to establish if these cells shed different vesicle kinds and eventually characterize their protein content. To this purpose, medium conditioned by subconfluent cells (3-24 hour incubation) was collected and after two low speed centrifugations aimed to remove cell debris, it was differentially centrifuged (fig. 15), using a variant of Heijnen's method (Heijnen et al., 1999) in order to sediment separately eventual different vesicle populations. Thus, vesicle fractions and cell lysate were separated by SDS-PAGE and analyzed by Western Blotting.

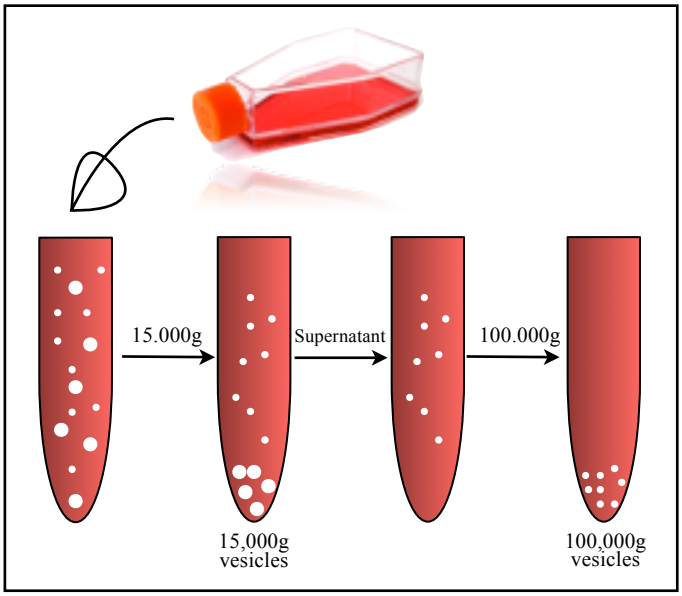

Fig. 15 Vesicle preparation. Conditioned medium from subconfluent cells is collected and differentially centrifuged to obtain two different vesicle fractions.

At first vesicular fractions were analyzed for the presence of β1-intergrin. As previously described (Dolo et al., 1998), β1-integrin is clustered in selective areas of cell membrane from which vesicle shedding occurs and it has been found in shed microvesicles. To investigate the presence of β1-integrin in the vesicle fractions, a western blot using an antibody against β1-integrin was performed (fig. 16).

Equal amount (15 µg) of proteins of cellular extract (WCL) and vesicle fractions (15V and 100V) were electrophoresed on a SDS-7.5% polyacrylamide gel under non reducing conditions, because the primary antibody recognizes a conformational epitope of the protein.

As expected, the 140kDa band correspondent to β1-integrin was found in the whole cell lysate (WCL) and vesicle fraction obtained by centrifugation at 15,000 xg (15V). The same band is under represented in the complementary fraction obtained by ultracentrifugation at 100,000 xg (100V).

Moreover, to discriminate between the fractions obtained by differential centrifugation, an immunoblot using anti Hsc70 (heat shock cognate protein 70) as primary antibody was performed. Heat shock proteins are a group of common proteins that play a role in the cell response to elevated temperature, infection, cytokine stimulation, metabolic starvation, and other environmental stresses.

Hsc70 had been already identified in the protein profile of exosomes by several research groups (Mears et al., 2004; Choi et al., 2007). Its presence therefore indicates that the pelleted fraction of shed material might contain exosomes.

For this analysis, proteins of cellular extract and vesicle fractions were electrophoresed on a SDS-12% polyacrylamide gel under reducing conditions. The image of the Western Blot (fig. 16) shows the presence of a band at 70kDa in WCL and in 100V fraction. The band is not visible in 15V fraction.

This finding, together with the first one, suggests that the differential centrifugation procedure led to the separation of different vesicle populations which are enriched in different proteins. In particular, low speed centrifugation may sediment membrane vesicles while smaller vesicles, i.e. exosomes, are pulled down at higher speed ultracentrifugation. It is also conceivable that 8701 BC cells shed different kinds of vesicles separable by differential centrifugation.

Moreover, the purity of such vesicle preparations has been checked. Recently it has been suggested that the mitochondrial protein cytochrome C may be required for cells to undergo apoptosis. Furthermore, different research groups used anti cytochrome C for checking the purity of vesicle preparations (Mears et al., 2004; Choi et al., 2007). For that reason, vesicles were tested by western blotting analysis using antibody against cytochrome C. WCL and vesicle proteins were electrophoresed on a SDS-15% polyacrylamide gel under reducing conditions. This analysis (fig. 16) confirms the presence of a band at about 15kDa which corresponds to the cytochrome C, in WCL. The same band is not detectable in any vesicle fraction. This result permits to exclude the presence of apoptotic vesicles in those preparations.

For all performed western blotting analyses the specificity of the secondary antibodies was proved by using a control membrane, which was treated only with the secondary antibody (data not shown).

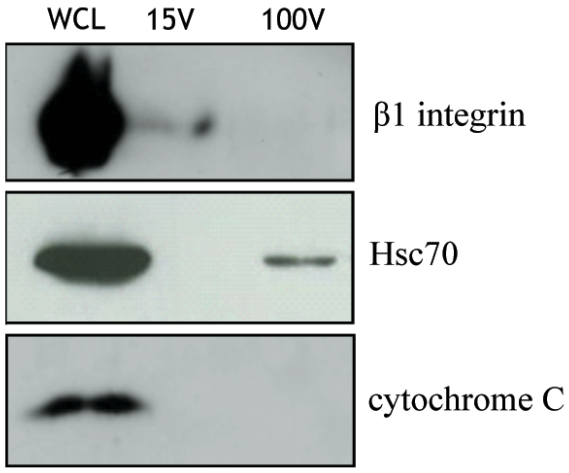

Fig. 16 Characterization of vesicles shed from 8701 BC. Proteins from cell lysates (WCL) and vesicles pelletted either at 15,000 x g (15V) or at 100,000 x g (100V) were separated by electrophoresis and analysed by immunoblotting using antibodies to ß1 Integrin (140 kDa), Hsc70 (70 kDa) and cytochrome C (15kDa).

Proteomic analysis of 8701 BC derived MVs.

To determine the protein composition of MVs released by 8701 BC cells, the vesicular fractions and the whole cell lysate were separated by 2D-PAGE. The gels were silver stained and analyzed through Image Master 2D Platinum software. The proteome of 8701 BC cells has already been characterized (Pucci-Minafra et al., 2006) and represents a reference map for this analysis.

Proteomic analysis (shown in fig. 17) revealed a high contamination of vesicle proteins, in both fractions, with serum components such as albumin and immunoglobulins. These proteins adhere to biological membranes thus being sedimented together with vesicles through centrifugation. Vesicles were so deeply contaminated by serum components that it was not possible to detect the spots belonging to the vesicles.

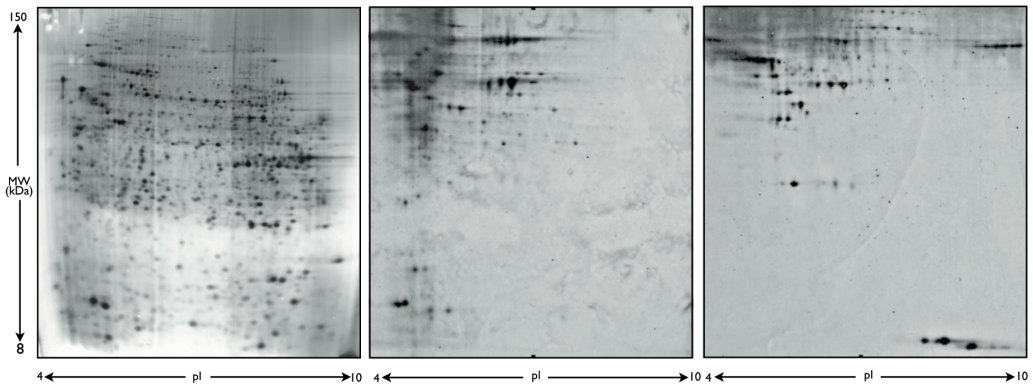

Fig. 17 Proteomic analysis of 8701 BC cells and shed vesicles. Total cell lysates, vesicles sedimented at 15,000 x g sedimented and vesicles sedimented at100,000 x g were separated by 2D-electrophoresis, detected by silver staining and analyzed in comparison with a proteome reference map of human breast cancer, already published and available on-line.

Afterwards, to exclude the visualization of serum proteins from vesicle proteomic maps, cells were grown for 16 hours in the presence of S^{35} radioactive methionine, that is exclusively incorporated in neo-synthetized proteins. After incubation, radioactive medium was replaced with non radioactive one. Conditioned medium was collected after 24 hours, purified from cell debris by two low speed centrifugation steps and ultracentrifuged for 90 min. In this case,

the step of centrifugation at 15,000 xg was avoided to limit the contact with radioactive material. Radioactive vesicles and cell lysates so obtained were separated by SDS PAGE and detected by S^{35} fluorography.

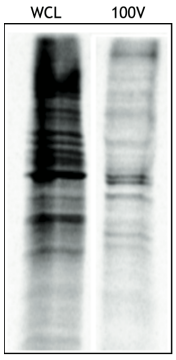

Fig. 18 Autoradiographic detection of SDS page. WCL: whole cell lysate; 100V: conditioned medium sedimented at 100,000 xg. The proteins were labelled with S^{35} methionine.

As it is shown in figure 18, vesicles and cell extracts have different protein profiles; in particular, some bands visible in vesicles are less detectable in cell lysate and *vice versa*. This result demonstrates that vesicles are enriched in specific components of the cells from which they take origin.

Radioactive vesicles and cell lysate were further labeled with cyanin fluorophores and analyzed by 2D-PAGE. Into the electropherogram, protein spot detection was performed by fluorography of both S^{35} Methionine and cyanin Cy5. The merge of the two maps (illustrated in fig. 19, on the top) permitted to distinguish between actual vesicular proteins and serum components; in particular serum proteins, that are highly abundant in cyanin-fluorescent maps, are instead undetectable in the other maps because they are not radioactive. On the other hand, vesicular proteins which are almost completely covered by the highly abundant contaminants in fluorescent maps, become visible in the radioactive maps. In contrast, the merge of cell lysate proteomic maps obtained by differential detection (illustrated in fig. 19, on the bottom) revealed a high degree of overlapping protein spots. Furthermore, analysis showed that vesicle proteome profile is distinct from the one of cell lysate. Nevertheless such a technique was

not useful for protein identification, since using radioactive material inside mass spectrometer is not recommended.

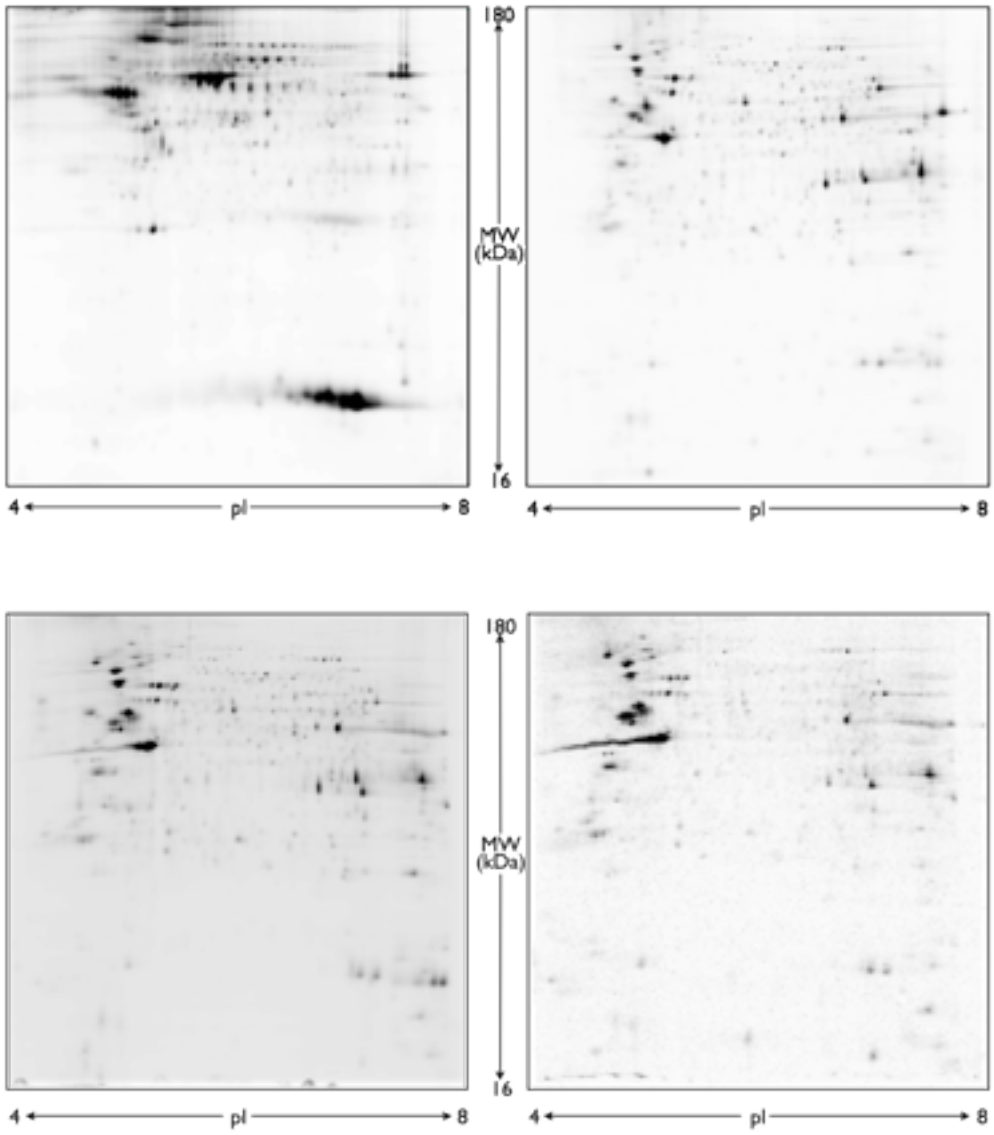

Fig. 19 2D-electrophoresis of vesicles sedimented at 100,000 x g (top) and cell lysate (bottom) from cell cultures incubated in the presence of S^{35}. The proteomic maps on the left are produced by flurographic detection of Cy5 labeled proteins; on the right, fluorographic detection of S^{35}-labeled newly synthetized proteins is shown.

Attempts of vesicles purification

In agreement with previous findings (Dolo et al., 1994) 8701 BC cells are found to shed vesicles only when cultured in the presence of fetal bovine serum (FBS). Therefore, in order to decrease serum contaminants from 8701 BC shed vesicles, several attempts of purification were performed.

Serum was ultracentrifuged to remove any sediment before addition to cell cultures. Moreover, vesicle pellet was washed twice in PBS before the analysis.

Figure 20 shows the SDS-page of the vesicles and medium sediment. Serum contaminants are revealed in vesicles obtained in the presence of ultracentrifuged serum (fig. 20, lane 2) as well as in vesicles produced in the presence of untreated serum and then washed twice in PBS (lanes 3, 4, 5). This treatment did not cause a relevant decrease in serum proteins. Finally, the protein pattern of the pellets obtained from unconditioned medium with/without serum, shown respectively in lanes 6 and 7, proved that most of the observed proteins belong to the fetal bovine serum.

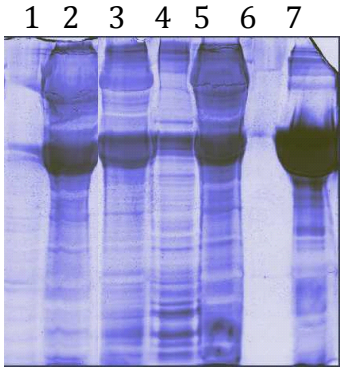

Fig. 20 SDS-PAGE analysis of vesicle preparations from 8701 BC cultures. 1) Vesicles (100000g) –FBS ; 2) Vesicles (100000g) +FBS previously ultracentrifuged; 3) whole vesicle pool (sedimented directly at 100000g) +FBS, after two washings in PBS; 4) Vesicles (15000g) +FBS, after two washings in PBS; 5) Vesicles (100000g) +FBS, after two washings in PBS ; 6) RPMI medium –FBS ; 7) RPMI medium +FBS. (FBS=fetal bovine serum; PBS=phosphate buffered saline).

In order to purify 8701 BC vesicles from serum contaminants, a centrifugation/ filtration device (Millipore), with cut off 100 kDa, has been used hoping to remove BSA (67kDa) which is the main contaminant of vesicles. The filtrate and the held fraction were then analyzed by electrophoresis, in parallel with the untreated vesicle pellet. For this test, only the fraction obtained by ultracentrifugation at 100,000 xg was used. As shown in the electropherograms (fig. 21), the untreated control vesicle sample (top left) produces one main peak correspondent to BSA (around at 64 kDa). The same peak is really small in the filtrate fraction (top right) while it is high in the held fraction (bottom left). This suggests that BSA, because of its sticky properties, could produce aggregates that, blocking the membrane pores, are kept in the held fraction together with the vesicles. Therefore this method failed in separating vesicles from contaminant proteins.

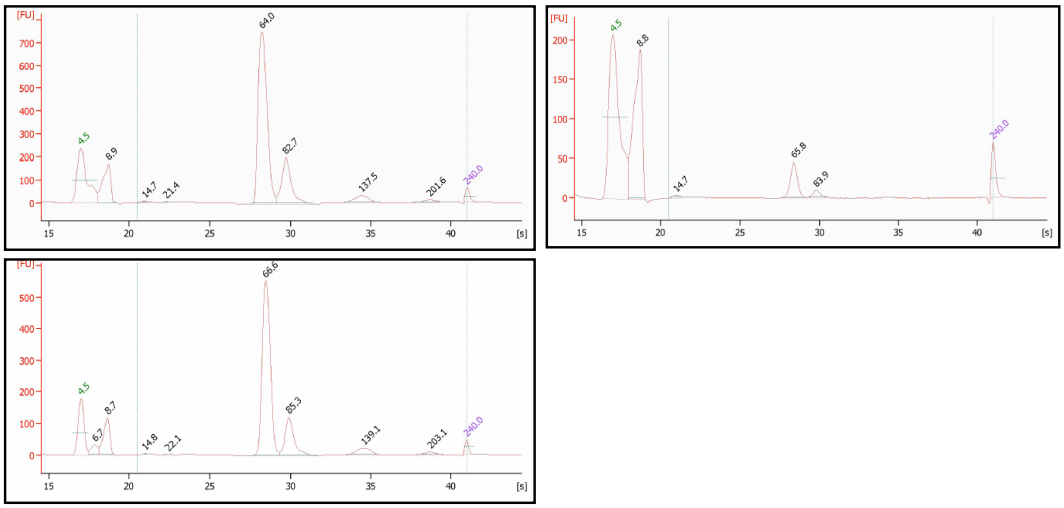

Fig. 21 Vesicle filtration/centrifugation through devices with 100 kDa cut off to remove BSA (67kDa). Electropherograms of vesicle preparation without treatment (top left); filtrate obtained after treatment (top right); held fraction obtained after treatment (bottom left).

For the same purpose, a gel filtration chromatography was performed. In this case the vesicles were expected to leave the column as first and BSA should be recovered later on. In the chromatogram (fig. 22) the peak correspondent to vesicles is very small and no peak correspondent to BSA is revealed. This indicates that BSA blocked the holes of the column avoiding both the passage of vesicles and its own outcome.

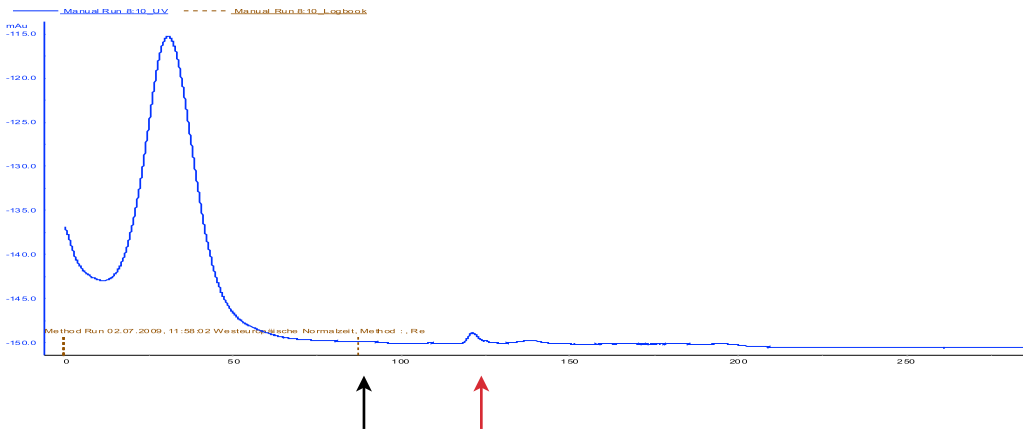

Fig. 22 Purification of vesicles by size exclusion chromatography through a Sepharose 2b column. X axis: time; Y axis: absorbance (280nm). The peak recorded before the black arrow is determined by the washing step of the column. After the sample loading (indicated by black arrow) we expected that the vesicles left the column as the leading fraction and that BSA went out of the column at the end. Actually the chromatogram shows that the putative vesicle peak (indicated by the red arrow) is very small and BSA doesn't give any peak at all.

Eventually, none of the mentioned methods succeed in obtaining a good purification.

Induction of vesicle shedding by Scatter Factor addition

In order to obtain a higher amount of vesicles and to decrease fetal bovine serum amount added to the culture, vesicle shedding could be induced in the presence of a growth factor that stimulates cell proliferation. Insulin had been reported to have a modest stimulatory effect on 8701 BC vesicle shedding (Cassarà et al., 1998). Hepatocyte growth factor/Scatter factor (HGF/SF) had not been tested. HGF however had been reported to stimulate the invasiveness of MDA MB 231 breast cancer cell line (Trusolino et al., 2000). It was therefore considered worthwhile to investigate its potential to increase vesicle shedding by breast carcinoma cells. A minimal amount of serum is necessary for HGF activity. Subconfluent 8701 BC cells were therefore incubated with/without HGF (40 ng/ µl) in the presence of 2.5% FBS. As control, cells were also incubated in the presence of 10% FCS, without HGF. Conditioned medium was collected after 3-24 hours and ultracentrifuged. Vesicle amount was measured by protein quantification using Bradford method. It was found that 8701 BC cells incubated in 2.5% FBS plus HGF shed twice the vesicle amount they released in its absence (fig. 23). Nevertheless the amount of shed vesicles was still rather low, moreover this method required a high amount of HGF, which is expensive, and BSA was still present in the vesicle pellets as contaminant (data not shown).

Overexpression of HGF produced by stromal cells has been found to act on breast cancer cells, through the binding to its receptor (c-met), where regulates the levels of unbound beta catenin favoring the E-cadherin junction disruption. Therefore HGF has been associated with a more aggressive phenotype (Logullo et al., 2010). Finally, the induction of vesicle production by HGF remarks the correlation between malignant phenotype and vesicle shedding.

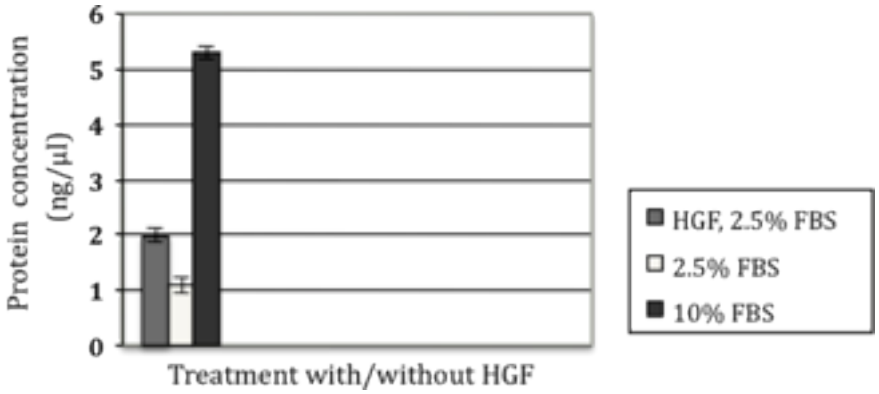

Fig. 23 Quantification of proteins in the vesicles shed from 8701 BC. Cell cultures were treated with/without HGF/SF. Shed vesicles were collected from conditioned medium by ultracentrifugation and analyzed by Bradford assay.

Purification and characterization of MDA MB 231 derived MVs.

In the second part of this study, MDA MB 231, a cell line derived from malignant pleural effusion of invasive breast cancer patient, has been chosen as system model for vesicle release. These cells had been shown to shed vesicles also in starvation from serum (Ginestra et al., 1998), thus leading to collect serum free vesicles. Although the cell line has been widely studied and characterized, the nature and the composition of shed vesicles are not yet investigated.

In this case, subconfluent cells were put in serum depleted medium. Conditioned medium was collected after 24 hours and treated as described above to obtain two vesicle fractions. In order to study vesicle morphology, transmission electron microscopy (TEM) analysis was performed. Electron micrographs revealed that the isolated extracellular particles consisted primarily of rounded vesicles with different size between the two fractions (fig. 24A). Quantitative analysis of those micrographs indicated a higher concentration of vesicles in the 100V fraction, around 6 times more than in the 15V fraction. As it is shown in the histogram (fig. 24B), a higher number of vesicles was recorded in the ultracentrifuged fraction (100V) for all the sizes, except for vesicles with diameter larger than 160 nm, which were more represented in 15V fraction. On the other hand, 100V fraction was found to contain vesicles with diameter ranging between 40 and 80 nm, which was compatible with the size previously reported for exosomes (Fevrier and Raposo, 2004).

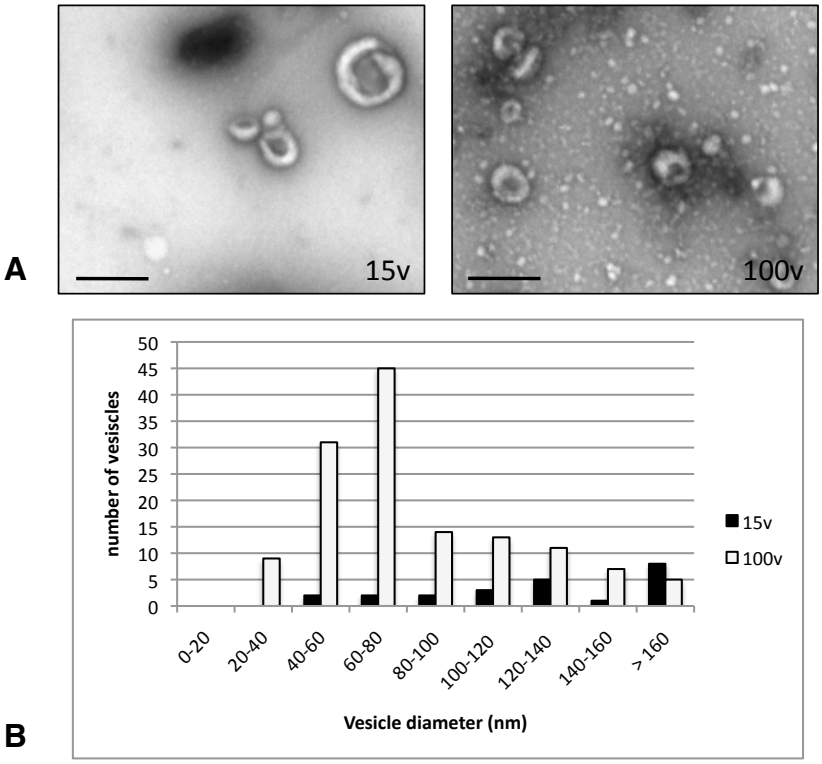

Fig. 24 Size distribution of microvesicles shed by MDA MB 231 in serum free medium. A). Representative transmission electron micrographs of negatively stained vesicles. Bar 200 nm. **B).** Histogram of quantitative analysis of vesicle diameter. For 15v fraction, n=23; for 100v fraction, n=134; n represents the number of analyzed vesicles. (15v) 15,000 x g fraction; (100v) 100,000 x g fraction.

Afterwards the protein content of those vesicles was examined. Western analysis showed the presence of vesicular markers such as Lamp1 and Hsc70 (fig. 25) in both the fractions, although at the higher levels in 100V than in 15V fraction.

Lamp1, that is lysosome-associated membrane glycoprotein 1, has the peculiarity to shuttle among lysosomes, endosomes and plasma membrane. Therefore it is acceptable its presence in cell lysate as well as in microvesicles, both membrane vesicles and exosomes. Moreover, since Lamp1 has been implicated in tumor metastasis, its presence in tumor derived microvesicles is in agreement with the data concerning the involvement of MVs in tumor progression.

Hsc70 is a chaperon with preferential localization in the cytoplasm and at the cell surface, taking part in several processes like cellular membrane organization

or post Golgi vesicle-mediated transport. It could assist the folding of the proteins carried out by vesicles.

Furthermore, western blotting analysis indicated that cytochrome C is not detectable in any of the fractions, leading to confirm the purity of vesicles from apoptotic blebs.

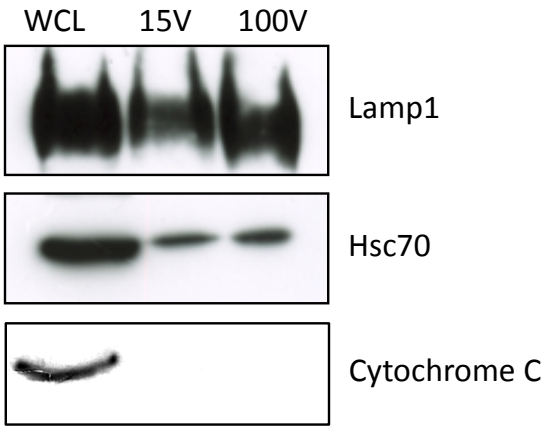

Fig. 25 Characterization of vesicles shed from MDA MB 231. Proteins from cell lysates (WCL) and vesicles pelletted either at 15,000 x g (15V) or at 100,000 x g (100V) were separated by electrophoresis and analysed by immunoblotting using antibodies to Lamp1 (125 kDa), Hsc70 (70 kDa) and cytochrome C (15kDa).

Immunofluorescence of MDA MB 231 cells

Vesicle shedding was further observed by immunofluorescence. Cells were grown on glass slides and once subconfluent they were fixed and labeled with antibodies against β1 integrin - known to be enriched in membrane vesicles (Dolo et al., 1998) - and Lamp1, or alternatively Hsc70 - both of which are known exosomal markers (Safaei et al., 2005; Mears et al., 2004). The proteins were detected by fluorophore-conjugated secondary antibodies. Analyses (shown in fig. 26a, 26c) led to observe that bigger size vesicles contain exclusively β1 integrin (marked by green fluorescence) while smaller vesicles may contain either β1 integrin or exosome markers (Lamp1 and Hsc70, marked by red fluorescence). In parallel, cells were grown into 3D collagene matrix and analyzed by confocal microscopy. Immunofluorescence image (fig. 26b) indicated that β1 integrin clusters into selective cell membrane areas. In some regions a co-localization of β1 integrin and Lamp1 was observed (marked by yellow fluorescence). It is presumable that membrane vesicles are shed from areas expressing only β1 integrin while regions containing also Lamp1 could represent points of exosome release.

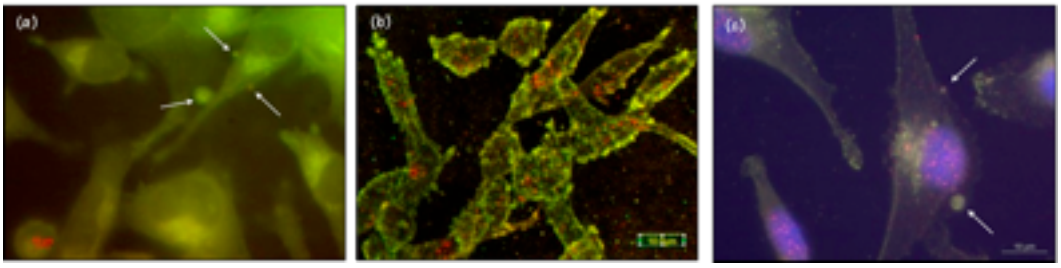

Fig. 26 Vesicle shedding by breast cancer MDA MB 231 cells. (a) Immunofluorescent microscopy of β1 integrin and Lamp1 in vesicles shed from cells grown on glass slides; (b) confocal microscopy of β1 integrin and Lamp1 in cells cultured in 3D collagene matrix; (c) immunofluorescent localization of β1 integrin and Hsc70 in vesicles shed by cells grown on glass slides. Anti-β1 integrin antibodies were revealed with FITC-conjugated secondary antibodies; anti-Lamp1 and anti-Hsc70 antibodies were revealed with TRITC-labeled secondary antibodies. Bar: 10 μm. Shed vesicles are indicated by arrows.

These observations confirmed that, as demonstrated for 8701 BC cells, MDA MB 231 cells release at least two vesicle populations that differ for size and protein composition. This finding encouraged the proteomic analysis of such vesicles.

Proteomic analysis of MDA MB 231 shed vesicles.

Afterwards, the attention was focused on proteomic analysis. Vesicles obtained by differential centrifugation were electrophoresed into 2D PAGE and the proteome profile was studied. The first vesicle maps showed still serum contaminants (fig. 27, left). This was due to the fact that the cells had been grown in the presence of serum until they reached 70-80% confluence.

To wash away the serum from cells before vesicle collection, an additional step was introduced during cell culture. In particular, serum depleted medium added to subconfluent cells was discarded after 4 hour incubation and fresh serum-free medium was added. Conditioned medium was collected after 24 hour incubation and used to obtain vesicle preparations. As shown in the proteomic maps (fig. 27), the new procedure led to an almost complete removal of serum proteins from vesicle preparations, thus becoming suitable for proteomic analysis.

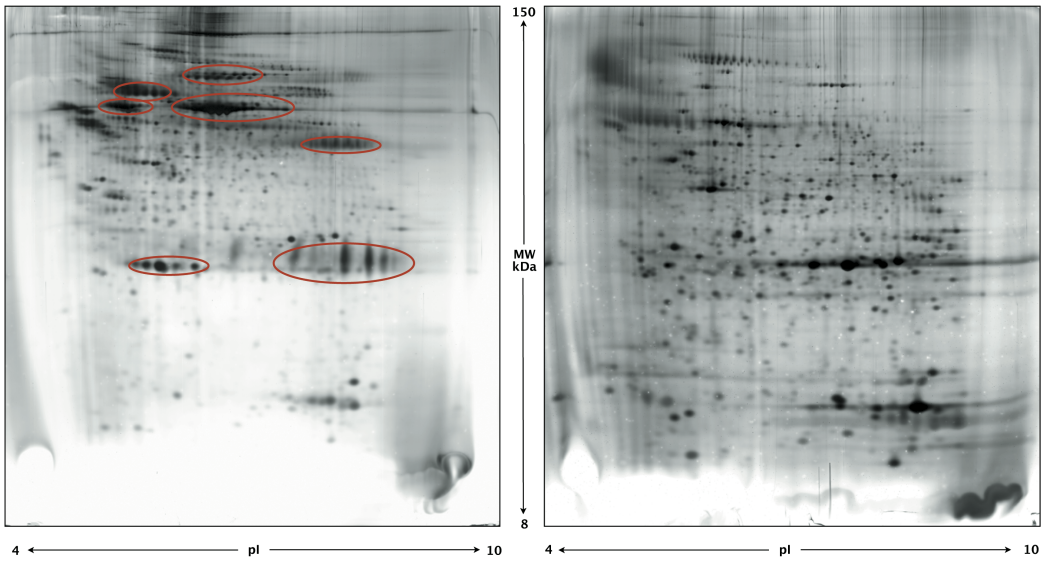

Fig. 27 Serum-free vesicles shed from MDA MB 231 cells. Proteomic map of vesicles (100V) obtained from 24 hour conditioned medium in serum-free conditions (left); proteomic map of vesicles (100V) from 24 hour-conditioned medium in serum-free conditions; in the latter case, a preliminary 4-hour wash of cells in serum-free medium was performed (new procedure, right). Red circles indicate serum proteins.

Using this procedure, 2D page analyses were performed in parallel for both the vesicles fractions and cell lysate. Representative 2-D gel images of whole cell

lysates and vesicles are shown in fig 28A and B. The protein identities, shown in 15V and 100V maps, are marked with packed labels corresponding to the accession numbers of the Swiss-Prot database, which also includes the major isoelectric variants of assigned proteins. The landmarks corresponding to the known proteins were found by gel matching with the reference proteomic maps present in the DOSAC-COBS 2D-PAGE database from the Expasy (Expert Protein Analysis System) server (http://expasy.org/world-2dpage/#DOSAC-COBS).

The gels were analyzed through the software Image Master 2D Platinum (Melanie V version) that allows both a qualitative and quantitative analysis. In particular, a quantitative analysis was carried out, comparing relative abundance of vesicular and cellular proteins, calculated for each spot as the relative percentage of spot intensity (integration of OD over the spot area) over the total spot intensity detected by the system in the map.

The proteins, whose ratio (vesicular amount: cellular amount) was at least 30% higher, were considered selectively targeted to the vesicles.

For what concerns the microvesicles obtained by ultracentrifugation (100V), all the proteins identified by gel matching and/or mass spectrometry sequencing are listed in table 1. Among these, 32 proteins were definitively found to be over represented in 100V in comparison with whole cell lysate.

The identities of the 32 protein spots (table 2) were successfully determined by mass spectrometry. The gel positions of those proteins are shown in the panel of the cropped images from 2-D matched gels (fig. 29) where qualitative differences among WCL, 15V and 100V fractions are also visible. Quantitative analysis is shown in the histogram plot below. Importantly, two independent vesicular preparations from MDA MB 231 were analyzed and showed a general good reproducibility, as it is indicated by the standard deviation values. Each vesicle preparation consisted of a pool of vesicles collected by several cell cultures, therefore the analysis on two samples can be considered statistically valid.

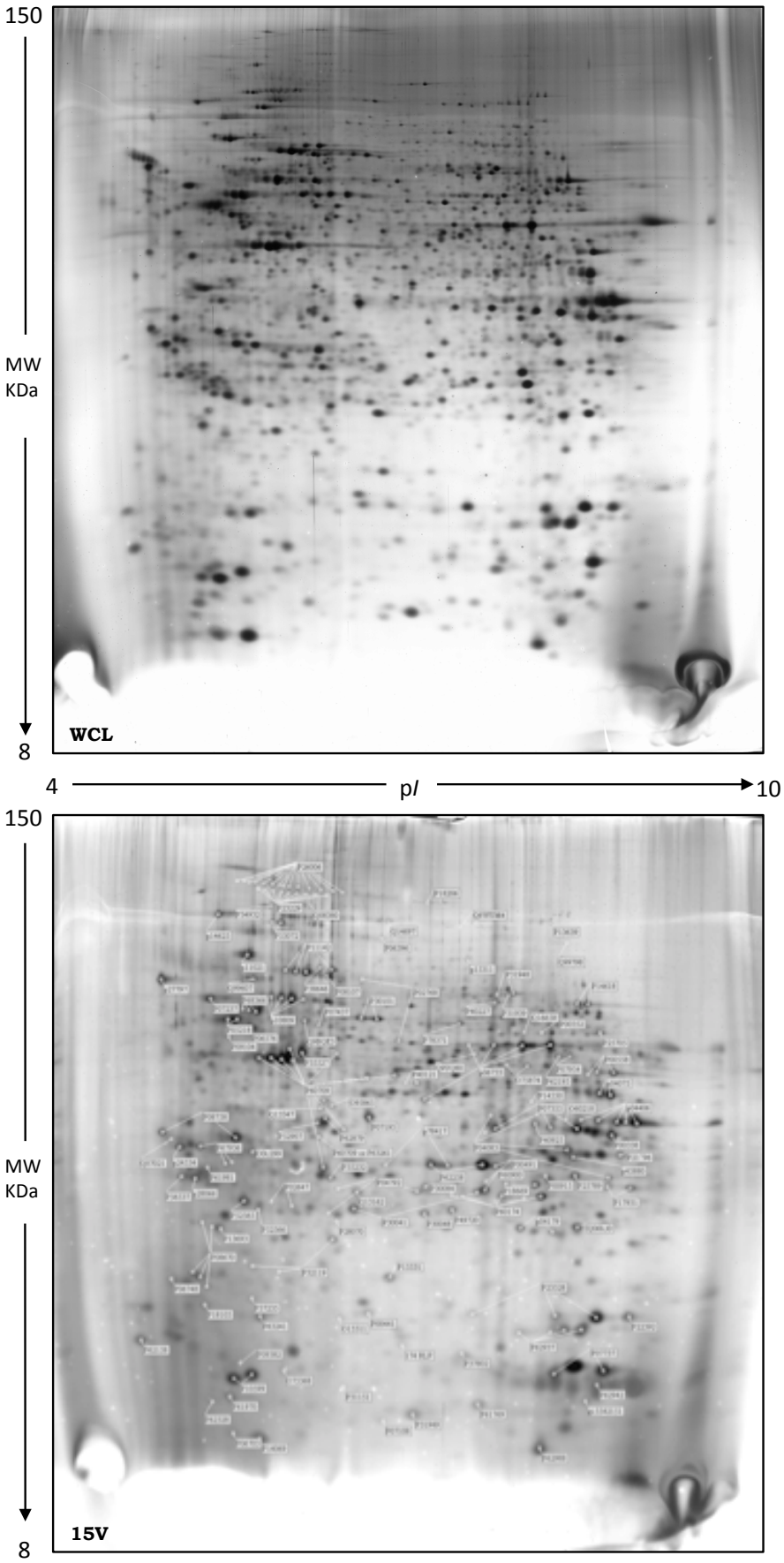

Fig. 28A Proteomic analysis of MDA MB 231 cells and shed vesicles.

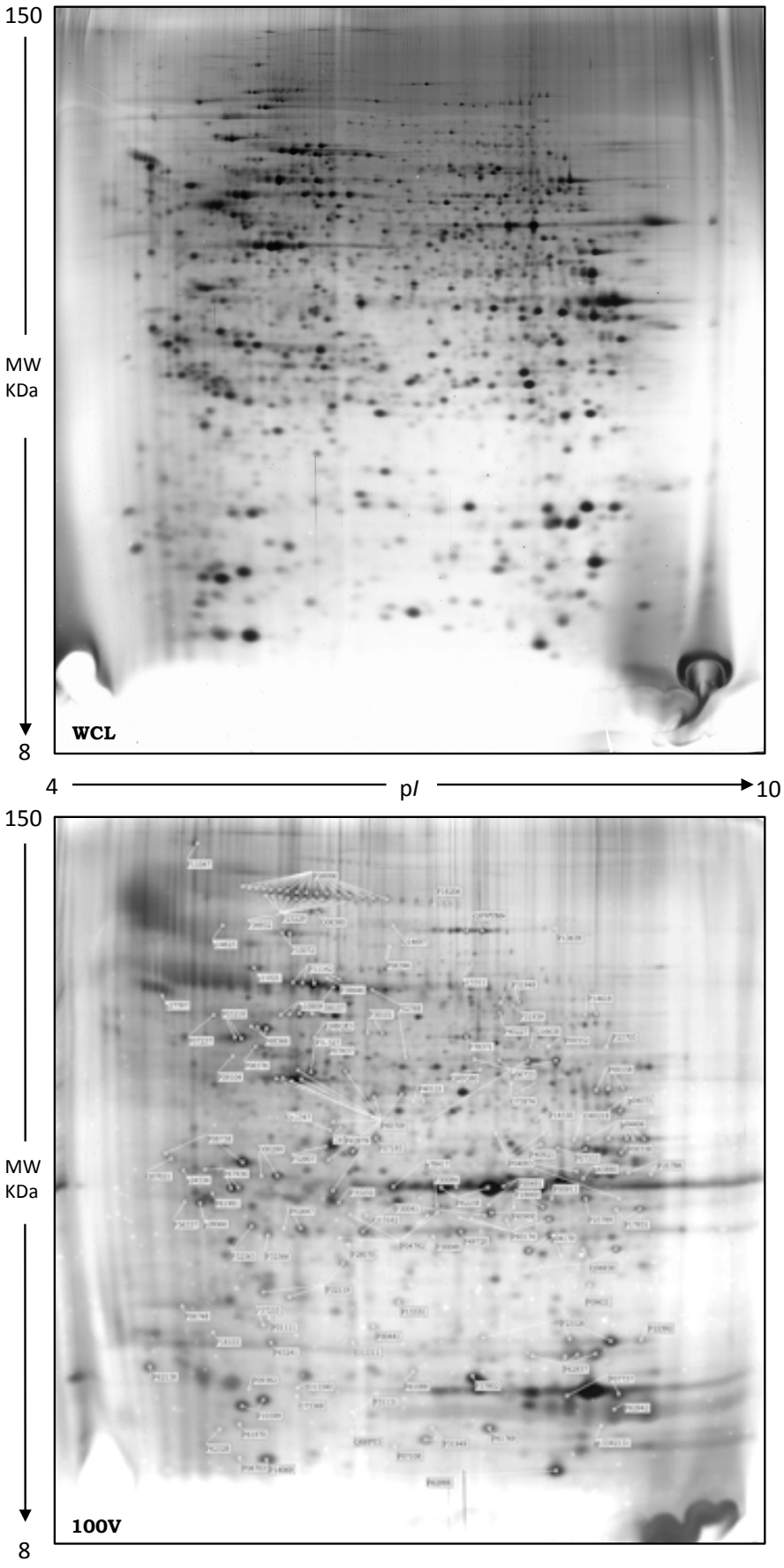

Fig. 28B Proteomic analysis of MDA MB 231 cells and shed vesicles.

Table1. Catalogue of the protein spots identified in the 2D-IPG map of 100V fraction, reported in fig. 28B, by gel matching with the reference maps present in DOSAC-COBS 2D database and/or by mass spectrometry sequencing. Protein names, accession numbers (AC) and abbreviated names correspond to the nomenclature used in the Swiss Prot database. The experimental values of pI and MW for every isoelectric spot were calculated with ImageMaster 2D Platinum system; the theoretical values represent the predicted MW and pI for each identified protein according to Swiss-Prot and TrEMBL databases.

Protein name	AC number	Abbreviated Name	Theor. MW	Exp. MW	Theor. Pi	Exp. Pi
14-3-3 protein gamma	P61981	1433G	28302	29134	4,8	4,87
14-3-3 protein epsilon	P62258	1433E a	29174	29859	4,63	5,76
14-3-3 protein epsilon	P62258	1433E b	29174	29859	4,63	6,44
Heterogeneous nuclear ribonucleoprotein A1	P09651	2UP1A (ROA1 chain A)	29386	19736	9,19	7,12
Acyl-CoA-binding protein	P07108	ACBP	10044	10157	6,12	5,88
Actin, cytoplasmic 1	P60709	ACTB/G	41737	42000	5,29	5,13
Actin, cytoplasmic 1	P60709	ACTB/G a	41737	45194	5,29	5,27
Actin, cytoplasmic 1	P60709	ACTB/G b	41737	45089	5,29	5,58
Actin, cytoplasmic 1	P60709	ACTB/G fr a	41737	40634	5,29	5,78
Actin, cytoplasmic 1	P60709	ACTB/G fr b	41737	41123	5,29	5,90
Actin, cytoplasmic 1	P60709	ACTB/G fr ab	41737	31828	5,29	5,39
Actin, cytoplasmic 1	P60709	ACTB/G fr c	41737	37265	5,29	5,51
Actin, cytoplasmic 1	P60709	ACTB/G fr e	41737	34234	5,29	5,64
Actin, cytoplasmic 1	P60709	ACTB/G fr g	41737	29454	5,29	5,51
Aldo-keto reductase family 1 member A1	P14550	AK1A1	36573	37737	6,32	6,43
Aldo-keto reductase family 1 member B10	O60218	AK1BA b	36021	35848	7,12	7,02
Retinal dehydrogenase 1	P00352	AL1A1	54862	50405	6,3	6,81
Serum albumin	P02768	ALBU	69367	69242	5,92	5,62
Serum albumin	P02768	ALBU fr	69367	46913	5,92	5,92
Fructose-bisphosphate aldolase A	p04075	ALDOA a	39420	38755	8,3	7,25
Fructose-bisphosphate aldolase A	p04075	ALDOA b	39356	38684	8,3	7,33
Annexin A1	P04083	ANXA1 a	38714	36856	6,57	6,50
Annexin A1	P04083	ANXA1 b	38714	36856	6,57	6,78
Annexin A1	P04083	ANXA1 sf1	38714	30801	6,57	7,04
Annexin A1	P04083	ANXA1 sf2	38714	28504	6,57	7,37
Annexin A2	P07355	ANXA2	38604	35236	7,57	7,05
Annexin A2	P07355	ANXA2 a	38604	36053	7,57	6,86
Annexin A5	P08758	ANXA5 a	35752	33762	4,83	4,51
Annexin A5	P08758	ANXA5 b	35752	31921	4,83	5,00
Annexin A6	P08133	ANXA6	75873	68300	5,42	5,30
Apolipoprotein A-I	P02647	APOA1 a	30778	24014	5,56	5,18
Apolipoprotein A-I	P02647	APOA1 b	30778	23885	5,56	5,24
Actin-related protein 2/3 complex subunit 5	O15511	ARPC5	16320	14634	5,47	5,64
ATP synthase subunit alpha, mitochondrial	P25705	ATPA	59751	50170	9,16	7,28
ATP synthase subunit beta, mitochondrial	P06576	ATPB	56560	50405	5,26	5,05
Beta-2-microglobulin	P61769	B2MG	13715	11910	6,06	6,45
Complement component 1 Q subcomponent-binding protein, mitochondrial	Q07021	C1QBP a	31362	32206	4,74	4,49
Carbonic anhydrase 1	P00915	CAH1	28870	28504	6,59	6,83
Calmodulin	P62158	CALM	16837	12118	4,09	4,36

Protein name	AC number	Abbreviated Name	Theor. MW	Exp. MW	Theor. Pi	Exp. Pi
Glutathione S-transferase omega-1	p78417	GSTO1 a	27566	29941	6,24	5,88
Glutathione transferase omega-1	p78417	GSTO1 b	27566	29941	6,24	6,21
Hippocalcin-like protein 1	P37235	HPCL1		16099	5,21	5,10
Heat shock protein beta-1	P04792	HSP27 a	22782	25337	5,98	5,62
Heat shock protein beta-1	P04792	HSP27 b	22783	25289	5,98	6,02
Heat shock protein beta-1	P04792	HSP27 c	22783	26306	5,98	5,79
Heat shock protein beta-1	P04792	HSP27 sf a	22783	24924	5,98	5,53
60 kDa heat shock protein, mitochondrial	p10809	HSP60 a	61055	59500	5,7	5,19
60 kDa heat shock protein, mitochondrial	p10809	HSP60 b	61055	59715	5,7	5,20
60 kDa heat shock protein, mitochondrial	p10809	HSP60 c	61055	59500	5,7	5,27
60 kDa heat shock protein, mitochondrial	p10809	HSP60 d	61055	59500	5,7	5,28
Heat shock 70 kDa protein 1	P08107	HSP71	70052	67997	5,48	5,45
Heat shock 70 kDa protein 4	P34932	HSP74	94331	110395	5,11	5,13
Heat shock cognate 71 kDa protein	P11142	HSP7C a	70898	68579	5,37	5,22
Heat shock cognate 71 kDa protein	P11142	HSP7C b	70898	68300	5,37	5,27
Heat shock cognate 71 kDa protein	P11142	HSP7C c	70898	68300	5,37	5,30
Heat shock cognate 71 kDa protein	P11142	HSP7C d	70898	69991	5,37	5,53
Isocitrate dehydrogenase [NADP] cytoplasmic	O75874	IDHC a	46659	42000	6,53	6,37
Isocitrate dehydrogenase [NADP] cytoplasmic	O75874	IDHC b	46659	42000	6,53	6,73
Eukaryotic translation initiation factor 3 subunit I	Q13347	IF32	36502	36502	5,38	5,44
Eukaryotic translation initiation factor 5A-1	P63241	IF5A	16832	14634	5,07	5,08
Eukaryotic translation initiation factor 6	P56537	IF6	26511	28117	4,63	4,68
Integrin alpha-3	P26006	ITA3 a	116612	115649	6,32	5,08
Integrin alpha-3	P26006	ITA3 b	116612	116338	6,32	5,28
Integrin alpha-3	P26006	ITA3 c	116612	117379	6,32	5,62
Integrin alpha-6	P23229	ITA6 a	126632	117205	6,39	5,02
Integrin alpha-6	P23229	ITA6 b	126632	117554	6,39	5,19
Integrin alpha-6	P23229	ITA6 c	126632	118254	6,39	5,42
Keratin, type I cytoskeletal 9	P35527	K1C9	62064	44881	5,14	5,27
Thiosulfate sulfurtransferase/rhodanese-like domain-containing protein 1	Q8NFU3	KAT	12530	11818	5,85	5,63
Pyruvate kinase isozymes M1/M2	P14618	KPYM a	57937	59500	7,96	7,08
Pyruvate kinase isozymes M1/M2	P14618	KPYM b	57937	59715	7,96	7,08
Laminin subunit gamma-1	P11047	LAMC1	177603	174282	5,01	4,94
L-lactate dehydrogenase A chain	P00338	LDHA	36689	33962	8,44	7,34
L-lactate dehydrogenase B chain	P07195	LDHB	36572	36493	5,7	5,71
Galectin-1	P09382	LEG1 b	14866	11414	5,32	5,10
Galectin-3	P17931	LEG3 a	26152	25728	8,58	7,44
Galectin-3	P17931	LEG3 b	26152	28801	8,58	7,46

Protein name	AC number	Abbreviated Name	Theor. MW	Exp. MW	Theor. Pi	Exp. Pi
Galectin-3-binding protein	Q08380	LG3BP	65331	112355	5,13	5,36
Malate dehydrogenase, cytoplasmic	P40925	MDHC	36426	35082	6,91	6,78
Macrophage Migration Inhibitory Factor	P14174	MIF b	12476	11350	7,73	7,30
Myosin regulatory light chain 12A	P19105	ML12A	19794	15512	4,67	4,88
Nucleoside diphosphate kinase A	P15531	NDKA	17208	17585	6,84	5,90
Nucleoside diphosphate kinase B	P22392	NDKB	17363	15837	6,97	7,52
Nucleophosmin	P06748	NPM fr	32560	16963	4,62	4,46
Nuclear transport factor 2	P61970	NTF2	14478	10970	5,1	4,60
Proliferation-associated protein 2G4	Q9UQ80	PA2G4	43787	45299	6,13	6,38
Programmed cell death 6-interacting protein	Q8WUM4	PDC6I a	96023	89509	6,13	6,11
Programmed cell death 6-interacting protein	Q8WUM4	PDC6I b	96023	89509	6,13	6,35
Protein disulfide-isomerase	P07237	PDIA1	57116	59500	4,76	4,89
Protein disulfide-isomerase A3	P30101	PDIA3 a	56782	52375	5,98	5,65
Protein disulfide-isomerase A3	P30101	PDIA3 b	56782	52265	5,98	5,77
Phosphoglycerate mutase 1	P18669	PGAM1 a	28804	27649	6,67	6,41
Phosphoglycerate mutase 1	P18669	PGAM1 b	28804	27091	6,67	6,78
Phosphoglycerate kinase 1	P00558	PGK 1 a	44615	41868	8,3	7,08
Phosphoglycerate kinase 1	P00558	PGK 1 b	44615	42000	8,3	7,27
Phosphoglycerate kinase 1	P00558	PGK 1 c	44550	42000	8,02	7,35
Prohibitin	P35232	PHB	29820	28040	5,57	5,46
Purine nucleoside phosphorylase	P00491	PNPH a	32118	30022	6,45	6,41
Purine nucleoside phosphorylase	P00491	PNPH b	32118	28172	6,45	6,45
Peptidyl-prolyl cis-trans isomerase A	P62937	PPIA b	18012	14853	7,68	6,71
Peptidyl-prolyl cis-trans isomerase A	P62937	PPIA c	18012	14676	7,68	6,95
Peptidyl-prolyl cis-trans isomerase A	P62937	PPIA d	18012	14853	7,68	7,19
Peptidyl-prolyl cis-trans isomerase A	P62937	PPIA e	18012	14429	7,68	7,19
Peroxiredoxin-1	Q06830	PRDX1	22176	22327	8,26	6,78
Peroxiredoxin-1	Q06830	PRDX1 b	22110	21208	8,27	7,06
Peroxiredoxin-1	Q06830	PRDX1 c	22110	21599	8,27	7,44
Peroxiredoxin-2	P32119	PRDX2	21892	22053	5,66	5,56
Peroxiredoxin-2	P32119	PRDX2 a	21892	18803	5,66	5,10
Peroxiredoxin-2	P32119	PRDX2 b	21892	18229	5,66	5,26
Peroxiredoxin-3	P30048	PRDX3	27693	23501	7,68	6,13
Peroxiredoxin-4	Q13162	PRDX4	30540	25289	5,86	5,66
Peroxiredoxin-6	P30041	PRDX6	25035	24538	6	5,68
Peroxiredoxin-6	P30041	PRDX6 b	25035	25289	6	6,37
Profilin-1	P07737	PROF1 a	15054	11486	8,44	6,97
Profilin-1	P07737	PROF1 b	14957	12217	8,46	7,40

Protein name	AC number	Abbreviated Name	Theor. MW	Exp. MW	Theor. Pi	Exp. Pi
Proteasome subunit alpha type-4	P25789	PSA4	29484	28504	7,58	7,05
Proteasome subunit alpha type-5	p28066	PSA5	26411	26350	4,74	4,84
Proteasome subunit alpha type-6	P60900	PSA6	27372	25483	6,35	6,47
Proteasome subunit beta type-3	P49720	PSB3	22949	24538	6,14	6,16
Proteasome subunit beta type-4	P28070	PSB4	29204	22131	5,72	5,61
Bifunctional purine biosynthesis protein PURH	P31939	PUR9	64616	63758	6,27	6,39
GTPase NRas		RASN	21229	16451	5,01	5,09
Protein S100-A6	P06703	S10A6 a	10180	9184	5,32	4,60
Protein S100-A6	P14069	S10A6 b	10051	8993	5,3	5,00
Protein S100-A7	P31151	S10A7 a	11471	11132	6,27	5,65
Protein S100-A11	P31949	S10AB a	11083	11910	5,28	6,11
Protein S100-A11	P31949	S10AB b	11083	10742	5,28	5,98
SH3 domain-binding glutamic acid-rich-like protein	O75368	SH3L1 b	12774	11486	5,22	5,28
Superoxide dismutase [Cu-Zn]	P00441	SODC	15943	16041	6,02	5,74
Superoxide dismutase [Mn], mitochondrial	P04179	SODM a	24722	21278	8,35	6,63
Superoxide dismutase [Mn], mitochondrial	P04179	SODM b	24722	21559	8,35	6,92
Stress-induced-phosphoprotein 1	P31948	STIP1 a	62639	66331	6,4	6,51
Stress-induced-phosphoprotein 1	P31948	STIP1 b	62639	66331	6,4	6,50
Transgelin-2	P37802	TAGL2	22391	12031	8,41	6,05
Tubulin alpha-1 chain	P68366	TBA1 a	49924	54581	4,95	5,10
Tubulin alpha-1 chain	P68366	TBA1 b	49924	54220	4,95	5,11
Tubulin alpha-1 chain	P68366	TBA1 c	49924	53152	4,95	5,00
Tubulin alpha-1C chain	Q9BQE3	TBA1C	49895	51609	4,96	5,30
Tubulin beta chain	P07437	TBB5 a	49671	51609	4,78	4,95
Tubulin beta chain	P07437	TBB5 b	49671	51802	4,78	4,98
Tubulin beta chain	P07437	TBB5 c				
T-complex protein 1 subunit beta	P78371	TCPB	57488	51718	6,01	6,11
T-complex protein 1 subunit zeta	P40227	TCPZ	58024	58908	6,24	6,43
Transitional endoplasmic reticulum ATPase	P55072	TERA a	89322	88952	5,14	5,17
Transitional endoplasmic reticulum ATPase	P55072	TERA b	89322	88767	5,14	5,2
Thioredoxin	p10599	THIO b	11737	11296	4,82	4,99
Triosephosphate isomerase	P60174	TPIS b	26669	25096	6,45	6,18
Triosephosphate isomerase	P60174	TPIS c	26669	25048	6,45	6,06
Triosephosphate isomerase	P60174	TPIS d	26669	24684	6,45	6,29
Triosephosphate isomerase	P60174	TPIS e	26669	24938	6,45	6,56
Triosephosphate isomerase	P60174	TPIS f	26669	25000	6,45	6,81
Tropomyosin alpha-4 chain	P67936	TPM4 b	28522	32180	4,67	4,76
Tropomyosin alpha-4 chain	P67936	TPM4 c	28522	29778	4,67	4,93
Tropomyosin alpha-4 chain	P67936	TPM4 d	28522	29859	4,67	4,70
Thymosin beta-4	P62328	TYB4	5053	12200	5,02	4,79
Ubiquitin-conjugating enzyme E2 N	P61088	UBE2N	17138	12074	6,13	5,94
Ubiquitin-60S ribosomal protein L40	P62987	RL40 b	14728	9363	9,87	6,89
Voltage-dependent anion-selective channel protein 1	P21796	VDAC1 a	30773	31017	8,62	7,41
Voltage-dependent anion-selective channel protein 1	P21796	VDAC1 b	30773	31393	8,62	7,56
Voltage-dependent anion-selective channel protein 2	P45880	VDAC2	31566	31017	7,5	7,06
Vinculin	P18206	VINC a	123799	119845	5,5	5,56
Vinculin	P18206	VINC b	123799	119667	5,5	5,95

Table2. List of the protein spots enriched in 100V fraction and identified by mass spectrometry. Protein names, accession numbers (AC) and abbreviated names correspond to the nomenclature used in the Swiss-Prot database. The experimental values of pI and MW for every isoelectric spot were calculated with ImageMaster 2D Platinum system; the theoretical values represent the predicted MWand pI for each identified protein according to Swiss-Prot and TrEMBL databases. Identification methods: 1, MALDI-TOF; 2, N-terminal sequencing by automated Edman degradation; 3, Liquid chromatography MS/MS.

Protein name	AC number	Abbreviated Name	Theor. MW	Exp. MW	Theor. Pi	Exp. Pi	ID methods	% MASSES MATCHED	Sequence coverage (%), N-terminal residues, Score
14-3-3 protein epsilon	P62258	1433E a	29174	29859	4,63	5,76	3		40,16
14-3-3 protein epsilon	P62258	1433E b	29174	29859	4,63	6,44	3		40,17
Actin, cytoplasmic 1	P60709	ACTB/G fr b	41737	42000	5,29	5,30	1	24	22
Annexin A5	P08758	ANXA5 a	35937	31921	4,94	5,00	1	53	64
Beta-2-microglobulin	P61769	B2MG	13715	9872	6,06	6,71	2	-	res. 21-30
Fascin	Q16658	FSCN1	54530	50170	6,84	6,56	1	60	29
Guanine nucleotide-binding protein G(I)/G(S)/G(T) subunit beta-2	P62879	GBB2	37331	35848	5,6	5,45	1	18	30
Heat shock 70 kDa protein 1	P08107	HSP71	70052	67568	5,48	5,63	1	38	38
Integrin alpha-3	P26006	ITA3 a	116612	115649	6,32	5,08	3		190,24
Integrin alpha-3	P26006	ITA3 b	116612	116338	6,32	5,28	1	64	9
Integrin alpha-3	P26006	ITA3 c	116612	117379	6,32	5,62	3		170,24
Integrin alpha-6	P23229	ITA6 a	126632	117205	6,39	5,02	3		220,23
Integrin alpha-6	P23229	ITA6 b	126632	117554	6,39	5,19	1	43	21
Integrin alpha-6	P23229	ITA6 c	126632	118254	6,39	5,42	3		310
Keratin, type I cytoskeletal 9	P35527	K1C9	62064	44881	5,14	5,27	1	18	11
Laminin subunit gamma-1	P11047	LAMC1	177603	174282	5,01	4,94	1	36	9
Galectin-3-binding protein	Q08380	LG3BP	65331	112355	5,13	5,36	1	38	21
Programmed cell death 6-interacting protein	Q8WUM4	PDC6I a	96023	89509	6,13	6,11	3		80,23
Programmed cell death 6-interacting protein	Q8WUM4	PDC6I b	96023	89509	6,13	6,35	1	53	8
Peroxiredoxin-2	P32119	PRDX2 a	21892	18803	5,66	5,10	1	18	36
Peroxiredoxin-2	P32119	PRDX2 b	21892	18229	5,66	5,26	1	17	36
Peroxiredoxin-6	P30041	PRDX6	25035	24538	6	5,68	1	53	34
Proteasome subunit alpha type-6	P60900	PSA6	27399		6,35		1	28	35
Proteasome subunit beta type-3	P49720	PSB3	22949	24538	6,14	6,16	1	100	34
Ubiquitin-60S ribosomal protein L40	P62987	RL40	14728	9363	9,87	6,89	1	80	61
Transgelin-2	P37802	TAGL2	22391	12031	8,41	6,05	1	39	33
Tubulin alpha-1C chain	Q9BQE3	TBA1C	49895	51609	4,96	5,30	1	60	19
Transitional endoplasmic reticulum ATPase	P55072	TERA	89322	88767	5,14	5,2	1	26	46
Tropomyosin alpha-4 chain	P67936	TPM4 d	28522	29859	4,67	4,70	1	63	10
Tropomyosin alpha-4 chain	P67936	TPM4 c	28522	29778	4,67	4,93	1	63	16

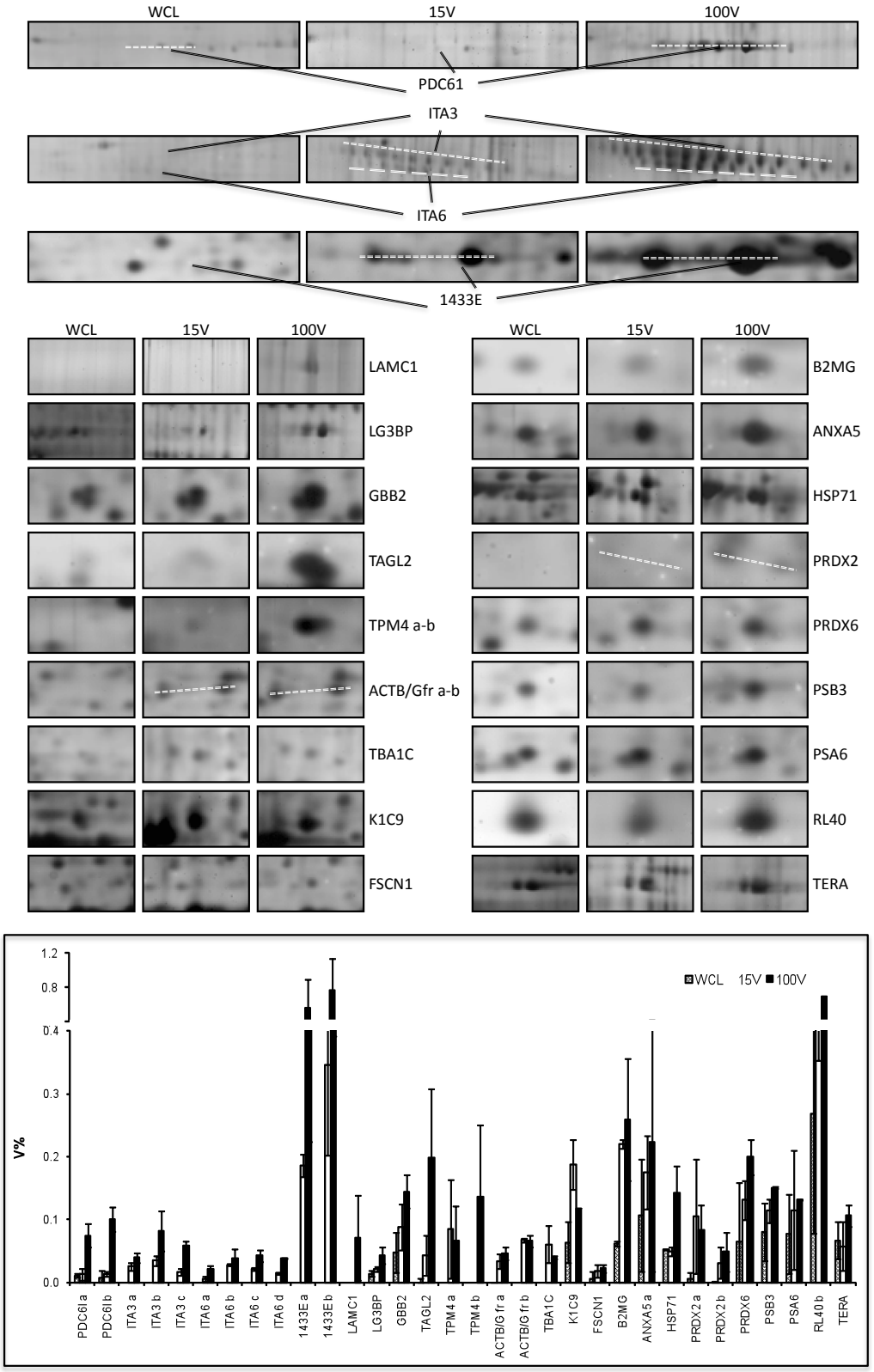

Fig. 29 Comparative qualitative/quantitative analysis of proteins enriched in 100V fraction. Above the cropped gel areas show the gel positions of the proteins found to be more abundant in 100V than in WCL and 15V. Below the histogram plot shows the quantitative analysis. V% represents the relative percentage volume.

Furthermore the 32 protein spots were grouped on the basis of their sub-cellular localization and biological processes in which they are known to be involved, using gene ontology classification taken by UniProt-K database (from Expasy server) and confirmed with Exocarta database (fig. 30). The majority of the proteins comes from the cytoplasm (36%), plasma membrane (29%), cytoskeleton (20%) and extracellular space (7%). Minor represented categories are endoplasmic reticulum, endosome membrane and lysosome (3% each one). For what concerns the major biological processes, the classification shows that most of the proteins are involved in cell adhesion (29%), cell structure and motility (19%), signal transduction (10%) and protein metabolism and modification (13%). Proteins involved in detoxification and redox reaction (10%), immune response (3%), protein transport (7%), antiapoptosis (6%) and developmental processes (3%) are also present.

subcellular localization						
cytoplasm	cytoskeleton	plasma membrane	endoplasmic reticulum	endosome membrane	lysosome	extracellular space
1433E a	ACTB/G fr b	B2MG	HSP71	RL40	PRDX6	LAMC1
1433E b	FSCN1	ITA3 a				LG3BP
ANXA5 a	K1C9	ITA3 b				
GBB2	TBA1C	ITA3 c				
PDC6I a	TPM4 c	ITA6 a				
PDC6I b	TPM4 d	ITA6 b				
PRDX2 a		ITA6 c				
PRDX2 b		ITA6 d				
PSB3		TAGL2				
TERA						
PSA6						

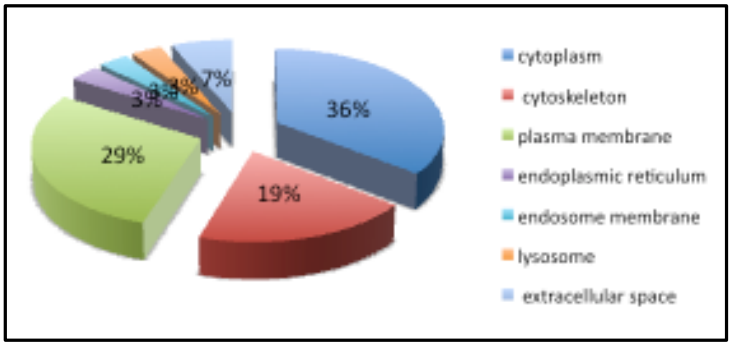

A

biological process								
cell structure and motility	cell adhesion	signal transduction	protein degradation/ modification	detoxification and redox proteins	immune response	protein transport	anti-apoptosis	developmental processes
ACTB/G fr b	ITA3 a	1433E a	PSA6	PRDX2 a	B2MG	PDC6I a	HSP71	TAGL2
FSCN1	ITA3 b	1433E b	PSB3	PRDX2 b		PDC6I b	ANXA5 a	
K1C9	ITA3 c	GBB2	RL40	PRDX6				
	ITA6 a		TERA					
TBA1C	ITA6 b							
TPM4 c	ITA6 c							
TPM4 d	ITA6 d							
	LAMC1							
	LG3BP							

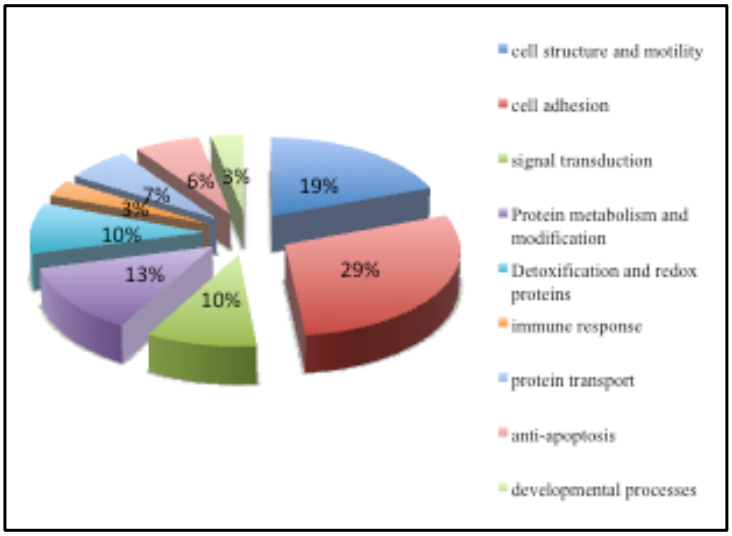

B

Fig. 30 Classification of identified proteins by (A) sub-cellular localization and (B) biological process. The categories are extrapolated from Gene Ontology from UniProtK and Exocarta databases.

Previous proteomic studies (Mathivanan et al., 2010; Choi et al., 2007; Mears et al., 2004) considered all proteins they found in vesicles as belonging to shed vesicles. Nevertheless a protein specifically destined to these particles is expected to be enriched in vesicle preparation compared to different cell regions. Therefore, in this study only the proteins that were at least 30% more abundant in vesicle preparations than in whole cell lysate, are considered to be really vesicular proteins. Other components could be due to the presence of cell debris.

In order to focus on the possible main functions of those microparticles, indicated by their protein composition, a brief description of the proteins found enriched in 100V fraction is added.

First PDC6I (2 isoforms), ITA3 (3 isoforms), ITA6 (3 isoforms) and 1433E (2 isoforms) are found to be highly abundant in 100V fraction, less present in 15V fraction (see the panel in fig. 29). The same spots are almost undetectable in the whole cell lysate. Certainly the lacking of those spots in the WCL does not imply the absence of the correspondent proteins in the cells. It may rather indicate that these proteins are under represented in the whole cellular protein extract and, therefore, their amount is under the sensitivity threeshold of the analytical method. PDC6I, namely programmed cell death 6-interacting protein, is documented to be involved in concentration and sorting of cargo proteins of the multivesicular body (MVB) for incorporation into intralumenal vesicles (ILVs) that are generated by invagination and scission from the limiting membrane of the endosome. After fusion of MVB with the plasma membrane ILVs are released in the extracellular space as exosomes. Therefore the presence of PDC6I in 100,000 xg fraction strengthens the exosomal nature of those vesicles. PDC6I has been found in other exosomal preparations from colon rectal cancer, melanoma and other cancers (Mathivanan et al., 2010b; Choi et al., 2007; Mears et al., 2004).

ITA3 (α3 integrin) and ITA6 (α6 integrin) are involved in cell-extracellular matrix adhesion. In particular, α3 integrin is usually found in association with β1 integrin. By the way, β1 integrin itself had been previously found enriched in breast cancer shed vesicles (Dolo et al., 1998). The heterodimer works as receptor

for several ECM components such as fibronectin, laminin, collagen, epiligrin, thrombospondin and CSPG4, favoring vesicle anchorage to ECM. In association with LGALS3, a lectin also found in exosomes (Mathivanan et al., 2010), α3/β1 receptor may mediate the stimulation of endothelial cells migration (Fukushi et al., 2004), having a further role in angiogenesis. A structural role in the hemidesmosomes is attributed to α6 integrin, associated with either β1 or β4 integrin. In epithelial cells, α6/β4 integrin is a receptor for laminin. Moreover, it has been found also an enrichment in galectin-3-binding protein (GL3BP), that promotes integrin-mediated cell adhesion.

Laminin subunit γ-1 was also found to be enriched in these microvesicles. Laminin is known to be involved in cell migration, in ECM disassembly as well as in cell proliferation, confirming the role of exosomes in several aspects of tumor progression.

Another protein highly expressed in exosomes is tyrosine 3-monooxygenase/ tryptophan 5-monooxygenase activation protein, epsilon polypeptide (two isoforms were identified), that is undetectable in WCL. It belongs to the 14-3-3 family. 14-3-3 proteins regulate many cellular processes that are implicated in cancer development and the seven 14-3-3 isoforms have different expression level and isoform-specific roles in different tumors. In particular, the overexpression of 14-3-3 epsilon has been demonstrated to prompt the abnormal growth of renal tumor cells *in vitro* (Liang et al., 2009). This protein has been found also in exosomes derived from biological fluids such as urine (Gonzales et al., 2009). Taken together, these data let to infer that 14-3-3 epsilon protein could represent an important new tumor biological marker.

Exosomes can vehicle also protein G, as demonstrated by the enrichment of guanine nucleotide-binding protein G(I)/G(S)/G(T) subunit beta-2 (GBB2). This protein has been already found in exosomes from breast cancer cells and breast milk (Staubach et al., 2009; Admyre et al., 2007).

Another protein found particularly abundant in exosomes is transgelin2 (TAGL2) already found in other origin exosomes, among them exosomes derived

from colorectal cancer (Choi et al., 2007; Mathivanan et al. 2010b). Furthermore, overexpression of TAGL2 has been recently indicated as potential new biomarker for predicting progression and prognosis of colon rectal cancer (Zhang et al., 2010). Transgelin-2 has not yet a defined role in microvesicles. Nevertheless, as it contains a calpoin-like repeat able to bind to actin and tropomyosin, a role of transgelin in cytoskeleton organization, aimed to the shedding process, can be supposed.

It is conceivable that extracellular vesicle shedding include a profound rearrangement of cytoskeleton. Therefore it is not surprising to find in microvesicles an enrichment in proteins involved in cell structure and motility, such as tropomyosin alpha-4 chain (two isoforms) that binds to actin filaments, contributing to cytoskeleton stabilization. Also actins (ACTB/G fr a-b) are highly represented in exosomes. It is found also an enrichment in fascin (FSCN1), a protein responsible of organizing filamentous actin into bundles present in microspikes, membrane ruffles, and stress fibers. Tubulin alpha-1C chain, involved in microtubule based movement, is highly abundant in exosomes, suggesting a role of microtubules also in microvesicle shedding. Another constituent of cytoskeleton highly expressed in exosomes is keratin type I cytoskeletal 9 (K1C9), a protein which plays a role in organization of intermediate filaments.

Among the proteins enriched in exosomes, there is also beta2 microglobulin (B2MG), the beta-chain of major histocompatibility complex class I molecules. Since this protein is involved in the presentation of peptide antigens to the immune system it could play an important role in immune system modulation during tumor progression. Moreover B2MG has been found in urine, where it could be released, at least in part, by a vesicle-mediated mechanism (Gonzales et al., 2009). This could render B2MG a potential tumor biomarker, easily recoverable from biological fluids.

Annexin A5 has been extensively demonstrated to be characteristic of vesicles. It has been found particularly abundant in exosomes, with possible implications in activation of anti-apoptotic pathways, thus helping cell survival.

Molecular chaperons are widely accepted to be typical in microvesicles. In exosomes it is found specifically an enrichment in heat shock 70 kDa protein 1, involved in protein folding. This protein has also been found enriched in exosomes from breast milk (Admyre et al., 2007).

Peroxiredoxin-2 (two isoforms) and peroxiredoxin-6, proteins involved in oxidation-reduction processes, are also highly represented in exosomes. The presence of PRDX-2, already documented in other cancer derived microvesicles (Staubach et al., 2009; Mathivanan et al., 2009), is challenging because it has been identified as early-stage breast cancer auto antigen, useful in earlier diagnosis of aggressive breast cancer (Desmetz et al., 2009). Also PRDX-6 has demonstrated to be related to breast cancer malignancy. In particular, overexpression of peroxiredoxin 6 leads to a more invasive phenotype and metastatic potential in human breast cancer (Chang et al., 2007). Its presence in tumor microvesicles suggests that it can be considered a potential biomarker for breast cancer. PRDX-6 was observed in microvesicles of different origin (Choi et al., 2007; Gonzales et al., 2009) but this is the first work in which PRDX-6 is observed in microvesicles derived from breast cancer.

Proteins taking part in the proteasome complex are also found to be typical of breast cancer exosomes. These include proteasome subunit beta type-3 (PSB3), proteasome subunit alpha type-6 (PSA6), ubiquitin-60S ribosomal protein L40 (RL40) and transitional endoplasmic reticulum ATPase (TERA). TERA is necessary for the vesicle budding that occurs for transferring membranes from transitional endoplasmic reticulum to the Golgi apparatus. TERA and RL40 had been already found in microvesicles of other origin (Choi et al., 2007), while, at our knowledge, PSA6 and PSB3 had not been mentioned before.

While 100V fraction shows a protein profile considerably different from WCL, the protein profile of 15V fraction is more similar to the whole cell lysate,

containing similar levels of metabolic enzymes. This fraction contains also typical vesicular proteins, found at lower levels than in 100V vesicles.

Nevertheless qualitative/quantitative analysis indicated that 15V fraction is particularly enriched in 6 proteins that are listed in table 3. Their identity has been found by mass spectrometry. The quantitative data are shown in the histogram plot (fig. 31).

As first, 15V is characterized by an enrichment in cytoskeleton proteins such as an isoform of cytoplasmic 1 actin (ACTB/G a). This fraction revealed the high presence of ETS-related transcription factor Elf-4 (ELF-4) that transactivates promoters of the hematopoietic growth factor genes CSF2, IL3, IL8 and has a role in tumorigenesis (Yi et al., 2009). The protein disulfide-isomerase A3 (PDIA3) is also found at high levels, in agreement with data reported in Exocarta database. Furthermore, high expression levels of peroxiredoxins have been discovered in this fraction. In particular analysis indicated enrichment in PRDX2 - an isoform different than the two observed in 100V - and PRDX3, that has also a significant role in cell cycle regulation and could be a potential proliferation marker in breast cancer (Chua et al., 2010).

Eventually five enriched protein spots analyzed by mass spectrometry corresponded to different fragments of vimentin. Vimentins are class-III intermediate filaments found in various non-epithelial cells, especially mesenchymal cells. Therefore their presence attests the epithelial-mesenchimal transition occuring in cell transformation towards a malignant phenotype. This is the first work in which vimentins have been observed in microvesicles derived from human cells.

Table 3. List of the protein spots enriched in the 2D-IPG map of 15V fraction and identified by mass spectrometry. Protein names, accession numbers (AC) and abbreviated names correspond to the nomenclature used in the Swiss Prot database. The experimental values of pI and MW for every isoelectric spot were calculated with ImageMaster 2D Platinum system; the theoretical values represent the predicted MWand pI for each identified protein according to Swiss-Prot and TrEMBL database. Identification methods: 1, MALDI-TOF; 2, N-terminal sequencing by automated Edman degradation.

Protein name	AC number	Abbreviated Name	Theor. MW	Exp. MW	Theor. Pi	Exp. Pi	ID methods	% MASSES MATHCHED	Sequence coverage (%), N-terminal residues, score
Actin, cytoplasmic 1	P60709	ACTB/G a	41737	45194	5,29	5,27	1	18	30
ETS-related transcription factor Elf-4	Q99607	ELF4	70730	69242	5,41	5,1	1	4	22
Protein disulfide-isomerase A3	P30101	PDIA3 b	56782	52265	5,98	5,77	1	57	27
Peroxiredoxin-2	P32119	PRDX2 c	21892	22053	5,66	5,56	2		177-191
Peroxiredoxin-3	P30048	PRDX3	27693	24697	7,68	6,11	1	22	64
Vimentin	P08670	VIME fr a	53652	22064	5,06	4,78	1	14	32
Vimentin	P08670	VIME fr b	53652	21599	5,06	4,82	1	29	18
Vimentin	P08670	VIME fr c	53652	18229	5,06	4,81	1	37	17
Vimentin	P08670	VIME fr d	53652	17299	5,06	4,76	1	52	30
Vimentin	P08670	VIME fr e	53652	16754	5,06	4,84	1	40	18

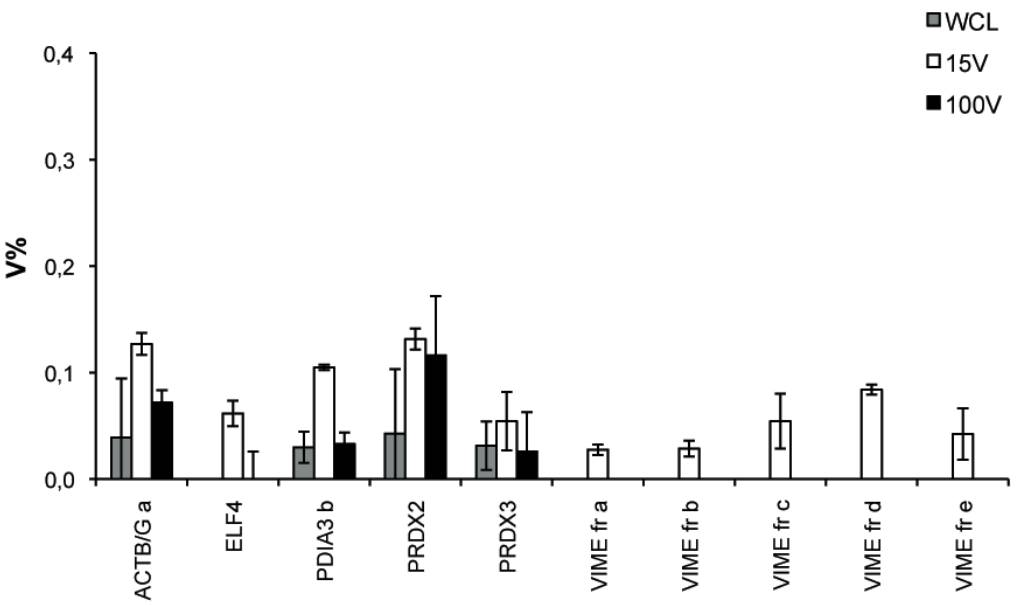

Fig. 31 Quantitative analysis of proteins enriched in 15V fraction. The histogram plot reports the values of percentage volume of the proteins found to be highly represented in 15V, in comparison with WCL and 100V.

Moreover, mass spectra of five other proteins being over represented in 15V fraction (less represented in 100V and almost undetectable in WCL) do not correspond to any known protein sequence present in databases. Figure 32 shows the gel positions (with pI and MW annotations) and the mass spectra of unidentified proteins.

Reported data indicate that 15V vesicles could represent a population of vesicles different from the one of exosomes (100V). It is in fact specifically enriched in a different subset of proteins. This fraction seems however to be partially contaminated by cell debris and by 100V exosomes. It is possible that a little part of exosomes is pull down already at 15,000 xg centrifugation.

Moreover about one half of the proteins which are enriched in 15V fraction are unknown. However, their high relative abundance in 15V suggests that they could play central roles in the function of these extracellular large vesicles and therefore they are worth to be more deeply investigated.

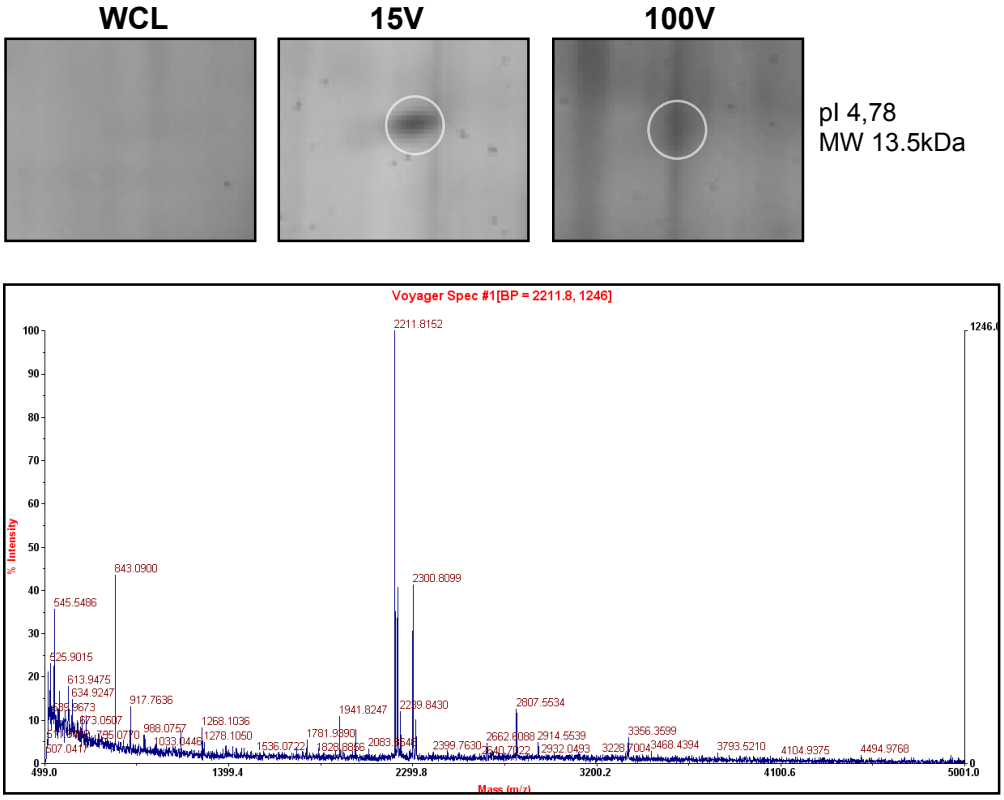

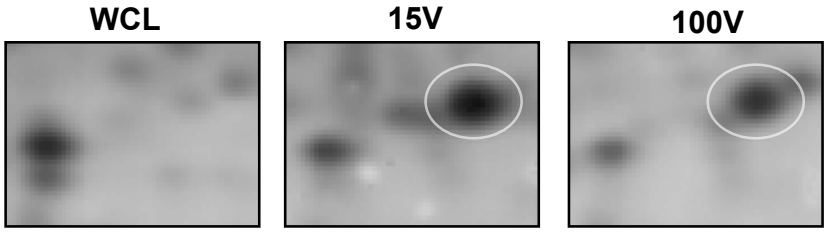

pI 6,13
MW 39kDa

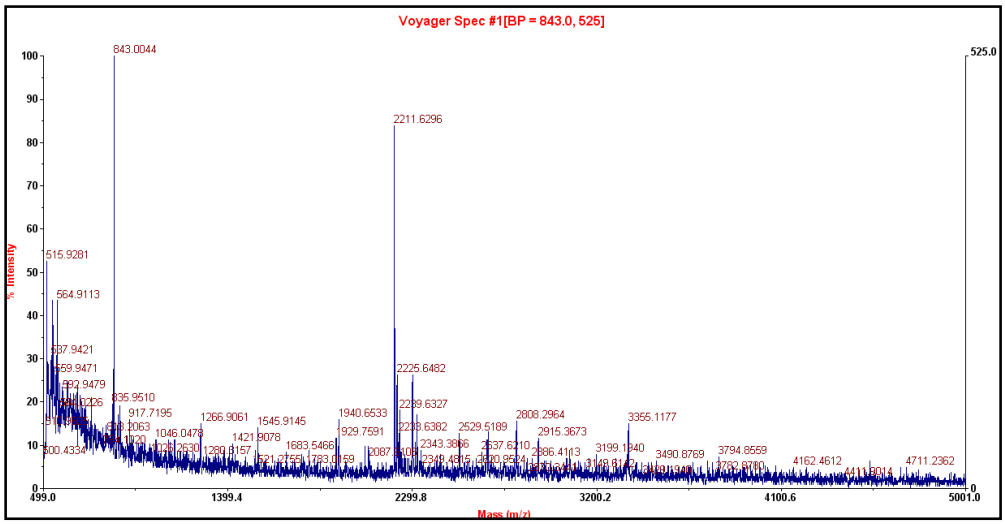

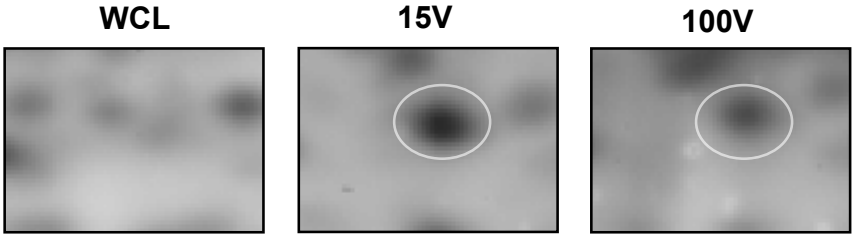

pI 5,65
MW 28.5kDa

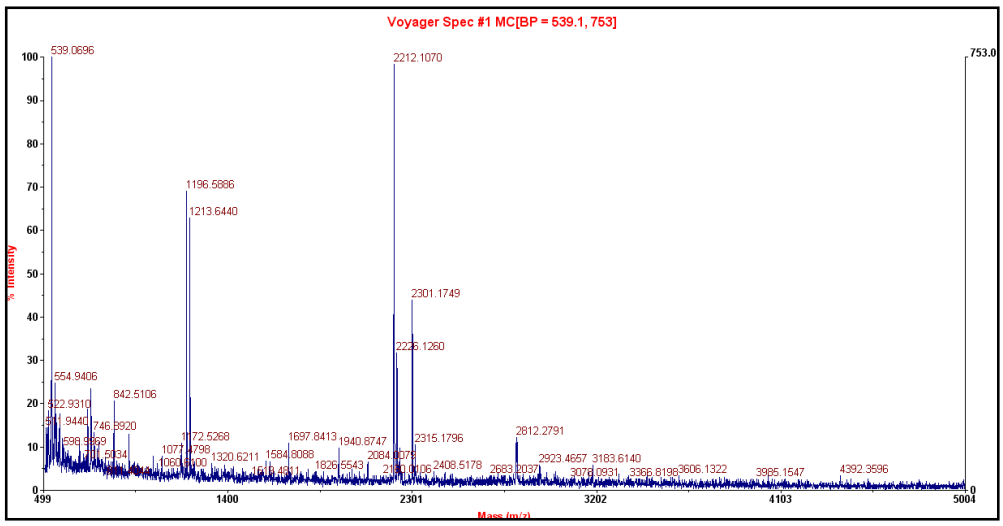

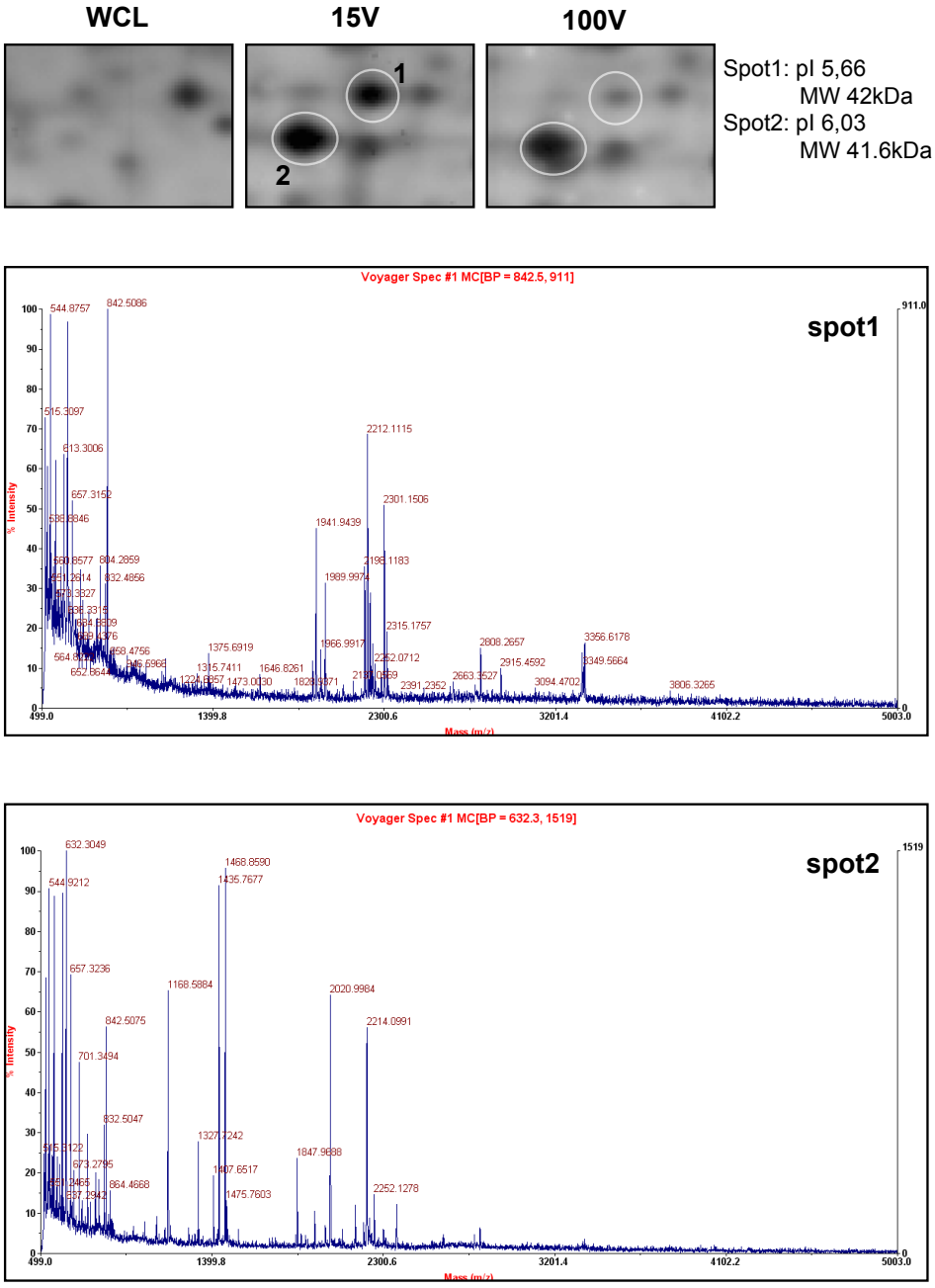

Fig. 32. Mass spectra of unknown protein spots found to be enriched in 15V. Mass spectra of 5 protein spots whose levels were particularly abundant in the 15V in comparison with WCL and 100V and that were not correspondent to any protein sequence present in Swiss Prot database. For each spot the cropped gel areas and the mass spectra are shown.

Finally table 4 lists the proteins that were at least 50% more abundant in WCL than in 100V, grouped by functional categories. A large number of the proteins which were identified as being under represented in 100V were metabolic enzymes, leading to confirm that 100V fraction is poorly contaminated by cellular components and mainly characterized by exosomes.

Table 4. Catalogue of the proteins, grouped for biological function, at least 50% more represented in 2D-IPG maps of WCL than in 100V fraction. These proteins have been found by gel matching with the reference proteomic maps of DOSAC-COBS 2D-PAGE database.

Protein name	AC number	Abbreviated Name	Theor. MW	Exp. MW	Theor. Pi	Exp. Pi
cytoskeleton and associated proteins						
Actin, cytoplasmic 1	P60709	ACTB/G	41737	42000	5,29	5,13
Actin, cytoplasmic 1	P60709	ACTB/G fr c	41737	37641	5,29	5,45
Actin, cytoplasmic 1	P60709	ACTB/G sf a	41737	41556	5,29	5,09
Actin, cytoplasmic 2	P63261	ACTG	41793	35760	5,31	5,45
Macrophage-capping protein	P40121	CAP G a	38498	39437	5,82	5,79
Macrophage-capping protein	P40121	CAP G b	38498	39437	5,82	5,65
Rho GDP-dissociation inhibitor 1	P52565	GDIR	23207	23501	5,03	5,02
Rho GDP-dissociation inhibitor 2	P52566	GDIS	22988	22644	5,1	5,09
Tubulin alpha-1 chain	P68366	TBA1 a	49924	54581	4,95	5,10
Tubulin alpha-1 chain	P68366	TBA1 b	49924	54220	4,95	5,11
Tubulin alpha-1 chain	P68366	TBA1 c	49924	53152	4,95	5,10
Tubulin beta chain	P07437	TBB5 b	49671	51802	4,78	4,98
Tropomyosin alpha-1 chain	P09493	TPM1	32708	31748	4,69	4,78
Tropomyosin beta chain	P07951	TPM2	32990	38647	4,63	4,84
Thymosin beta-4	P62328	TYB4	5053	12200	5,02	4,79
Myosin light polypeptide 6	P60660	MYL6	16930	14537	4,56	4,43
metabolic enzymes						
Aconitase	O75944	ACON a	65347	78855	7,96	6,96
Retinal dehydrogenase 1	P00352	AL1A1	54862	50866	6,3	6,79
Fructose-bisphosphate aldolase A	p04075	ALDOA b	39420	38684	8,3	7,33
Apolipoprotein A-I	P02647	APOA1 a	30778	24730	5,56	5,17
ATP synthase subunit alpha, mitochondrial	P25705	ATPA	59751	51052	9,16	7,26
ATP synthase subunit beta, mitochondrial	P06576	ATPB	56560	50405	5,26	5,05
Bifunctional purine biosynthesis protein PURH	P31939	PUR9	64616	62263	6,27	6,32
Carbonic anhydrase 1	P00915	CAH1	28870	28671	6,59	6,83
D-dopachrome decarboxylase	P30046	DOPD a	12712	11068	6,72	6,96
D-dopachrome decarboxylase	P30046	DOPD b	12712	11219	6,72	7,16
Alpha-enolase	p06733	ENOA c	47169	46791	7,01	6,49
Alpha-enolase	p06733	ENOA d	47169	46628	7,01	6,65
Alpha-enolase	p06733	ENOA e	47169	46791	7,01	6,84
Alpha-enolase	p06733	ENOA sf a	47169	38517	7,01	6,11
Fumarate hydratase, mitochondrial	P07954	FUMH	54637	44762	8,85	7
Gamma-enolase	P09104	ENOG	47269	46995	4,91	4,94
Glyceraldehyde-3-phosphate dehydrogenase	p04406	G3P b	36053	35500	8,57	7,27
Glyceraldehyde-3-phosphate dehydrogenase	p04406	G3P c	36053	35236	8,57	7,38
Glyceraldehyde-3-phosphate dehydrogenase	p04406	G3P d	36053	35500	8,57	7,43
Glyceraldehyde-3-phosphate dehydrogenase	p04406	G3P e	36053	35959	8,57	7,52
Isocitrate dehydrogenase [NADP] cytoplasmic	O75874	IDHC a	46659	42000	6,53	6,34
Pyruvate kinase isozymes M1/M2	P14618	KPYM a	57937	59715	7,96	7,08
Pyruvate kinase isozymes M1/M2	P14618	KPYM b	57937	59715	7,96	7,14

Protein name	AC number	Abbreviated Name	Theor. MW	Exp. MW	Theor. Pi	Exp. Pi
L-lactate dehydrogenase A chain	P00338	LDHA	36689	33962	8,44	7,34
L-lactate dehydrogenase B chain	P07195	LDHB	36638	36493	5,71	5,71
Nucleoside diphosphate kinase A	P15531	NDKA	17149	17557	5,83	5,86
Nucleoside diphosphate kinase A	P15532	NDKA sf	17149	15076	5,83	5,84
Nucleoside diphosphate kinase B	P22392	NDKB	17298	15837	8,52	7,52
Malate dehydrogenase, cytoplasmic	P40925	MDHC	36426	35224	6,91	6,78
Protein disulfide-isomerase	P07237	PDIA1	57116	59500	4,76	4,89
Protein disulfide-isomerase A3	P30101	PDIA3 a	56782	56445	5,98	5,76
Phosphoglycerate mutase 1	P18669	PGAM1 b	28804	27091	6,67	6,78
Phosphoglycerate mutase 1	P18669	PGAM1a	28804	28801	6,67	6,47
Phosphoglycerate kinase 1	P00558	PGK 1 c	44615	42000	8,3	7,35
Purine nucleoside phosphorylase	P00491	PNPH b	32118	28172	6,45	6,45
Peptidyl-prolyl cis-trans isomerase A	P62937	PPIA b	18012	14853	7,68	6,71
Peptidyl-prolyl cis-trans isomerase A	P62937	PPIA d	18012	14853	7,68	7,19
Triosephosphate isomerase	P60174	TPIS b	26669	25181	6,45	5,88
Triosephosphate isomerase	P60174	TPIS c	26669	24905	6,45	6,19
Triosephosphate isomerase	P60174	TPIS d	26669	24684	6,45	6,29
Triosephosphate isomerase	P60174	TPIS e		24938		6,56
Triosephosphate isomerase		TPIS f		25000		6,81
Triosephosphate isomerase		TPIS a sf	26669	25581	6,45	4,9
V-type proton ATPase subunit F	Q16864	VATF	13370	11158	5,29	5,17
molecular chaperons						
Peptidyl-prolyl cis-trans isomerase FKBP1A	P62942	FKB1A	11951	11091	7,89	7,39
75 kDa glucose-regulated protein	P38646	GRP75	73680	69991	5,87	5,37
Endoplasmin	P14625	GRP94a	92469	91200	4,76	4,9
Endoplasmin	P14626	GRP94b	92469	89007	4,77	4,98
Endoplasmin	P14627	GRP94c	92469	87930	4,78	5,04
Heat shock protein beta-1	P04792	HSP27 a	22782	26680	5,98	5,42
Heat shock protein beta-2	P04792	HSP27 c	22782	26108	5,98	5,56
60 kDa heat shock protein, mitochondrial	p10809	HSP60 c	61055	59500	5,7	5,27
60 kDa heat shock protein, mitochondrial	p10809	HSP60 d	61055	59500	5,7	5,29
Heat shock cognate 71 kDa protein	P11142	HSP7C d	70898	69991	5,37	5,47
Peptidyl-prolyl cis-trans isomerase B	P23284	PPIB	23742	16404	9,42	7,87
Transitional endoplasmic reticulum ATPase	P55072	TERA b	89322	88767	5,14	5,19
Translationally-controlled tumor protein	P13693	TCTP	19595	22267	4,84	4,9
membrane associated proteins with multiple activities						
Annexin A1	P04083	ANXA1 b	38714	35652	6,57	6,80
Annexin A1	P04083	ANXA1 sf2	38714	28854	6,57	7,44
Galectin-3	P17931	LEG3 a	26152	25728	8,58	7,44
Voltage-dependent anion-selective channel protein 1	P21796	VDAC1 b	30773	31393	8,62	7,56
cell growth and proliferation regulators						
14-3-3 protein gamma	P61981	1433G	28302	28309	4,8	4,85
Protein S100-A11	P31949	S10AB b	11740	10,472	6,56	5,56

Protein name	AC number	Abbreviated Name	Theor. MW	Exp. MW	Theor. Pi	Exp. Pi
Protein S100-A2	P29034	S10A2	11117	12090	4,68	4,60
Proliferation-associated protein 2G4	Q9UQ80	PA2G4	43787	44857	6,13	6,40
Prohibitin	P35232	PHB	29804	28040	5,57	5,46
Acidic leucine-rich nuclear phosphoprotein 32 family member A	P39687	AN32A	28585	29837	3,99	4,11
Calreticulin	p27797	CALR	48142	59300	4,29	4,52
Chloride intracellular channel protein 1	O00299	CLIC1 a	26923	31938	5,09	5,01
Protein S100-A6	P06703	S10A6 a	10180	9184	5,32	4,92
Protein S100-A6	P06703	S10A6 b	10180	8993	5,32	5
SH3 domain-binding glutamic acid-rich-like protein	O75368	SH3L1	12774	12374	5,22	5,23
protein transport						
Endoplasmic reticulum resident protein 29	P30040	ERP29	28993	28040	6,77	5,87
Fatty acid-binding protein, epidermal	Q01469	FABP5	15164	12395	6,6	5,92
Fatty acid-binding protein, brain	O15540	FABP7 b	14889	11551	5,4	5,65
Eukaryotic translation initiation factor 5A-1	P63241	IF5A	16832	14897	5,07	5,08
Transthyretin	P02766	TTHY	15887	13411	5,52	5,35
detoxification and redox proteins						
Aldose reductase	P15121	ALDR b	35853	34974	6,52	6,66
Peroxiredoxin-1	Q06830	PRDX1 b	22110	21208	8,27	7,07
Peroxiredoxin-1	Q06830	PRDX1 c	22110	21599	8,27	7,33
Peroxiredoxin-6	P30041	PRDX6 a	25035	26680	6	5,67
Peroxiredoxin-6	P30041	PRDX6 b	25035	25181	6	6,36
Superoxide dismutase [Mn], mitochondrial	P04179	SODM b	24722	21559	8,35	6,92
Thioredoxin	p10599	THIO b	11737	10557	4,82	5,01
Thioredoxin	p10600	THIO mut	11737	12821	4,82	4,9
protein degradation and modification						
Cathepsin D	P07339	CATD a	44552	31174	6,1	5,29
Proteasome subunit alpha type-1	P25786	PSA1	29556	31017	6,15	5,88
26S protease regulatory subunit 8	P62195	PRS8	45626	44762	7,11	6,91
Proteasome subunit beta type-4	P28070	PSB4	29204	22131	5,72	5,61
Proteasome activator complex subunit 1	Q06323	PSME1	28723	29131	5,78	5,8
proteins with extracellular activity						
Cystatin-B	P04080	CYTB	11139	12306	6,96	6,60
Cystatin-B	P04080	CYTB sf	11139	10649	6,96	6,88
Macrophage Migration Inhibitory Factor	P14174	MIF a	12476	10995	7,73	7,11
Macrophage Migration Inhibitory Factor	P14174	MIF b	12476	11350	7,73	7,30
Protein S100-A7	P31151	S10A7	11471	10466	6,27	5,82
Protein S100-A8	P05109	S10A8	10834	10673	6,51	6,82
protein biosynthesis						
Elongation factor 1-beta	p24534	EF1B	24764	31938	4,5	4,65
Eukaryotic translation initiation factor 6	P56537	IF6	26599	26942	4,56	4,67
39S ribosomal protein L12, mitochondrial	P52815	RM12	21348	19355	9,05	5,09
Heterogeneous nuclear ribonucleoproteins A2/B1	P22626	ROA2	37430	32407	8,97	7,83
40S ribosomal protein SA	P08865	RSSA	32854	41247	4,79	4,85
stress response						
Stress-induced-phosphoprotein 1	P31948	STIP1 a	62639	66331	6,4	6,51
Stress-induced-phosphoprotein 2	P31948	STIP1 b	62639	65808	6,4	6,45
Hypoxia up-regulated protein 1	Q9Y4L1	HYOU1	111335	173310	5,16	5,19

Conclusions

Breast cancer represents one of the most diffused cancers among women around the world. In the last decades the rate of death is decreasing because of the improved therapies. Nevertheless, the battery of biomarkers usually used not always is suitable to all the specific cases, due to a wide heterogeneity of molecular causes beyond breast cancer. Identification of new tumor biomarkers is therefore necessary. A possible source of biomarkers consists of extracellular microvesicles which appear to play a central role in transporting informations among cells, thus favoring tumor invasiveness and metastasis.

This work demonstrated that two breast cancer cell lines, 8701 BC and MDA MB 231, release *in vitro* at least two different vesicle populations separable by differential centrifugation and with a specific protein composition.

In the first part of the research, the limits caused by the presence of serum in vesicles collected by 8701 BC cell cultures are enlightened. In fact serum proteins stickly adhere to microvesicle membranes and therefore they interfere with the extensive identification of vesicular proteins. Even though western blot analysis suggests that the fraction sedimented at 15,000 xg contains mainly membrane vesicles enriched in β1 integrin while the further ultracentrifugation pulls down the exosomes enriched in heat shock cognate protein 70.

In the second part of this study, the proteomic analysis successfully applied to microvesicles derived from MDA MB 231 cells, together with TEM analysis and western blot revealed that the vesicles pulled down at high speed centrifugation are suitable to be considered as exosomes for dimension and protein content. They carry key factors in endosomal pathway and especially in multivesicular bodies genesis such as PDC6I. They are particularly enriched in molecules responsible of cell adhesion to extracellular matrix such as alpha integrins, laminins and galectin binding proteins that may favor anchoring of these structures to ECM. Proteins involved in immune response such as beta2 microglobulin have been considered typical of those exosomes. In the same time, microvesicles are found to express high levels of proteins related to tumor progression such as 14-3-3 epsilon and

transgelin 2 that could represent novel tumor biomarkers for prediction and prognosis of breast cancer.

Other proteins which can be considered as tumor markers have been identified in the exosomes. These include PRDX-2, a protein which was identified as early-stage breast cancer auto antigen, useful in earlier diagnosis of aggressive breast cancer (Desmetz et al., 2009) and PRDX-6 which was shown to be related to breast cancer malignancy (Chang et al., 2007).

Therefore this work has demonstrated to be useful in defining the whole protein content of exosomes derived from breast cancer, opening arguments on their putative roles in tumor progression and metastasis and searching for novel possible tumor biomarkers.

Eventually this work reports for the first time the proteomic analysis of the 15,000 xg sedimented fraction that in previous works had been washed away or included in the whole ultracentrifuged material. The proteomic study revealed that this fraction has a proteome profile more similar to the one of cell lysate, being more enriched in metabolism related proteins. The same fraction contains also some proteins, although at lower levels, found highly abundant in the complementary fraction obtained by ultracentrifugation. Therefore, it can be argued that 15,000 xg sediment is partially contaminated by exosomes and probably by cell debris.

Nevertheless the 15,000 xg vesicle fraction is also specifically enriched in some proteins, among them an isoform of PRDX2 different from the two observed in exosomes and PRDX3, that could be a potential proliferation marker in breast cancer. This fraction also revealed the high presence of ETS-related transcription factor Elf-4 which has a role in tumorigenesis and the protein disulfide-isomerase A3 (PDIA3). Five enriched protein spots analysed by mass spectrometry corresponded to different fragments of vimentin and one corresponds to an isoform of cytoplasmic 1 actin, i. e. cytoskeleton components.

Some proteins selectively abundant in 15,000 xg fraction could not be identified by mass spectrometry and searching in databases of known protein sequences, suggesting that they are completely new proteins not yet discovered.

Although these proteins are still unknown, their high relative abundance exclusively in this fraction remarks that the sediment obtained by centrifugation at 15,000 xg may contain different vesicles than exosomes, not only for size, as illustrated by microscopy, but also for protein composition. Therefore these unknown proteins are worth to be more deeply investigated, in order to get new insight into the nature and potential roles *in vivo* of extracellular large vesicles that, because of lack of informations, are under appreciated structures.

References

1. Admyre C, Johansson SM, Qazi KR, Filén JJ, Lahesmaa R, Norman M, Neve EP, Scheynius A, Gabrielsson S. (2007) Exosomes with immune modulatory features are present in human breast milk. J Immunol. 179(3): 1969-78.

2. Al-Nedawi K, Meehan B, Kerbel RS, Allison AC, Rak J. (2009). Endothelial expression of autocrine VEGF upon the uptake of tumor-derived microvesicles containing oncogenic EGFR. *Proc Natl Acad Sci USA*, 106(10): 3794-9.

3. Al-Nedawi K, Meehan B, Micallef J, Lhotak V, May L, Guha A, Rak J. (2008). Intercellular transfer of the oncogenic receptor EGFRvIII by microvesicles derived from tumour cells. *Nat Cell Biol,* 10: 619–624.

4. Andre F, Schartz NE, Movassagh M, Flament C, Pautier P, Morice P, Pomel C, Lhomme C, Escudier B, Le Chevalier T, Tursz T, Amigorena S, Raposo G, Angevin E, Zitvogel L. (2002). Malignant effusions and immunogenic tumour-derived exosomes. *Lancet*, 360: 295–305.

5. Andreola G, Rivoltini L, Castelli C, Rivoltini L, Castelli C, Huber V, Perego P, Deho P, Squarcina P, Accornero P, Lozupone F, Lugini L, Stringaro A, Molinari A, Arancia G, Gentile M, Parmiani G, Fais S. (2002) Induction of lymphocyte apoptosis by tumor cell secretion of FasL-bearing microvesicles. *J Exp Med*, 195: 1303–1316.

6. Arciero C, Somiari SB, Shriver CD, Brzeski H, Jordan R, Hu H, Ellsworth DL, Somiari RI. (2003). Functional relationship and gene ontology classification of breast cancer biomarkers. *Int J Biol Markers*, 18(4):241-72.

7. Baj-Krzyworzeka M, Szatanek R, Weglarczyk K, Baran J, Urbanowicz B, Brański P, Ratajczak MZ, Zembala M. (2006). Tumour-derived microvesicles carry several surface determinants and mRNA of tumour cells and transfer some of these determinants to monocytes. *Cancer Immunol Immunother*, 55: 808–818.

8. Baj-Krzyworzeka M, Szatanek R, Weglarczyk K, Baran J, Zembala M. (2007). Tumour-derived microvesicles modulate biological activity of human monocytes. *Immunol Lett*, 113: 76–82.

9. Bard MP, Hegmans JP, Hemmes A, Luider TM, Willemsen R, Severijnen LA, van Meerbeeck JP, Burgers SA, Hoogsteden HC, Lambrecht BN. (2004). Proteomic analysis of exosomes isolated from human malignant pleural effusions. *Am J Respir Cell Mol Biol*, 31(1): 114-21.

10. Caby MP, Lankar D, Vincendeau-Scherrer C, Raposo G, Bonnerot C. (2005). Exosomal-like vesicles are present in human blood plasma. *Int Immunol*, 17: 879–887.

11. Cantin R, Diou J, Belanger D, Tremblay AM, Gilbert C. (2008). Discrimination between exosomes and HIV-1: purification of both vesicles from cell-free supernatants. *J Immunol Meth*, 338: 21–30.

12. Cassarà D., Ginestra A., Dolo V., Miele M., Caruso G., Lucania G., Vittorelli ML. (1998). Modulation of vesicle shedding in 8701 BC human breast carcinoma cells. *J. Submicrosc. Cytol. Pathol,* 30 (1): 45-53.

13. Castellana D, Zobairi F, Martinez MC, Panaro MA, Mitolo V, Freyssinet JM, Kunzelmann C. (2009a). Membrane Microvesicles as Actors in the Establishment of a Favorable Prostatic Tumoral Niche: A Role for Activated Fibroblasts and CX3CL1-CX3CR1 Axis. *Cancer Res*, 69:785-793.

14. Castellana D, Kunzelmann C, Freyssinet JM. (2009b). Pathophysiologic significance of procoagulant microvesicles in cancer disease and progression. *Hämostaseologie,* 29(1):51-7.

15. Chang XZ, Li DQ, Hou YF, Wu J, Lu JS, Di GH, Jin W, Ou ZL, Shen ZZ, Shao ZM. (2007) Identification of the functional role of peroxiredoxin 6 in the progression of breast cancer. *Breast Cancer Res.* 9(6): R76.

16. Choi DS, Lee JM, Park GW, Lim HW, Bang JY, Kim YK, Kwon KH, Kwon HJ, Kim KP, Gho YS. (2007). Proteomic analysis of microvesicles derived from human colorectal cancer cells. *J Proteome Res,* 6: 4646–4655.

17. Chua PJ, Lee EH, Yu Y, Yip GW, Tan PH, Bay BH. (2010). Silencing the Peroxiredoxin III gene inhibits cell proliferation in breast cancer. *Int J Oncol.* 36(2) :359-64.

18. Cocucci E, Racchetti G, Meldolesi J. (2009). Shedding microvesicles: artefacts no more. *Trends in Cell Biol*, 19: 43-51.

19. Coghlin C, Murray GI. (2010). Current and emerging concepts in tumour metastasis. *The J. Pathol*, 222: 1–15.

20. Coussens LM, Werb Z. (1996). Matrix metalloproteinases and the development of cancer. *Chem Biol*, 3(11): 895-904.

21. Desmetz C, Bascoul-Mollevi C, Rochaix P, Lamy PJ, Kramar A, Rouanet P, Maudelonde T, Mangé A, Solassol J. (2009). Identification of a new panel of serum autoantibodies associated with the presence of in situ carcinoma of the breast in younger women. *Clin Cancer Res.* 15(14): 4733-41.

22. Dolo V, Adobati E, Canevari S, Picone MA, Vittorelli ML. (1995a). Membrane vesicles shed into the extracellular medium by human breast carcinoma cells carry tumor-associated surface antigens. *Clin Exp Metastasis,* 13(4): 277-86.

23. Dolo V, D'Ascenzo S, Violini S, Pompucci L, Festuccia C, Ginestra A, Vittorelli ML, Canevari S, Pavan A. (1999). Matrix-degrading proteinases are shed in membrane vesicles by ovarian cancer cells in vivo and in vitro. *Clin Exp Metastasis,* 17(2):131-40.

24. Dolo V, Ginestra A, Cassarà D, Violini S, Lucania G, Torrisi MR, Nagase H, Canevari S, Pavan A, Vittorelli ML. (1998). Selective localization of matrix

metalloproteinase 9, beta1 integrins, and human lymphocyte antigen class I molecules on membrane vesicles shed by 8701-BC breast carcinoma cells. *Cancer Res*, 58(19): 4468-74.

25. Dolo V, Ginestra A, Ghersi G, Nagase H, and Vittorelli ML. (1994). Human breast carcinoma cells cultered in the presence of serum shed vesicles rich in gelatinolytic activities. *J. Submicrosc. Cytol. Pathol.*, *26*, 173-180.

26. Dolo V, Pizzurro P, Ginestra A, Vittorelli ML. (1995b). Inhibitory effects of vesicles shed by human breast carcinoma cells on lymphocyte 3H-thymidine incorporation, are neutralised by anti TGF-beta antibodies. *J Submicrosc Cytol Pathol,* 27(4): 535-41.

27. Dowsett M, Cooke T, Ellis I, Gullick WJ, Gusterson B, Mallon E, Walker R. (2000). Assessment of HER2 status in breast cancer: why, when and how? *Eur J Cancer*, 36(2):170-6.

28. Fevrier B, Raposo G. (2004) Exosomes: endosomal-derived vesicles shipping extracellular messages. *Curr Op Cell Biol,* 16(4): 415–421.

29. Fishman DA, Bafetti LM, Banionis S, Kearns AS, Chilukuri K, Stack MS. (1997). Production of extracellular matrix-degrading proteinases by primary cultures of human epithelial ovarian carcinoma cells. *Cancer*, 80(8):1457-63.

30. Fukushi J., Makagiansar I.T., Stallcup W.B. (2004) NG2 proteoglycan promotes endothelial cell motility and angiogenesis via engagement of galectin-3 and alpha3beta1 integrin. Mol. Biol. Cell 15: 3580-3590.

31. Ginestra A, La Placa MD, Saladino F, Cassarà D, Nagase H, Vittorelli ML. (1998). The amount and proteolytic content of vesicles shed by human cancer cell lines correlates with their *in vitro* invasiveness. *Anticancer Res*, 18(5A): 3433-7.

32. Ginestra A, Miceli D, Dolo V, Romano FM, Vittorelli ML. (1999). Membrane vesicles in ovarian cancer fluids: a new potential marker. *Anticancer Res*, 19 (4C): 3439-45.

33. Giusti I, D'Ascenzo S, Millimaggi D, Taraboletti G, Carta G, Franceschini N, Pavan A, Dolo V. (2008). Cathepsin B mediates the pH-dependent proinvasive activity of tumor-shed microvesicles. *Neoplasia*, 10(5):481-8.

34. Gonzales PA, Pisitkun T, Hoffert JD, Tchapyjnikov D, Star RA, Kleta R, Wang NS, Knepper MA. (2009). Large-scale proteomics and phosphoproteomics of urinary exosomes. *J Am Soc Nephrol.* 20(2): 363-79.

35. Graves LE, Ariztia EV, Navari JR, Matzel HJ, Stack MS, Fishman DA. (2004). Proinvasive properties of ovarian cancer ascites-derived membrane vesicles. *Cancer Res*, 64(19):7045-9.

36. Hegmans JP, Bard MP, Hemmes A, Luider TM, Kleijmeer MJ, Prins JB, Zitvogel L, Burgers SA, Hoogsteden HC, Lambrecht BN. (2004). Proteomic

analysis of exosomes secreted by human mesothelioma cells. *Am J Pathol*, 164: 1807–1815.

37. Heijnen HFG, Schiel AE, Fijnheer R, Geuze HJ, Sixma JJ (1999). Activated Platelets Release Two Types of Membrane Vesicles: Microvesicles by Surface Shedding and Exosomes Derived From Exocytosis of Multivesicular Bodies and alpha-Granules. *Blood*, 94: 3791-3799.

38. Iero M, Valenti R, Huber V, Filipazzi P, Parmiani G, Fais S, Rivoltini L. (2008). Tumour-released exosomes and their implications in cancer immunity. *Cell Death Differ*, 15: 80–88.

39. Janowska-Wieczorek A, Wysoczynski M, Kijowski J, Marquez-Curtis L, Machalinski B, Ratajczak J, Ratajczak MZ. (2005). Microvesicles derived from activated platelets induce metastasis and angiogenesis in lung cancer. *Int J Cancer*, 113: 752–760.

40. Jeffery N, McLean MH, El-Omar EM, Murray GI. (2009). The matrix metalloproteinase/tissue inhibitor of matrix metalloproteinase profile in colorectal polyp cancers. *Histopathology*, 54: 820–828.

41. Kalluri R, Zeisberg M. (2006). Fibroblasts in cancer. *Nat Rev*, 6: 392–01.

42. Keller S, König AK, Marmé F, Runz S, Wolterink S, Koensgen D, Mustea A, Sehouli J, Altevogt P. (2009). Systemic presence and tumor-growth promoting effect of ovarian carcinoma released exosomes. *Cancer Lett*, 278(1): 73-81.

43. Kim CW, Lee HM, Lee TH, Kang C, Kleinman HK, Gho YS. (2002) Extracellular membrane vesicles from tumor cells promote angiogenesis via sphingomyelin. *Cancer Res*, 62(21): 6312-7.

44. Kim HK, Song KS, Park YS et al. (2003). Elevated levels of circulating platelet microparticles, VEGF, IL-6 and RANTES in patients with gastric cancer: possible role of a metastatic predictor. *Eur J Cancer*, 39: 184–191.

45. Kim JW, Wieckowski E, Taylor DD, Reichert TE, Watkins S, Whiteside TL. (2005). Fas ligand-positive membranous vesicles isolated from sera of patients with oral cancer induce apoptosis of activated T lymphocytes. *Clin Cancer Res,* 11(3): 1010-20.

46. Kirfel G, Rigort A, Borm B, Herzog V. (2004). Cell migration: mechanisms of rear detachment and formation of migration tracks. *Eur J Cell Biol,* 83: 717–724.

47. Logullo AF, Nonogaki S, Pasini FS, Osório CA, Soares FA, Brentani MM. (2010). Concomitant expression of epithelial-mesenchymal transition biomarkers in breast ductal carcinoma: association with progression. *Oncol Rep*, 23(2): 313-20.

48. Liang S, Xu Y, Shen G, Liu Q, Zhao X, Xu Z, Xie X, Gong F, Li R, Wei Y. (2009). Quantitative protein expression profiling of 14-3-3 isoforms in human

renal carcinoma shows 14-3-3 epsilon is involved in limitedly increasing renal cell proliferation. *Electrophoresis.* 30(23): 4152-62.

49. Liu C, Yu S, Zinn K, Wang J, Zhang L, Jia Y, Kappes JC, Barnes S, Kimberly RP, Grizzle WE, Zhang HG. (2006). Murine mammary carcinoma exosomes promote tumor growth by suppression of NK cell function. *J Immunol*, 176: 1375–1385.

50. Mareel M, Maria JO, Madani I. (2009). Cancer invasion and metastasis: interacting ecosystems. *Virchows Arch*, 454: 599–622.

51. Mathivanan S, Ji H, Simpson RJ. (2010). Exosomes: Extracellular organelles important in intercellular communication. J proteom. 73: 1907-1920.

52. Mathivanan S, Lim JW, Tauro BJ, Ji H, Moritz RL, Simpson RJ. (2010b). Proteomics analysis of A33 immunoaffinity-purified exosomes released from the human colon tumor cell line LIM1215 reveals a tissue-specific protein signature. *Mol Cell Proteomics.* 9(2): 197-208.

53. Mathivanan S, Simpson RJ. (2009). ExoCarta: A compendium of exosomal proteins and RNA. *Proteomics*, 9: 4997–5000.

54. Mears R, Craven RA, Hanrahan S, Totty N, Upton C, Young SL, Patel P, Selby PJ, Banks RE. (2004). Proteomic analysis of melanomaderived exosomes by two dimensional polyacrylamide gel electrophoresis and mass spectrometry. *Proteomics*, 4: 4019–31.

55. Millimaggi D, Mari M, D'Ascenzo S et al. (2007). Tumor vesicle-associated CD147 modulates the angiogenic capability of endothelial cells. *Neoplasia*, 9: 349–357.

56. Minafra S, Morello V, Glorioso F, La Fiura A, Tomasino R.M, Feo S, Mcintosh D, and Wolley D.E. (1989). A new cell line (8701-BC) from primari ductal infiltrating carcinoma of human breast. *Br. J. Cancer,* 60: 185-192.

57. Muralidharan-Chari V, Clancy JW, Sedgwick A, D'Souza-Schorey C. (2010). Microvesicles: mediators of extracellular communication during cancer progression. *J Cell Science,* 123: 1603-1611.

58. Nickel W (2003). The mystery of nonclassical protein secretion: a current view on cargo proteins and potential export routes. *Eur J Biochem*, 270: 2109–2119.

59. Paget S. (1889). The distribution of secondary growths in cancer of the breast. *Lancet*, 133: 571–573.

60. Pucci Minafra I, Cancemi P, Fontana S, Minafra L, Feo S, Becchi M, Freyria AM and Minafra S. (2006). Expanding the protein catalogue in the proteome reference map of human breast cancer cells. *Proteomics* 6: 2609–2625.

61. Rigogliuso S, Donati C, Cassarà D, Taverna S, Salamone M, Bruni P, Vittorelli ML. (2010). An active form of sphingosine kinase-1 is released in the extracellular medium as component of membrane vesicles shed by two human tumor cell lines. *J Oncol.*

62. Safaei R, Larson BJ, Cheng TC, Gibson MA, Otani S, Naerdemann W, Howell SB. (2005). Abnormal lysosomal trafficking and enhanced exosomal export of cisplatin in drug-resistant human ovarian carcinoma cells. *Mol Cancer Ther*, 4 (10): 1595-604.

63. Schiera G, Proia P, Alberti C, Mineo M, Savettieri G, Di Liegro I. (2007). Neurons produce FGF2 and VEGF and secrete them at least in part by shedding extracellular vesicles. *J Cell Mol Med*, 11(6):1384-94.

64. Shedden K, Xie XT, Chandaroy P et al. (2003). Expulsion of small molecules in vesicles shed by cancer cells: association with gene expression and chemosensitivity profiles. *Cancer Res*, 63: 4331–4337.

65. Sidhu SS, Mengistab AT, Tauscher AN, LaVail J, Basbaum C (2004). The microvesicle as a vehicle for EMMPRIN in tumor-stromal interactions. *Oncogene.* 23(4):956-63.

66. Skog J, Würdinger T, van Rijn S, Meijer DH, Gainche L, Sena-Esteves M, Curry WT Jr, Carter BS, Krichevsky AM, Breakefield XO. (2008) Glioblastoma microvesicles transport RNA and proteins that promote tumour growth and provide diagnostic biomarkers. *Nat Cell Biol.* 10(12):1470-6.

67. Staubach S, Razawi H, Hanisch FG. (2009). Proteomics of MUC1-containing lipid rafts from plasma membranes and exosomes of human breast carcinoma cells MCF-7. *Proteomics*. 9(10): 2820-35.

68. Taraboletti G, D'Ascenzo S, Borsotti P, Giavazzi R, Pavan A, Dolo V. (2002). Shedding of the matrix metalloproteinases MMP-2, MMP-9, and MT1-MMP as membrane vesicle-associated components by endothelial cells. *Am J Pathol,* 160(2):673-80.

69. Taraboletti G, D'Ascenzo S, Giusti I, Marchetti D, Borsotti P, Millimaggi D, Giavazzi R, Pavan A, Dolo V. (2006). Bioavailability of VEGF in tumor-shed vesicles depends on vesicle burst induced by acidic pH. *Neoplasia*. 8(2): 96-103.

70. Taverna S, Ghersi G, Ginestra A, Rigogliuso S, Pecorella S, Alaimo G, Saladino F, Dolo V, Dell'Era P, Pavan A, Pizzolanti G, Mignatti P, Presta M, Vittorelli ML. (2003) Shedding of membrane vesicles mediates fibroblast growth factor-2 release from cells. *J Biol Chem*, 278(51):51911-9.

71. Taylor DD, Gercel-Taylor C. (2008). MicroRNA signatures of tumor-derived exosomes as diagnostic biomarkers of ovarian cancer. *Gynecol Oncol*, 110: 13–21.

72. Taylor DD, Gerçel-Taylor C. (2005). Tumour-derived exosomes and their role in cancerassociated T-cell signalling defects. *Br J Cancer*, 92: 305–311.

73. Trusolino L, Cavassa S, Angelini P, Andó M, Bertotti A, Comoglio PM, Boccaccio C. (2000). HGF/scatter factor selectively promotes cell invasion by increasing integrin avidity. *FASEB J*, 14(11): 1629-40.

74. Valenti R, Huber V, Filipazzi P, Pilla L, Sovena G, Villa A, Corbelli A, Fais S, Parmiani G, Rivoltini L. (2006). Human tumor-released microvesicles promote the differentiation of myeloid cells with TGF-β mediated suppressive activity on T lymphocytes. *Cancer Res*, 66: 9290–9298.

75. Valenti R, Huber V, Iero M, Filipazzi P, Parmiani G, Rivoltini L. (2007). Tumor-released microvesicles as vehicles of immunosuppression. *Cancer Res.* 67(7): 2912-5

76. van Niel G, Porto-Carreiro I, Simoes S, Raposo G. (2006). Exosomes: a common pathway for a specialized function. *J Biochem*, 140: 13–21.

77. Viaud S, Terme M, Flament C, Taieb J, Andre F, Novault S, Escudier B, Robert C, Caillat-Zucman S, Tursz T, Zitvogel L, Chaput N. (2009). Dendritic cell-derived exosomes promote natural killer cell activation and proliferation: a role for NKG2D ligands and IL-15Ralpha. *PLoS ONE.*

78. Vittorelli ML. (2003). Shed membrane vesicles and clustering of membrane-bound proteolytic enzymes. *Curr Top Dev Biol*, 54: 411-32.

79. World Health Organization. (2003). Who Disease and injury country estimates. Retrieved 2009.

80. Wysoczynski M, Ratajczak MZ. (2009). Lung cancer secreted microvesicles: underappreciated modulators of microenvironment in expanding tumors. *Int. J. Cancer,* 125: 1595–1603.

81. Yi CH, Zheng T, Leaderer D, Hoffman A, Zhu Y. (2009). Cancer-related transcriptional targets of the circadian gene NPAS2 identified by genome-wide ChIP-on-chip analysis. *Cancer Lett.* 284(2): 149-56.

82. Zhang Y, Ye Y, Shen D, Jiang K, Zhang H, Sun W, Zhang J, Xu F, Cui Z, Wang S. (2010). Identification of transgelin-2 as a biomarker of colorectal cancer by laser capture microdissection and quantitative proteome analysis. Cancer Sci. 101(2): 523-9.

Acknowledgements:

The first part of this work, i.e. characterization of vesicles shed by 8701 BC cells, was carried out in:

- the laboratory of prof. Maria Letizia Vittorelli, DBCS, University of Palermo;
- the laboratory of prof. Anna Maria Puglia, DBCS, University of Palermo;
- the laboratory of prof. Daniel Gygax, FHNW, University of Life Sciences, Basel, Switzerland.

The second part of this work, i.e. characterization of vesicles shed by MDA MB 231 cells, was carried out in:

- the laboratory of prof. Italia Di Liegro, BioNeC, University of Palermo;
- the laboratory of prof. Daniel Gygax, FHNW, University of Life Sciences, Basel; Switzerland.
- the laboratory of prof. Ida Pucci-Minafra, DOSAC-COBS, University of Palermo, with the support of Dr. Nadia Ninfa Albanese and Dr. Gianluca Di Cara.

Transmission electron micrographs were taken by Vesna Olivieri at the Biozentrum, Basel, Switzerland.

Gel chromatography experiment was performed at the Department of Chemistry, University of Basel, with the support of Dr. Ozana Onaca.

Special thanks:

I would like really to thank all the persons that contributed to this work with their human and scientific support:

Prof. Maria Letizia Vittorelli, Prof. Anna Maria Puglia, Dr. Giuseppe Gallo, Prof. Daniel Gygax, Prof. Uwe Pieles, Prof. Italia Di Liegro, Dr. Gabriella Schiera, Dr. Patrizia Proia, Dr. Monica Salamone, Prof. Ida Pucci-Minafra, Dr. Gianluca Di Cara and Dr. Nadia Ninfa Albanese.